Die Funktion von Three rows bei der Schwesterchromatiden-Trennung in *Drosophila melanogaster*

Dissertation

zur Erlangung des Grades eines

Doktors der Naturwissenschaften

- Dr. rer. nat. -

der Fakultät für Biologie, Chemie und Geowissenschaften

der Universität Bayreuth

vorgelegt von

Alf Herzig

aus Marbach am Neckar

2002

Promotionsgesuch eingereicht am:

Erstgutachter: Prof. Dr. Christian F. Lehner

Zweitgutachter:

Tag der mündlichen Prüfung:

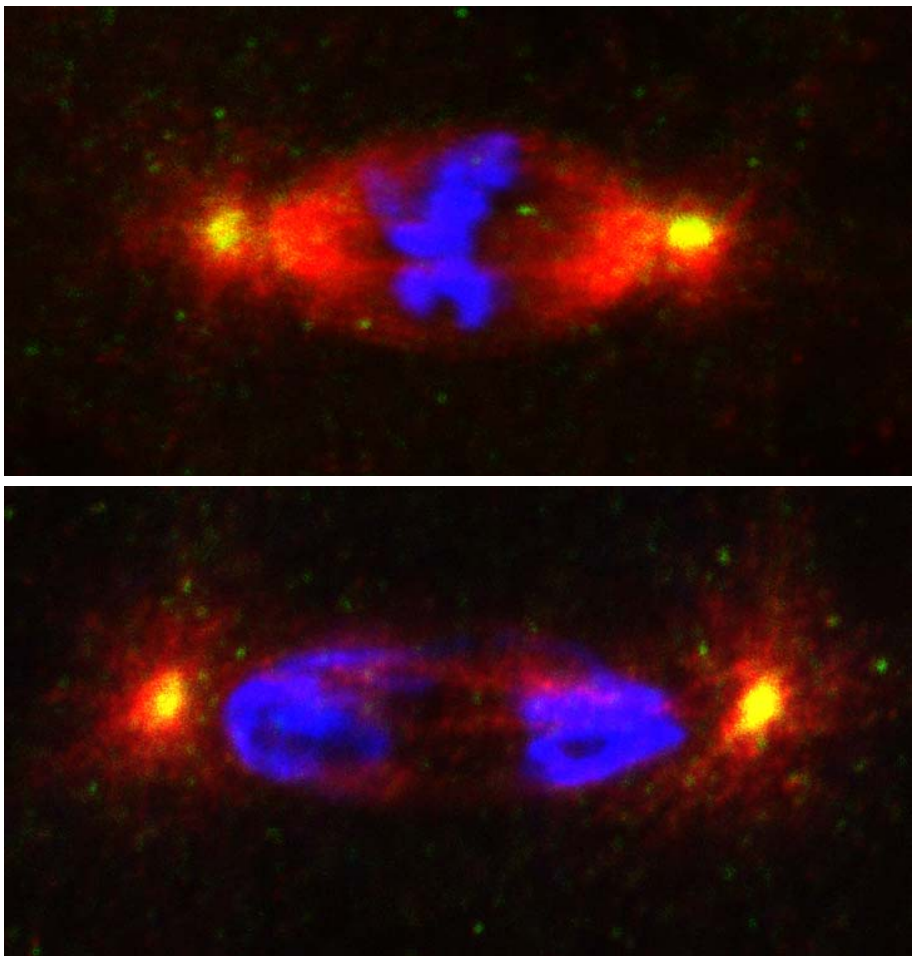

Höre Viele, tue Deines

(Sprichwort der Massai)

Für Honey Bunny und Philip

Danksagung:

Diese Arbeit wurde am Lehrstuhl für Genetik der Universität Bayreuth unter der Anleitung von Prof. Dr. Christian F. Lehner angefertigt.

Bei Christian Lehner bedanke ich mich nicht nur für die hervorragende Betreuung während meiner Promotion, sondern insgesamt für meine wissenschaftliche Ausbildung. Seit meinen „ersten Schritten“ am Friedrich-Miescher-Laboratorium in Tübingen war er mir ein scharfsinniger, hartnäckiger, hilfsbereiter und verantwortungsvoller akademischer Lehrer. Für seine einzigartige Anleitung zur Wissenschaft bin ich ihm sehr dankbar.

Darüber hinaus möchte ich mich bei den derzeitigen und ehemaligen Mitgliedern des Labors für ihre Zusammenarbeit, Diskussionsbereitschaft und nicht zuletzt den Spaß bedanken, den wir zusammen hatten. Nur exemplarisch seien hier Stefan Heidmann (mit „f“), Hubert Jäger (die Schwaben-Unterstützung), Oliver Leismann (mit seinen unschätzbaren Gesangseinlagen) und Claas Meyer (mit seinen weisesten aller Ratschlägen) genannt.

Mein besonderer Dank gilt Jörg Höflich, der seine Diplomarbeit unter meiner Anleitung „durchleiden“ durfte. Im Rahmen dieser Arbeit hat er zur Charakterisierung der THR/PIM Interaktion im Hefe-Two-Hybrid-System beigetragen.

Des weiteren möchte ich mich bei den Damen der Spül- und Futterküche, sowie den technischen Assistentinnen für ihre vielfältige und unschätzbare Hilfe bedanken.

Abseits der Wissenschaft danke ich ganz besonders meinen Eltern, die mich lange Jahre unterstützt und motiviert haben.

Inhaltsverzeichnis

1 Zusammenfassung

In der Mitose werden die Schwesterchromatiden getrennt und auf beide Tochterzellen verteilt. Die Trennung der Schwesterchromatiden erfordert die proteolytische Spaltung des Scc1-Proteins. Scc1 ist Bestandteil des Kohäsin-Komplexes, der die Schwesterchromatiden nach ihrer Entstehung in der S-Phase bis zum Beginn der Anaphase gepaart hält. Die Protease, die durch Scc1-Spaltung die Schwesterchromatiden-Trennung einleitet, heißt Separase. Die Separase wird erst dann aktiviert, wenn alle Chromosomen bipolar mit dem mitotischen Spindelapparat verbunden sind. Die Aktivierung der Separase erfordert die Ubiquitin-abhängige Degradation des Securins, einer inhibitorischen Untereinheit der Separase. Weitere Mechanismen der Separase-Regulation sind noch nicht vollständig verstanden.

Das Securin von *Drosophila melanogaster* ist das Protein Pimples (PIM). Die Separase (SSE) von *D. melanogaster* besitzt zwar eine Protease-Domäne, aber die N-terminale regulatorische Domäne, die in Separasen anderer Eukaryoten gefunden wird, fehlt in SSE fast vollständig. In dieser Arbeit wurde gezeigt, dass PIM und SSE einen heterotrimeren Komplex mit dem Protein Three rows (THR) bilden. THR besitzt Bindungsstellen für PIM und SSE. In anderen Organismen besitzt die N-terminale Separase-Domäne Bindungsstellen für das Securin und die Protease-Domäne der Separase. Diese Ergebnisse legen nahe, dass THR strukturell der N-terminalen Domäne anderer Separasen entspricht. Die Separase aus *D. melanogaster* scheint demnach aus zwei Untereinheiten aufgebaut zu sein.

Während SSE die katalytische Domäne der Separase beinhaltet, wurde hier gezeigt, dass THR eine regulatorische Separase-Untereinheit ist. THR wird nach dem Metaphasen-Anaphasen-Übergang proteolytisch gespalten. Diese Spaltung erfolgt nur in funktionellen Separase-Komplexen, und die Spaltstelle in THR entspricht dem Konsensus einer Separase-Spaltstelle. Mutationen in dieser Spaltstelle unterbinden die THR-Spaltung. Diese Daten legen nahe, dass THR durch die katalytische Untereinheit der Separase gespalten wird. Die Expression von nicht spaltbaren THR-Varianten führt zu frühembryonaler Letalität bei erniedrigter Temperatur. Diese Letalität wird unterdrückt wenn die katalytische Aktivität der Separase erniedrigt wird. Die Spaltung von THR trägt demnach zur Inaktivierung der Separase bei. Die Spaltung von THR ist vor allem während der Zellularisierung wichtig, einem insektenspezifischen Prozess in der Embryonalentwicklung von *D. melanogaster*. Während der Zellularisierung führt die ausbleibende Inaktivierung der Separase zu Defekten im Tubulin-Zytoskelett. Dieses Ergebnis legt nahe, dass die Separase in *D. melanogaster* weitere Substrate neben den Kohäsinen und andere Funktionen als in der Schwesterchromatiden-Trennung hat.

2 Summary

In mitosis, sister chromatids are separated and distributed onto two daughter cells. Separation of sister chromatids depends on proteolytic cleavage of Scc1. Scc1 is part of the cohesin complex, that holds sister chromatids together after they are synthesized in S-phase until they are separated in anaphase. The protease that initiates sister chromatid separation by cleavage of Scc1 is called separase. Separase is only activated when all chromosomes are attached to the mitotic spindle in a bipolar fashion. Activation of separase involves ubiquitin-dependent degradation of securin, an inhibitory separase subunit. Additional mechanisms that regulate separase activity are still poorly understood.

In *Drosophila melanogaster*, Pimples (PIM) is the securin. The separase (SSE) from *D. melanogaster* has a protease domain although it lacks most of the N terminal regulatory domain found in all other eukaryotic separases. It is shown here, that PIM and SSE form a heterotrimeric complex with Three rows (THR). THR has binding sites for both PIM and SSE. The N-terminal domains of other separases have binding sites for the securin and the protease domain of separase. These data suggest that THR structurally corresponds to the N-terminal domain of other separases. Therefore, the separase from *D. melanogaster* appears to consist of two independent subunits.

While SSE includes the catalytic separase domain, THR was found to be a regulatory separase subunit. THR is cleaved after the metaphase-to-anaphase transition. Cleavage only occurs in functional SSE complexes and in a region that matches the separase cleavage site consensus. Mutations in this region abolish THR cleavage. These results indicate that THR is cleaved by the catalytic separase subunit. Expression of noncleavable THR variants results in early-embryonic lethality at lowered temperature. This lethality can be suppressed by a reduction of catalytically active separase levels, indicating that THR cleavage contributes to inactivation of separase. THR cleavage is particularly important during cellularization, an insect specific process in early-embryonic development of *D. melanogaster*. During cellularization the lack of separase inactivation severely disrupts organization of the tubulin-cytoskeleton. These results suggest that *D. melanogaster* separase has other targets in addition to cohesin subunits and might have other functions than sister chromatid separation.

3 Einleitung

Diese Arbeit befasst sich mit der Verteilung des genetischen Materials auf die Tochterzellen. Aufgrund seiner zentralen zellulären Bedeutung scheint dieser Prozess in Eukaryoten evolutionär konserviert zu sein. (Zur Übersicht: Nasmyth, 2002).

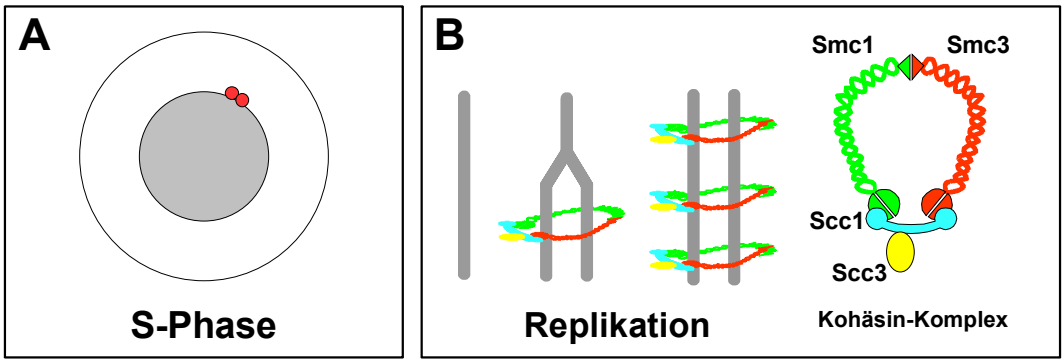

Abbildung 1: S-Phase und Aufbau der Schwesterchromatiden-Kohäsion

(*A*) Schematische Darstellung einer Zelle in der S-Phase. Die dekondensierte DNA befindet sich im Zellkern (grau). An der Kernmembran sind die Zentrosomen lokalisiert (rot).
(*B*) Etablierung der Schwesterchromatiden-Kohäsion während der Replikation in der S-Phase. Während der Verdopplung der DNA-Stränge (grau) bindet der Kohäsin-Komplex an die DNA. Dargestellt ist außerdem ein mögliches, räumliches Modell für den Kohäsin-Komplex aus *S. cerevisiae*, mit den Proteinen Smc1, Smc3, Scc1 und Scc3. (Modell modifiziert nach: Nasmyth, 2002)

Eine Voraussetzung für die korrekte Verteilung der Schwesterchromatiden ist, dass sie von ihrer Entstehung in der S-Phase an bis in die Mitose verbunden bleiben (Uhlmann und Nasmyth, 1998). Diese Verbindung, die als Schwesterchromatiden-Kohäsion bezeichnet wird, bewahrt die Information darüber, welche Chromatiden exakte Kopien voneinander sind. Diese müssen in der Mitose in unterschiedliche Tochterzellen segregiert werden. In *Saccharomyces cerevisiae* wurde gezeigt, dass die Kohäsion der Schwesterchromatiden durch die Proteine Scc1/Mcd1, Scc3, Smc1 und Smc3 vermittelt wird, die so genannten Kohäsine (Michaelis et al., 1997; Toth et al., 1999). Mittlerweile wurden Kohäsine auch in anderen Organismen, wie *Schizosaccharomyces pombe*, *Drosophila melanogaster*, *Xenopus laevis* und dem Menschen beschrieben (Losada et al., 1998; Tomonaga et al., 2000; Warren et al., 2000a; Hauf et al., 2001). Die Kohäsine bilden einen Proteinkomplex, der während der S-Phase an die entstehenden Schwesterchromatiden bindet und so deren Zusammenhalt etabliert (Abb. 1). Neuere, ultrastrukturelle Analysen haben zu einem räumlichen Modell des Kohäsin-Komplexes geführt (Haering et al., 2002). Danach legt sich ein Heterodimer aus Smc1 und Smc3 wie eine Spange um die beiden DNA Stränge. Diese Spange wird an ihrem offenen Ende von einem Heterodimer aus Scc1 und Scc3 zusammengehalten (Abb. 1).

In *S. cerevisiae* erfolgt die Trennung der Schwesterchromatiden durch die proteolytische Spaltung des Kohäsins Scc1 (Uhlmann et al., 1999). In höheren Eukaryoten erfolgt die Auflösung der Kohäsion in zwei Schritten. Während der Prophase dissoziiert der Kohäsin-Komplex unabhängig von Scc1-Spaltung von den Armen der Chromosomen. Die Dissoziation des Kohäsin-Komplexes im Bereich der Chromosomen-Arme wird über Phosphorylierung der Scc1- und Scc3-Untereinheiten reguliert (Sumara et al., 2002). Lediglich im zentromernahen Bereich bleibt die Kohäsion der Schwesterchromatiden in der Prophase noch erhalten (Sumara et al., 2000; Waizenegger et al., 2000; Warren et al., 2000b, siehe auch Abb. 2). Der zweite Schritt, bei dem während dem Übergang von der Metaphase in die Anaphase die Kohäsion am Zentromer aufgelöst wird, ist auch in höheren Eukaryoten von Scc1-Spaltung abhängig (Waizenegger et al., 2000).

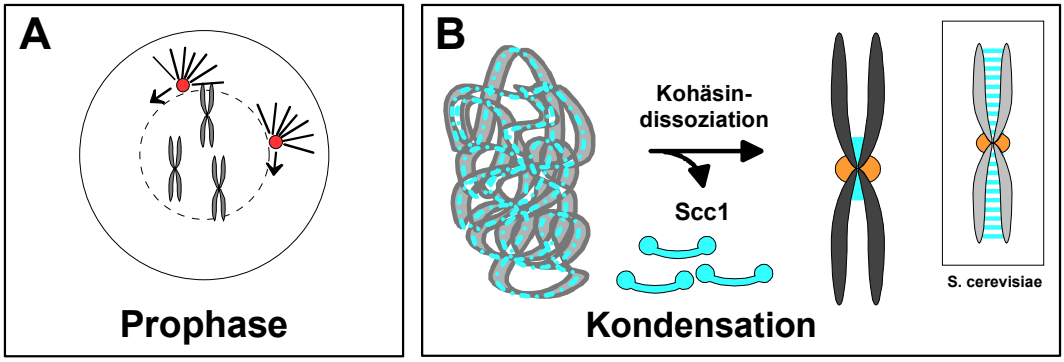

Abbildung 2: Prophase und Kondensation des Chromatins

(*A*) Schematische Darstellung einer Zelle in der Prophase der Mitose. Innerhalb der Zelle werden die Chromosomen sichtbar (grau) und die Kernmembran löst sich auf (gestrichelter Kreis). Die Zentrosomen (rot) wandern auseinander um später gegenüberliegende Pole der mitotischen Spindel zu bilden (Pfeile). Währenddessen beginnen sich astrale Mikrotubuli auszubilden (schwarz).
(*B*) Kondensation und Kohäsion der Schwesterchromatiden. Während der Kondensation des Chromatins wird in höheren Eukaryoten die Kohäsion an den Armen der Chromosomen aufgelöst. Dieser Vorgang erfordert keine Spaltung von Scc1. Im Bereich der Zentromere, auf denen die Kinetochore aufgebaut sind (orange), bleibt die Kohäsion erhalten. In *S. cerevisiae* bleibt während der weniger ausgeprägten Kondensation des Chromatins, die Kohäsion auf der ganzen Länge der Chromatiden erhalten (kleiner Kasten).

Die Scc1-Spaltung und endgültige Trennung der Schwesterchromatiden erfolgt erst dann, wenn alle Chromosomen korrekt in der so genannten Metaphasen-Platte angeordnet sind (Abb. 3). Erreicht wird dieser Zustand durch die Wechselwirkung der Chromosomen mit dem mitotischen Spindelapparat, der sich während der Metaphase als eine bipolare Struktur herausbildet (Zur Übersicht: Sharp et al., 2000; Karsenti und Vernos, 2001).

An den Chromosomen-Armen wird über Mikrotubuli und Chromatin-gebundene Motorproteine, eine von den Polen wegweisende Kraft erzeugt, der so genannte „polar wind“ (blaue Pfeile in Abb. 3). Dieser Mechanismus ist essentiell für die Ausrichtung der Chromosomen in der Metaphase. An den Kinetochoren, die auf den Zentromeren der Chromosomen aufgebaut sind, werden Mikrotubuli

ebenfalls über Motorproteine gebunden. Am Kinetochor wird jedoch eine Kraft erzeugt, die zum jeweiligen Pol hinweist (grüne Pfeile in Abb. 3). Die Bindung der Mikrotubuli am Kinetochor bleibt instabil, solange ein Chromosom nur mit einem der beiden Spindel-Pole verbunden ist. Erst wenn beide Schwester-Kinetochore mit entgegengesetzten Spindel-Polen verknüpft sind, wird die Bindung der Mikrotubuli am Kinetochor stabilisiert. Das Ergebnis der Chromosomen-Ausrichtung in der Metaphase ist ein stabiler Zustand, bei dem die Schwester-Kinetochore eines Chromosoms mit entgegengesetzten Spindel-Polen verknüpft sind. Diese bipolare Verknüpfung mit der Spindel erlaubt die Trennung der Schwesterchromatiden. Da die Schwesterchromatiden mit gegenüberliegenden Polen verbunden sind, werden sie, sobald die Kohäsion gelöst ist, zu gegenüberliegenden Polen segregiert. Auf diese Weise wird sichergestellt, dass jede Tochterzelle eines und nur eines der beiden Duplikate eines Chromosoms erhält.

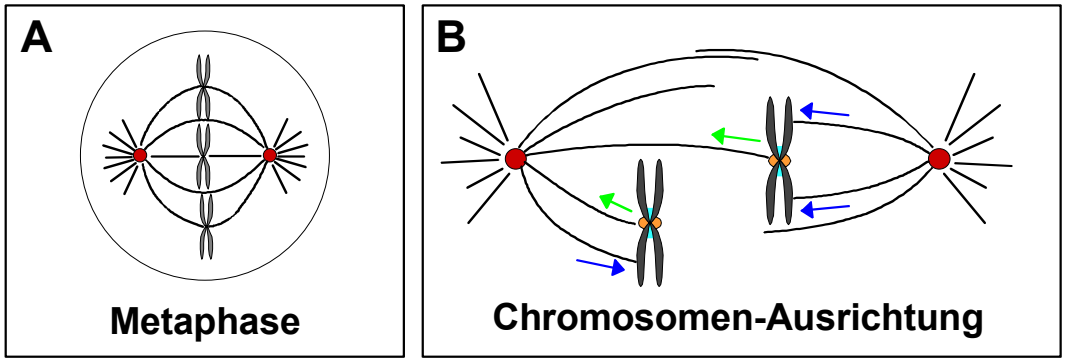

Abbildung 3: Metaphase und Ausrichtung der Chromosomen in der Metaphasen-Platte

(*A*) Schematische Darstellung einer Zelle in der Metaphase der Mitose. Die Chromosomen (grau) ordnen sich in der Metaphasen-Platte an. Die Zentrosomen (rot) befinden sich an gegenüberliegenden Polen der mitotischen Spindel (schwarz).
(*B*) Modell der Chromosomen-Ausrichtung in der Metaphase. An den Chromosomen-Armen erzeugen Mikrotubuli und Motorproteine eine vom Pol wegweisende Kraft (blaue Pfeile). An den Kinetochoren wird über andere Motorproteine eine zum Pol hinweisende Kraft erzeugt (grüne Pfeile). Diese Prozesse wirken zusammen bei der Ausbildung der Metaphasen-Platte.

Die bipolare Verknüpfung der Chromosomen mit der Spindel ist eine unabdingbare Voraussetzung für die Schwesterchromatiden-Trennung (Abb.4). Auf molekularer Ebene wird diese Abhängigkeit durch einen Kontrollmechanismus gewährleistet, den sogenannten „spindle assembly checkpoint“. Dieser Kontrollmechanismus verhindert die Einleitung der Anaphase, solange Kinetochore vorliegen, die nur mit einem Spindel-Pol verbunden sind (Zur Übersicht: Amon, 1999). Schon in sehr frühen Arbeiten hatte sich gezeigt, dass für die Einleitung der Anaphase Ubiquitin-abhängige proteolytische Degradation erforderlich ist (Holloway et al., 1993). In der Folge wurde die kritische E3-Ubiquitin-Ligase identifiziert, der sogenannte „anaphase promoting complex/cyclosome“ (APC/C). In der Mitose benötigt der APC/C eine aktivierende Untereinheit, das Fizzy/Cdc20 Protein. Solange der „spindle assembly checkpoint“ aktiv ist, verhindert er die Fizzy/Cdc20-APC/C-abhängige Degradation eines Anaphase-Inhibitors (Zur Übersicht: Peters, 2002).

Zu den am besten charakterisierten Substraten des APC/C gehören die mitotischen Cycline (Glotzer et al., 1991; Hershko et al., 1991). Als positive, regulatorische Untereinheiten der Cyclin-abhängigen Kinasen (Cdk) sind sie essentiell für den Eintritt in die Mitose. In den mitotischen Cyclinen konnte ein Sequenzelement, die sogenannte „destruction box“ (D-Box) identifiziert werden, welches für ihren APC/C-abhängigen Abbau hinreichend und notwendig ist (Glotzer et al., 1991). Der Abbau der mitotischen Cycline ist erforderlich um die Mitose zu beenden. Wird die Degradation der mitotischen Cycline verhindert, unterbleibt die Dekondensation des Chromatins und die Depolymerisation der mitotischen Spindel. Experimente mit nicht degradierbaren Cyclinen haben jedoch gezeigt, dass die Trennung der Schwesterchromatiden nicht vom Abbau der mitotischen Cycline abhängig ist (Holloway et al., 1993; Irniger et al., 1995; Tugendreich et al., 1995).

Daraus ergab sich das Postulat, dass mindestens ein weiteres Protein existieren muss, welches ein Substrat des APC/C ist und als Anaphase-Inhibitor wirkt. Proteine mit diesen Eigenschaften konnten mittlerweile in vielen Organismen identifiziert werden (Cohen-Fix et al., 1996; Funabiki et al., 1996; Zou et al., 1999, Teilarbeit A). Diese Proteine stellen sicher, dass keine verfrühte Schwesterchromatiden-Trennung erfolgt und sie werden heute als Securine bezeichnet.

Alle bislang charakterisierten Securine binden an eine Protease, die essentiell für die Trennung der Schwesterchromatiden ist (Funabiki et al., 1996a; Ciosk et al., 1998; Zou et al., 1999; Teilarbeit B). Diese als Separase bezeichnete Protease vermittelt die Spaltung der Scc1-Kohäsin-Untereinheit und damit die Trennung der Schwesterchromatiden (Uhlmann et al., 2000). Die Bindung des Securins inhibiert die Aktivität der Separase (Hornig et al., 2002; Waizenegger et al., 2002). Demnach erlaubt die Degradation des Securins am Metaphasen-Anaphasen-Übergang die Aktivierung der Separase (Abb. 4). Dieser Mechanismus zur Aktivierung der Separase scheint in allen Organismen konserviert zu sein. Obwohl die Trennung der Schwesterchromatiden ein konservierter Prozess ist, zeigen die Securine, abgesehen von Degradationssignalen (D-Box, KEN-Box) keine Verwandtschaft auf Sequenzebene. Die Identifizierung der Securine erfolgte daher anhand funktioneller Kriterien. Bei den Separasen handelt es sich um Cystein-Proteasen aus der CD-Familie, zu denen auch die Caspasen gehören. Wie die Caspasen sind die Separasen sequenzspezifische Endoproteasen, deren Erkennungssequenz einem evolutionär konservierten Konsensus entspricht (Hauf et al., 2001). Im Gegensatz zu den Securinen zeigen die Separasen deutliche Sequenzhomologien zueinander. Diese Homologien beschränken sich jedoch auf eine C-terminale Domäne, in der sich das katalytisch aktive Zentrum der Protease befindet. In der N-terminalen Domäne, die für die Bindung der Securine benötigt wird, zeigen die Separasen dagegen keine Sequenzähnlichkeiten. (Funabiki et al., 1996a; Uhlmann et al., 2000).

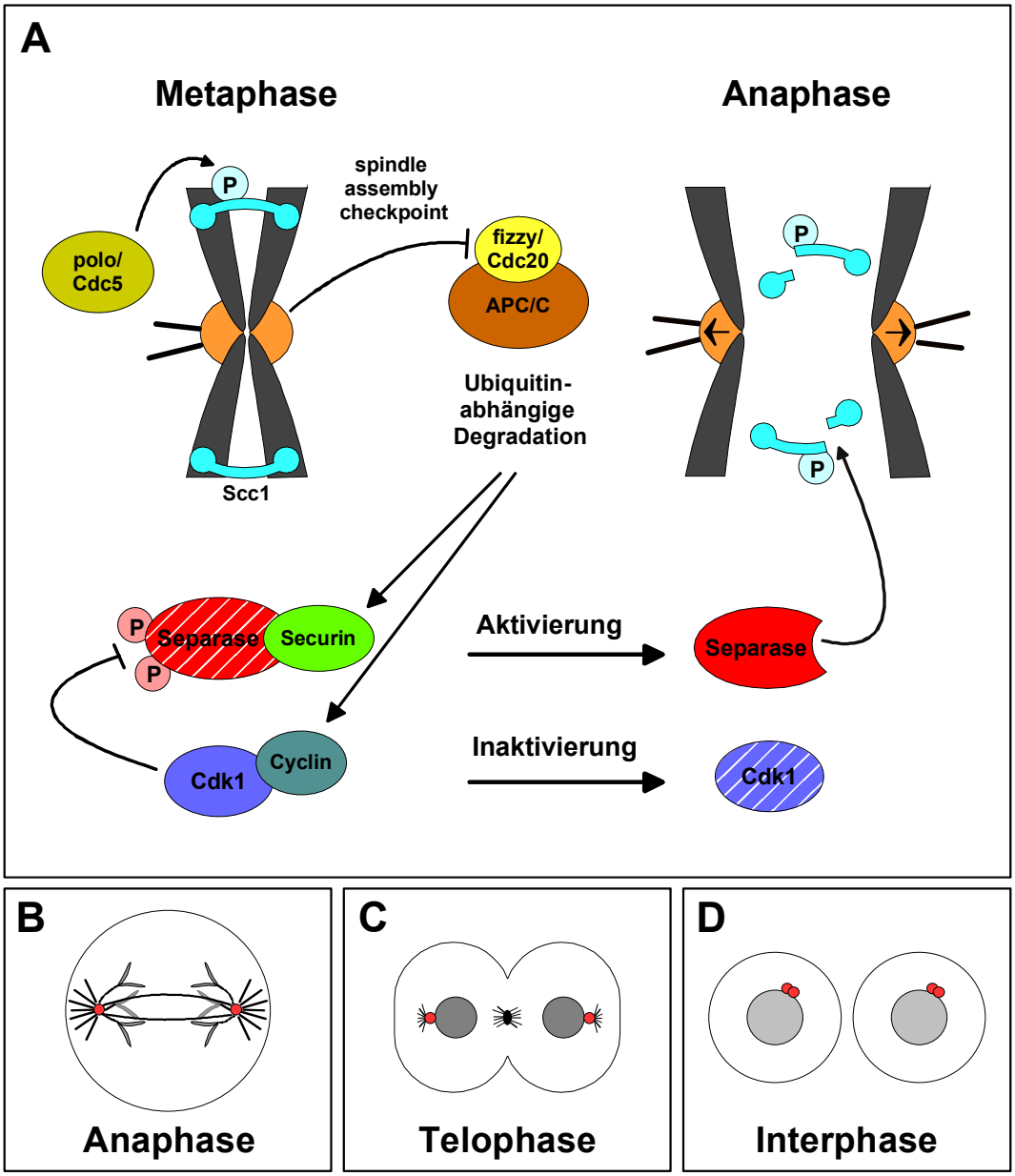

Abbildung 4: Metaphasen-Anaphasen-Übergang und Zytokinese

(***A***) Schematische Darstellung des Metaphasen-Anaphasen-Übergangs. Der „spindle assembly checkpoint" verhindert, dass die Anaphase eingeleitet wird solange Kinetochore vorliegen, die nicht bipolar mit der Spindel verknüpft sind. Dies geschieht durch die Inhibition des fizzy/Cdc20 Aktivators der APC/C Ubiquitin-Ligase. Nachdem die Kinetochore bipolar mit der Spindel verknüpft sind, wird der APC/C durch fizzy/Cdc20 aktiviert. Der APC/C vermittelt die Ubiquitin-abhängige Degradation der mitotischen Cycline und des Securins. Die Auswirkung der Degradation ist in beiden Fällen verschieden. Der Abbau der mitotischen Cycline führt zur Inaktivierung der Cdk1-Kinase und zum Austritt aus der Mitose. Der Abbau des Securins führt zur Aktivierung der Separase. Die aktive Separase spaltet das Scc1-Kohäsin, wodurch die Trennung der Schwesterchromatiden ermöglicht wird. Die beiden Schwesterchromatiden werden daraufhin durch die mitotische Spindel zu gegenüberliegenden Polen segregiert. In Vertebraten kann die Aktivität der Separase über inhibitorische Phosphorylierung durch die Cdk1-Kinase reguliert werden. In *S. cerevisiae* wurde gezeigt, dass die polo/Cdc5-Kinase das Scc1 phosphoryliert, wodurch die Spaltung von Scc1 unterstützt wird.
(***B-D***) Schematische Darstellung von Zellen nach dem Metaphasen-Anaphasen-Übergang. Dargestellt sind DNA (grau), Mikrotubuli (schwarz) und Zentrosomen (rot).
(***B***) Anaphase der Mitose. Die getrennten Schwesterchromatiden werden durch die Spindel zu gegenüberliegenden Spindel-Polen segregiert.
(***C***) Telophase der Mitose. Das Chromatin beginnt zu dekondensieren und die mitotische Spindel bildet sich zurück. Im Zentrum der Zelle bildet sich der Mittelkörper aus Mikrotubuli und die Zytokinese beginnt mit der Einschnürung der Zellmembran.
(***D***) Interphase. Nach der vollendeten Zytokinese tritt die Zelle in die Interphase ein. Während der Interphase findet die Replikation der dekondensierten DNA und die Duplikation der Zentrosomen statt.

Die Aktivität der Separase wird außer durch die Degradation des Securins durch weitere Mechanismen reguliert. Diese Mechanismen sind nicht vollständig verstanden und scheinen evolutionär divergent zu sein. Die Securine aus *D. melanogaster* und *S. pombe*, PIM und Cut2, wirken beispielsweise nicht nur inhibitorisch auf die Separase. Im Gegenteil, sie sind absolut essentiell für die Schwesterchromatiden-Trennung. Diese Securine sind daher auch für die Aktivierung der Separase erforderlich. (Funabiki et al., 1996b; Stratmann und Lehner, 1996). Die Securine aus *S. cerevisiae* und *H. sapiens*, Pds1 und PTTG, haben diese essentielle Funktion nicht (Yamamoto et al., 1996; Jallepalli et al., 2001; Mei et al., 2001; Wang et al., 2001). Im Fall von PTTG könnten dafür funktionelle Redundanzen verantwortlich sein, da in der menschlichen Genom-Sequenz zwei weitere, zu PTTG homologe Gene identifiziert wurden (Chen et al., 2000). Es konnte gezeigt werden, dass die Separasen Esp1 aus *S. cerevisiae* und Cut1 aus *S. pombe* in einer Securin-abhängigen Weise in den Zellkern importiert und dort an die mitotische Spindel lokalisiert werden (Kumada et al., 1998; Jensen et al., 2001, Hornig et al., 2002). In *S. cerevisiae* kann dieser Mechanismus nicht essentiell sein. Das Securin (Pds1) ist nur bei erhöhter Temperatur essentiell, ansonsten läuft die Schwesterchromatiden-Trennung auch in Pds1 Deletions-Mutanten normal ab. In *S. pombe* ist das Securin (Cut2) jedoch essentiell und die subzelluläre Lokalisation der Separase könnte tatsächlich einen Beitrag zur Aktivierung der Separase leisten. In jüngerer Vergangenheit wurde in Vertebraten außerdem ein Securin-unabhängiger Mechanismus zur Regulation der Separase-Aktivität gefunden. Es konnte gezeigt werden, dass die Separase-Aktivität durch multiple, Cdk1-abhängige Phosphorylierungen inhibiert werden kann (Stemmann et al., 2001).

Neben der Regulation der Separase-Aktivität scheinen weitere Mechanismen zu existieren, durch die eine verfrühte Schwesterchromatiden-Trennung verhindert wird. In *S. cerevisiae* kann in Pds1-Deletions-Mutanten die Aktivität der Separase nicht durch die Bindung des Securins inhibiert werden. Es wurde gezeigt, dass die Separase in Pds1-Deletions-Mutanten während des gesamten Zellteilungszyklus aktiv ist. Dennoch findet keine verfrühte Schwesterchromatiden-Trennung statt. Daher muss in *S. cerevisiae* eine zusätzliche Ebene der Regulation existieren. In der Tat konnte gezeigt werden dass Scc1 in *S. cerevisiae* kurz vor dem Metaphasen-Anaphasen-Übergang durch die polo/Cdc5-Kinase phosphoryliert und seine Spaltung dadurch stimuliert wird (Alexandru et al., 2001, siehe auch Abb. 4). Dieser Mechanismus ist jedoch in Anwesenheit von Pds1 nicht essentiell, und seine Bedeutung in anderen Organismen ist nicht geklärt.

4 Problemstellung

Zu Beginn dieser Arbeit waren in *D. melanogaster* zwei Gene bekannt, *pimples* (*pim*) und *three rows* (*thr*), die spezifisch für die Trennung der Schwesterchromatiden benötigt werden (D'Andrea et al., 1993; Philp et al., 1993; Stratmann und Lehner, 1996). Der Funktionsverlust von *pim* oder *thr* führt zum kompletten Ausfall der Schwesterchromatiden-Trennung. Die von diesen Genen kodierten Proteine, Pimples (PIM) und Three Rows (THR), zeigen auf Sequenzebene keine Ähnlichkeiten zu anderen bekannten Proteinen. Sie enthalten auch keine Sequenzelemente, über die auf ihre molekulare Wirkungsweise geschlossen werden könnte.

Die Fragestellung dieser Arbeit war, welche Funktionen PIM und THR in der Schwesterchromatiden-Trennung übernehmen. Von PIM war bekannt, dass es am Metaphasen-Anaphasen-Übergang degradiert wird (Stratmann und Lehner, 1996). Diese Beobachtung gab Anlass zur Hypothese, dass es sich bei PIM um das *D. melanogaster* Securin handeln könnte. Diese Hypothese konnte belegt werden (Teilarbeit A). Im Verlauf dieser Arbeit wurde das Gen für *Separase* (*Sse*) in *D. melanogaster* identifiziert (Teilarbeit B). Es konnte gezeigt werden, dass PIM an SSE bindet. Daraus ergab sich die Frage, ob THR eine weitere, neue Komponente im Separase-abhängigen Mechanismus der Schwesterchromatiden-Trennung ist, oder über einen anderen Weg zur Schwesterchromatiden-Trennung beiträgt. Es konnte gezeigt werden, dass THR einen heterotrimeren Komplex mit PIM und SSE ausbildet (Teilarbeit B). Auf diesen Ergebnissen aufbauend, wurde die Bedeutung von THR in der Regulation der Schwesterchromatiden-Trennung näher analysiert (Teilarbeit C).

5 Ausführliche Zusammenfassung und Diskussion der Ergebnisse

5.1 Bindungspartner von THR

Zunächst wurde untersucht ob THR einen Protein-Komplex mit PIM oder SSE ausbilden kann. Dazu wurden zwei sich ergänzende methodische Ansätze verfolgt. Einerseits wurden Immunpräzipitations-Experimente durchgeführt und andererseits Interaktionsstudien im Hefe-Two-Hybrid-System. Durch diese Experimente konnte gezeigt werden, dass THR einen heterotrimeren Komplex mit PIM und SSE ausbildet.

Mit Immunpräzipitations-Experimente wurde untersucht, ob THR *in vivo* Komplexe ausbildet, die PIM oder SSE enthalten. Ein wichtiges Hilfsmittel für diese Experimente waren Epitop-markierte Versionen von THR und PIM. Diese Proteine, THR-myc und PIM-myc, tragen mehrere Kopien des myc-Epitops an ihrem C-Terminus. THR-myc und PIM-myc wurden durch die Transgene *gthr-myc* und *gpim-myc* in *D. melanogaster* exprimiert. Diese Transgene enthalten die regulatorischen Bereiche des jeweiligen endogenen Gen-Locus. Durch genetische Komplementations-Tests wurde gezeigt, dass *gthr-myc* die Funktion von *thr*, und *gpim-myc* die Funktion von *pim* ersetzen kann (Stratmann und Lehner, 1996, Teilarbeit A). Daraus folgt, dass die Epitop-Markierung keinen wesentlichen Einfluß auf die Funktion von THR oder PIM hat. Ein Vorteil der Epitop-Markierung von THR und PIM liegt darin, dass ein sehr spezifischer Antikörper gegen das myc-Epitop zur Verfügung steht. THR-myc wurde mit Antikörpern gegen das myc-Epitop aus Proteinextrakten angereichert. Die Immunpräzipitate wurden durch Immuno-Blotting analysiert. Daraus ging hervor, dass PIM mit THR-myc ko-präzipitiert wird (Teilarbeit A, Fig. 1). Die Signifikanz dieses Ergebnisses wurde durch Kontrollexperimente mit Cdk1-myc belegt, welches weder mit PIM noch mit THR assoziiert. Nach der Charakterisierung des *Separase*-Gens (*Sse*) konnte gezeigt werden, dass THR auch mit SSE in einem Proteinkomplex vorliegt (Teilarbeit B, Fig. 5C).

Im Hefe-Two-Hybrid-System wurde überprüft, ob THR, PIM und SSE auch in einem heterologen System, ohne die Anwesenheit weiterer *D. melanogaster* Proteine miteinander wechselwirken können. Diese Experimente geben daher einen Hinweise darauf, ob THR direkt an PIM oder SSE bindet. Auch im Hefe-Two-Hybrid-System konnte eine Interaktion von THR mit PIM und SSE nachgewiesen werden (Teilarbeit B, Fig. 3). Allerdings war es dazu nötig eine verkürzte THR-Variante (THR 1-933) zu verwenden, denn mit einem vollständigen THR Protein (THR 1-1379) konnte keine Interaktion beobachtet werden. Diese Tatsache ist

vermutlich darauf zurückzuführen, dass THR 1-1379 aufgrund seiner Größe nicht in den Zellkern von *S. cerevisiae* gelangt, wo die Aktivierung der Reportergene stattfinden muss. Im Hefe-Two-Hybrid-System konnte außerdem eine Wechselwirkung von PIM und SSE gefunden werden (Teilarbeit B, Fig. 3). Das bestätigt Immunpräzipitations-Experimente, die mit Antikörpern gegen SSE durchgeführt wurden (Hubert Jäger, Teilarbeit B, Fig. 4). Diese Ergebnisse legen eine direkte Interaktion der drei Proteine THR, PIM und SSE nahe. Allerdings beweisen sie noch nicht, dass THR, PIM und SSE *in vivo* heterotrimere Komplexe bilden.

Um zu untersuchen ob *in vivo* heterotrimere Komplexe aus THR, PIM und SSE gebildet werden, wurden weitere Immunpräzipitations-Experimente durchgeführt.

Für die bereits beschriebenen Immunpräzipitations-Experimente wurden Proteinextrakte aus Embryonen hergestellt, deren Zellen zum überwiegenden Teil mitotisch proliferierten. In diesen Extrakten liegen THR, PIM und SSE in vergleichbar hoher Konzentration vor, da alle drei Proteine für die Teilung von Zellen benötigt werden (D'Andrea et al., 1993; Philp et al., 1993; Stratmann und Lehner, 1996, Teilarbeit B). In späteren Stadien der Embryogenese nimmt die Anzahl an proliferierenden Zellen ab, und die Menge an THR, PIM und SSE geht sehr stark zurück. In Embryonen dieses Entwicklungsstadiums wurde entweder *thr-myc* oder *pim-myc* durch geeignete Transgene überexprimiert. Gleichzeitig wurde in beiden Fällen *HA-Sse*, eine mit HA-Epitopen markierte, voll funktionsfähige Variante von *Sse*, ektopisch exprimiert (Teilarbeit B). Dadurch wurden Extrakte erhalten, in denen die Kombinationen HA-SSE und THR-myc bzw. HA-SSE und PIM-myc in hoher Konzentrationen vorhanden waren, nicht jedoch PIM oder THR. Aus diesen Extrakten wurde HA-SSE immunpräzipitiert. Das Ergebnis dieser Experimente war, dass HA-SSE und THR-myc einen stabilen Komplex ausbilden können. Im Gegensatz dazu bilden HA-SSE und PIM-myc *in vivo* keinen stabilen Komplex. Eine stabile Interaktion von HA-SSE mit PIM-myc wird erst dann möglich, wenn gleichzeitig THR-myc exprimiert wird und an den Komplex bindet (Teilarbeit B, Fig. 5A,B). Demzufolge ist die Wechselwirkung von SSE mit PIM abhängig von der gleichzeitigen Bindung von THR. Damit wurde gezeigt, dass SSE, PIM und THR *in vivo* einen heterotrimeren Komplex ausbilden können.

Die Stöchiometrie der Komponenten im Separase-Komplex wurde ebenfalls durch Immunpräzipitations-Experimente aufgeklärt. Aus Extrakten die sowohl THR als auch THR-myc enthielten, wurde mit einem Antikörper gegen das myc-Epitop THR-myc angereichert, nicht aber THR (Teilarbeit A, Fig. 1). Das bedeutet, dass Separase-Komplexe, die THR-myc enthalten, kein THR enthalten. Somit liegt jeweils nur ein Molekül THR pro Separase-Komplex vor. Analoge Ergebnisse wurden mit PIM-myc und PIM, sowie mit HA-SSE und SSE erhalten (Teilarbeit A, Fig.

1 und Daten nicht gezeigt). Daraus ergibt sich, dass der Separase-Komplex nicht mehr als jeweils ein Molekül THR, PIM und SSE enthält.

5.2 Modell für THR-Separase-Komplexe in *D. melanogaster*

Mit weiteren Interaktionsstudien im Hefe-Two-Hybrid-System und durch Immunpräzipitations-Experimente mit THR-Deletionsvarianten wurden die Bindungsstellen charakterisiert, über die THR, PIM und SSE miteinander wechselwirken (Teilarbeit B, Fig. 3 und Fig. 4). Zusammen mit den bereits dargestellten Ergebnissen, wurden diese Daten in ein Modell integriert (Abb. 5A, vergleiche auch Teilarbeit B, Fig. 6).

Entsprechend diesem Modell liegt während der Interphase des Zellzyklus ein heterotrimerer Komplex aus THR, PIM und SSE vor. In diesem Komplex vermittelt PIM die Assoziation von THR und SSE. Dies trägt der Tatsache Rechnung, dass PIM im Hefe-Two-Hybrid-System über seinen N-Terminus mit SSE und über seinen C-Terminus mit THR interagiert (Teilarbeit B, Fig. 3). Außerdem wird dadurch berücksichtigt, dass PIM und THR an denselben Bereich im N-Terminus von SSE binden (Teilarbeit B, Fig. 3). Da dieser Bereich nicht weiter eingeengt wurde, ist es allerdings nicht ausgeschlossen, dass THR auch eine Bindungsstelle in SSE besitzt, die nicht mit der Bindungsstelle von PIM überlappt.

Im Hefe-Two-Hybrid-System können Interaktionen nachgewiesen werden, die *in vivo* scheinbar nicht stabil sind. Im Gegensatz zum Two-Hybrid-System bindet PIM *in viv*o nicht effizient an SSE. Dies geschieht *in vivo* nur, wenn PIM auch mit THR wechselwirken kann. Ebenso wird ein mutantes PIM-Protein (PIM Δ110-114 oder PIM^2-myc, Stratmann und Lehner, 1996), das im Hefe-Two-Hybrid-System an THR aber nicht an SSE binden kann, *in vivo* nicht effizient in den Separase-Komplex eingebaut (Teilarbeit B, Fig. 3 und Fig. 5). Die Diskrepanzen zwischen den Ergebnissen aus dem Hefe-Two-Hybrid-System und den Daten aus Immunpräzipitations-Experimenten könnten darauf zurückzuführen sein, dass die Proteine im Hefe-Two-Hybrid-System sehr stark exprimiert werden und so auch schwache Wechselwirkungen nachweisbar sind. Es wäre jedoch ebenfalls möglich, dass in *D. melanogaster* Mechanismen existieren, die sicherstellen, dass PIM nur dann stabil in den Separase-Komplex eingebaut wird, wenn es gleichzeitig an THR und SSE binden kann.

Entsprechend seiner Funktion als Securin, reprimiert PIM während der Interphase die Aktivität von SSE. Am Übergang von der Metaphase in die Anaphase wird PIM degradiert, und die Separase aktiviert. Nach dem hier vorgeschlagenen Modell wird durch die Degradation von PIM ein direkter Kontakt zwischen THR und SSE ermöglicht. Daher könnte die inhibitorische Funktion von PIM darin be-

stehen, eine aktivierende Wechselwirkung zwischen THR und SSE zu unterbinden.

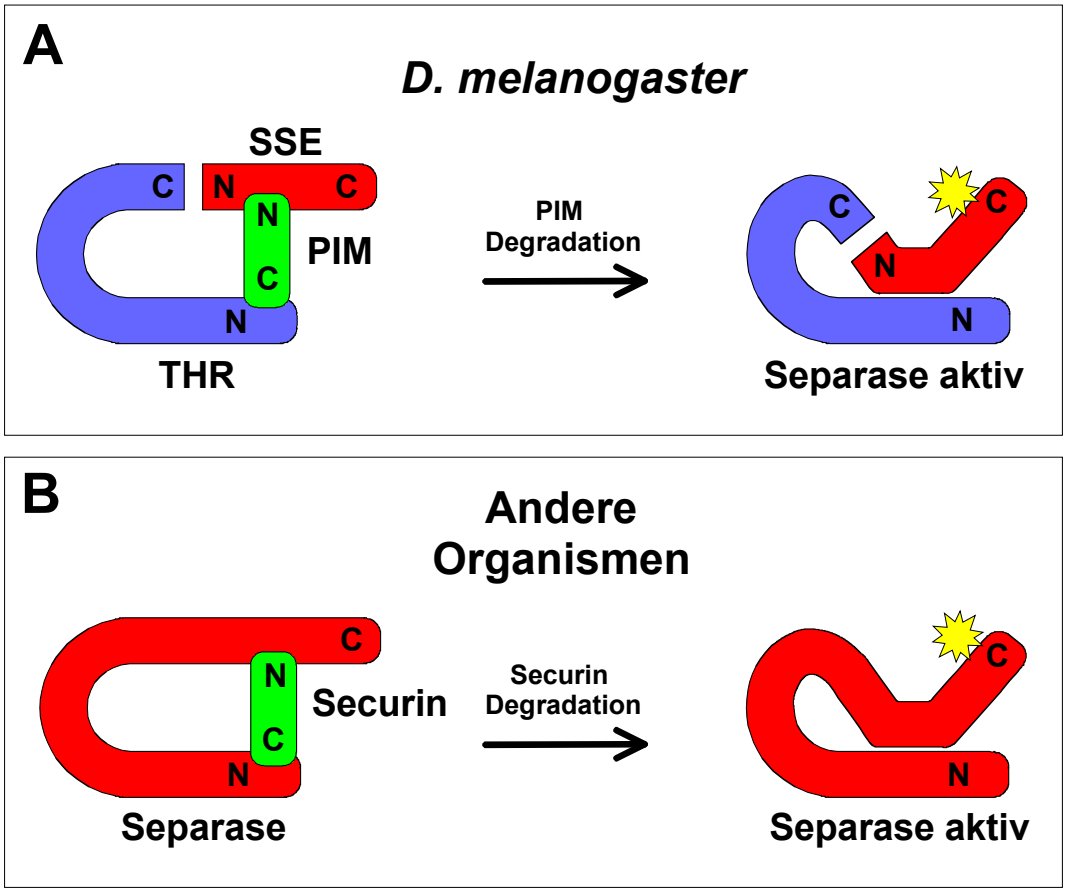

Abbildung 5: Modell für den Aufbau des Separase-Komplexes.

(***A***) In *D. melanogaster* ist der Separase-Komplex während der Interphase aus den Proteinen THR, SSE und PIM zusammengesetzt. PIM inhibiert als Securin die katalytische Aktivität von SSE. Nach der Degradation von PIM wird SSE durch die Wechselwirkung mit THR aktiviert (angedeutet durch einen Stern). Im Gegensatz zu den Securin/Separase-Komplexen anderer Organismen besteht die Separase in *D. melanogaster* aus zwei Untereinheiten, THR und SSE.
(***B***) In anderen Organismen hat das Securin nach diesem Modell zwei Bindungsstellen in der Separase. Nach der Degradation des Securins, erfolgt die Aktivierung der Separase durch eine intramolekularen Wechselwirkung zwischen N- und C-Terminus der Separase.

Eine Frage die dieses Modell nicht beantworten kann ist, warum PIM neben der Inhibition der Separase auch eine positive Funktion bei der Trennung der Schwesterchromatiden hat. Der aktive Separase-Komplex besteht in der Anaphase vermutlich aus einem THR/SSE Heterodimer. Das ist konsistent mit der Degradation von PIM am Metaphasen-Anaphasen-Übergang, und der Tatsache, dass THR und SSE einen stabilen Komplex ohne PIM ausbilden können. Ein Komplex zwischen THR und SSE sollte sich demnach auch dann ausbilden, wenn PIM aufgrund von Mutationen nicht gebildet werden kann. In *pim*-Mutanten werden die Schwesterchromatiden aber nicht getrennt, die gebildeten Separase-Komplexe sind demnach vermutlich nicht aktiv. Daraus ergibt sich, dass die Bindung von PIM den Separase-Komplex in einer bislang nicht verstandenen Weise aktiviert.

Im Rahmen dieser Arbeit wurden Versuche unternommen einen *in vitro* Assay für die Aktivität der Separase aus *D. melanogaster* zu etablieren. Für die humane Separase konnte ein solcher Assay bereits erfolgreich etabliert werden (Waizenegger et al., 2000). In diesen bereits beschriebenen Experimenten wurde humane Separase immunpräzipitiert, und das mit der Separase assoziierte Securin durch die Inkubation der Präzipitate in mitotischen *Xenopus*-Extrakten degradiert. Diese „aktivierten" Separase-Präzipitate konnten erfolgreich zur Spaltung von *in vitro* translatiertem humanen Scc1-Protein verwendet werden. Analog dazu wurden in dieser Arbeit Immunpräzipitate des *D. melanogaster* Separase-Komplexes in mitotischen *Xenopus*-Extrakten inkubiert. Dadurch konnte die Degradation von PIM erreicht werden. Die Spaltung von *in vitro* translatiertem *D. melanogaster* Scc1-Protein konnte jedoch nicht erreicht werden (Daten nicht gezeigt). Es ist unklar warum dieser Assay für Separase-Aktivität nicht auf *D. melanogaster* übertragbar ist. Diese Tatsache deutet jedoch an, dass die Aktivität der Separase aus *D. melanogaster* durch weitere Mechanismen neben der Degradation des Securins reguliert wird. Dazu könnte die subzelluläre Lokalisation der Separase oder die Interaktion der Separase mit weiteren Proteinen zählen, die nicht im Separase-Komplex vorliegen. Konsistent damit wurde gefunden, dass in Zellen in der Mitose ein Teil von THR an der mitotischen Spindel lokalisiert ist (Daten nicht gezeigt). Diese Lokalisation entspricht der Lokalisation der Separasen aus *S. cerevisiae* und *S. pombe*. Für PIM und SSE konnte die subzelluläre Lokalisation nicht untersucht werden, da die vorhandenen Antikörper gegen diese Proteine nicht die erforderliche Sensitivität des Nachweises ermöglichen (Daten nicht gezeigt).

Die hier vorgeschlagenen Modelle für den Aufbau des Separase-Komplexes aus *D. melanogaster* und aus anderen Organismen sind prinzipiell sehr ähnlich (Abb. 5). In dieser Arbeit wurden jedoch deutliche Hinweise darauf erhalten, dass THR in *D. melanogaster* strukturell dem N-Terminus der Separasen anderer Organismen entspricht. SSE ist im Vergleich zu den Separasen anderer Organismen außergewöhnlich klein und entspricht fast ausschließlich der in allen Separasen konservierten C-terminalen Protease-Domäne (Teilarbeit B, siehe auch Abb. 5A). Die N-terminale Domäne umfasst in allen Separasen außer SSE mehr als 110 kD und ist auf Sequenzebene nicht konserviert. THR ist ein Protein von etwa 160 kD und zeigt auf Sequenzebene keine Homologien zu anderen Proteinen. Strukturvorhersagen zeigen jedoch, dass in THR und den N-terminalen Domänen anderer Separasen gleiche Strukturelemente, sogenannte „Armadillo-repeats", vorhanden sein könnten (H. Sticht, Lehrstuhl Biopolymere, Universität Bayreuth, persönliche Mitteilung). Neben strukturellen Gemeinsamkeiten hat THR auch funktionelle Gemeinsamkeiten mit der N-terminalen Domäne anderer Separasen. Verschiedene Untersuchungen haben gezeigt, dass die N-terminalen Domäne der Separasen eine Bindungsstelle für das Securin enthält (Kumada et al., 1998; Jensen et al.,

2001, siehe auch Abb. 5B). In Übereinstimmung damit liegt in THR eine Bindungsstelle für PIM. In *D. melanogaster* hat PIM jedoch eine zweite Bindungsstelle in SSE. Neuere Ergebnisse haben bestätigt, dass das Securin in anderen Organismen ebenfalls eine zweite Bindungsstelle im C-Terminus der Separase besitzt (Hornig et al., 2002). Dieselbe Untersuchung hat außerdem gezeigt, dass zur Aktivierung der Separase aus *S. cerevisiae* eine intramolekulare Wechselwirkung zwischen den N- und C-terminalen Domänen erforderlich ist (Abb. 5B). Dies entspräche der bereits vorgeschlagenen, aktivierenden Wechselwirkung zwischen THR und SSE (Abb. 5A).

Der Vergleich zu anderen Organismen lässt vermuten, dass *thr* und *Sse* im Laufe der Evolution durch eine Genspaltung aus einem ursprünglichen *Separase*-Gen hervorgegangen sind. Daraus ergab sich die Frage welche funktionelle Bedeutung der Aufteilung der Separase auf zwei unabhängige Untereinheiten zukommt.

5.3 Mitotische Spaltung der THR-Untereinheit

Unter der Annahme, dass THR eine regulatorische Untereinheit des Separase-Komplexes sein könnte, wurde zunächst die Stabilität von THR während der Zellteilung untersucht. Dazu wurden zwei experimentelle Ansätze verfolgt.

Auf der einen Seite wurden Immunfluoreszenz-Färbungen an *D. melanogaster* Embryonen durchgeführt. Die Embryonen wurden in einem Entwicklungsstadium fixiert, in dem die Zellteilung in einem reproduzierbaren räumlichen und zeitlichen Muster stattfindet. Die Zellen dieser fixierten Embryonen befinden sich daher in verschiedenen Stadien des Zellteilungszyklus. Vor der Mitose verfügen diese Zellen über hohe Mengen an Cyclin B, eines der mitotischen Cycline in *D. melanogaster*. In der Mitose wird Cyclin B am Metaphasen-Anaphasen-Übergang degradiert. In Zellen unmittelbar nach der Mitose ist Cyclin B nicht nachweisbar. Durch die Immunfluoreszenz-Färbung von Cyclin B wird also erkennbar welche Zellen die Mitose durchlaufen haben (Teilarbeit C, Fig. 1B,D). Durch eine Doppelmarkierung von Cyclin B und THR-myc konnte gezeigt werden, dass THR-myc ebenfalls degradiert wird, wenn Zellen die Mitose durchlaufen (Teilarbeit C, Fig. 1A,B). Die Degradation von THR-myc ist jedoch weniger vollständig als der Abbau von Cyclin B. Während der Mitose können die einzelnen Stadien durch Fluoreszenz-Markierung der DNA identifiziert werden. Dabei wurde deutlich, dass THR-myc erst beim Austritt aus der Mitose degradiert wird, und nicht am Metaphasen-Anaphasen-Übergang wie Cyclin B (Teilarbeit C, Fig. 1F).

Auf der anderen Seite wurde die Stabilität von THR durch Immuno-Blotting analysiert. Dafür wurden Embryonen in einem früheren Entwicklungsstadium verwendet als für die Immunfluoreszenz-Färbungen. Während dieser frühen Entwick-

lung befinden sich die Zellkerne der Embryonen in einem Synzytium und fast alle Zellkerne durchlaufen den Zellzyklus synchron. Embryonen während dieser synzytialen Kernteilungen wurden fixiert und anhand einer DNA-Markierung nach Zellzyklus-Stadien sortiert. Aus diesen Embryonen wurden Proteinextrakte hergestellt und durch Immuno-Blotting analysiert. Als überraschendes Ergebnis zeigte dieses Experiment, dass sowohl THR als auch THR-myc nach dem Metaphasen-Anaphasen-Übergang proteolytisch gespalten werden (Teilarbeit C, Fig 1H). Die Abundanz des Spaltprodukts nimmt nach der Telophase bis zur nächsten Metaphase kontinuierlich ab. Die synchronen Kernteilungen verlaufen mit 6-12 min pro Zyklus sehr schnell (Foe und Alberts, 1983) und daher zeigt dieses Experiment, dass die nachgewiesenen Spaltprodukte von THR und THR-myc instabil sind.

Durch Immuno-Blotting wurde jeweils nur ein Spaltprodukt von THR oder THR-myc nachgewiesen. Die polyklonalen Antikörper gegen THR sind gegen C-terminale Epitope gerichtet, und die myc-Epitope in THR-myc sind am C-Terminus von THR lokalisiert. Daher beinhaltet das nachgewiesene Spaltprodukt den C-Terminus von THR. Das N-terminale Spaltprodukt konnte in diesen Experimenten nicht nachgewiesen werden. Epitop-Markierungen am N-Terminus von THR bewirken einen Funktionsverlust von THR und verhindern die Spaltung von THR (Daten nicht gezeigt). Daher liegen keine Informationen über die Stabilität des N-terminalen Spaltprodukts vor. Für die Immunfluoreszenz-Färbung wurde ein Antikörper gegen die myc-Epitope von THR-myc verwendet. Daher wurde hier ebenfalls das instabile, C-terminale Spaltprodukt von THR-myc nachgewiesen. Es ist daher anzunehmen, dass der Abbau von THR-myc am Austritt aus der Mitose die Lebensdauer des C-terminalen Spaltprodukts widerspiegelt.

5.4 THR-Spaltung durch Separase-Aktivität

Zur Identifikation der Protease, die für die Spaltung von THR verantwortlich ist, wurde zunächst die Spaltstelle in THR charakterisiert. Die Position der Spaltstelle wurde durch den Vergleich der gelelektrophoretischen Mobilität des C-terminalen Spaltprodukts mit *in vitro* translatierten THR Fragmenten auf einige Aminosäuren genau festgelegt. (Teilarbeit C, Fig. 2A). In dieser Region von THR befindet sich die Aminosäure-Sequenz 1031 VEPIRKQ 1037. Diese Sequenz ist in THR-Proteinen aus verschiedenen *Drosophila*-Spezies konserviert, obwohl *thr* ein schnell evolvierendes Gen ist (H. Jäger, C. F. Lehner, S. Heidmann, unveröffentlichte Ergebnisse). Außerhalb dieser Sequenz existiert nur ein Protein-Bereich in THR, der vergleichbar konserviert ist. Die Sequenz 1031 VEPIRKQ 1037 entspricht dem Konsensus einer Separase-Spaltstelle. Aus der Analyse verschiedener Separase-Spaltstellen ging hervor, dass ein D/ExxR Motiv essentiell für die Spaltung durch die Separase ist. Die Spaltung erfolgt dabei unmittelbar C-terminal

des Arginin-Restes. Ein Austausch dieses Arginin-Restes gegen Asparaginsäure oder Alanin unterbindet die Separase-abhängige Spaltung in Scc1 (Uhlmann et al., 1999; Hauf et al., 2001; Waizenegger et al., 2002). Daraus ergab sich die Vermutung, dass die Spaltung der THR-Untereinheit durch die Separase selbst erfolgt. Um diese Vermutung zu überprüfen wurde die vermeintliche Spaltstelle in THR-myc inaktiviert. Dies wurde einerseits durch eine Deletion der Sequenz 1031 VEPIRKQ 1037 ($THR^{\Delta VQ}$-myc) und andererseits durch den Austausch von Arginin 1035 gegen Asparaginsäure (THR^{RD}-myc) erreicht (Teilarbeit C, Fig. 2B). Beide THR-Varianten werden nach dem Metaphasen-Anaphasen-Übergang nicht mehr gespalten (Teilarbeit C, Fig. 2C,D). Dieses Ergebnis weist darauf hin, dass THR durch die katalytische Untereinheit der Separase gespalten wird.

Wenn die katalytische SSE-Untereinheit der Separase für die mitotische Spaltung von THR verantwortlich ist, sollte THR stabilisiert werden sobald keine Separase-Aktivität mehr vorhanden ist. Eine Inaktivierung der Separase wurde durch zwei experimentelle Ansätze erhalten. Zum einen wurden Embryonen mit dem Spindelgift Demecolcin behandelt, wodurch der „spindle assembly checkpoint“ ausgelöst wird. Zum anderen wurden *pim*-Mutanten untersucht, in denen die Schwesterchromatiden-Trennung ausbleibt und die Separase vermutlich inaktiv bleibt. In beiden Fällen wird THR-myc stabilisiert (Teilarbeit C, Fig. 3). Diese Resultate sind konsistent damit, dass die Spaltung der THR-Untereinheit durch die SSE-Untereinheit erfolgt.

Um weiter zu überprüfen ob die katalytische Aktivität der Separase direkt für die Spaltung der THR-Untereinheit verantwortlich ist, wurden THR-Deletionsvarianten untersucht. Diese Varianten, THR 445-1379-myc und THR 1-1204-myc, wurden durch die Transgene *gthr445-1379-myc* und *gthr1-1204-myc* in *D. melanogaster* exprimiert. THR 445-1379-myc und THR 1-1204-myc assoziieren mit der SSE-Untereinheit (Teilarbeit B, Fig. 5C und Daten nicht gezeigt). In genetischen Komplementations-Tests wurde jedoch gezeigt, dass keines der beiden Transgene in der Lage ist einen Funktionsverlust von *thr* zu ersetzen (Daten nicht gezeigt). Daraus folgt, dass die SSE-Untereinheit im Komplex mit diesen Deletionsvarianten vermutlich inaktiv ist. THR 445-1379-myc und THR 1-1204-myc beinhalten die wildtypische THR-Spaltstelle. Es wurde untersucht ob THR 445-1379-myc und THR 1-1204-myc nach dem Metaphasen-Anaphasen-Übergang gespalten werden. Beide THR-Deletionsvarianten werden in der Mitose stabilisiert (Teilarbeit C, Fig. 4). Die Expression der THR-Deletionsvarianten erfolgte in einem wildtypischen Hintergrund. Daher waren in diesen Experimenten, neben den durch die Deletionsvarianten inaktivierten Separase-Komplexen, auch funktionelle Separase-Komplexe vorhanden. Diese Resultate legen also nahe, dass die Spaltung

der THR-Untereinheit nur innerhalb eines Separase-Komplexes, durch die direkt assoziierte SSE-Untereinheit, erfolgt.

Die Charakterisierung von Mutationen in der THR Spaltstelle, sowie die Abhängigkeit der THR Spaltung von Separase-Aktivität, sind deutliche Hinweise dafür, dass die THR-Untereinheit der Separase ein Substrat der SSE-Untereinheit ist. Das C-terminale THR-Spaltprodukt wird nach der Spaltung rasch degradiert. In Analogie zu den Scc1-Spaltprodukten aus *S. cerevisiae*, könnte das durch den Ubiquitin-abhängigen „N-end-rule“ Mechanismus geschehen (Rao et al., 2001). Konsistent mit dieser Vermutung läßt sich aus der Sequenz der THR-Spaltstelle schließen, dass das C-terminale Spaltprodukt mit einem Lysin-Rest beginnt, welcher nach der „N-end-rule“ destabilisierend wirkt (Varshavsky, 1996).

5.5 Expression von nicht spaltbaren THR-Varianten

Die THR-Untereinheit ist eine essentielle Komponente des Separase-Komplexes. Daher lag die Vermutung nahe, dass die Spaltung der THR-Untereinheit einen Einfluss auf die Funktion der Separase hat. Zunächst wurde geklärt ob die THR-Spaltung für einen bestimmten biologischen Prozess benötigt wird. Darauf aufbauend wurde untersucht ob die Spaltung der THR-Untereinheit zur Regulation der Separase beiträgt.

Amorphe Mutationen in *thr* führen zu Letalität. Die nicht spaltbaren THR-Varianten wurden durch Transgene in *D. melanogaster* eingebracht, welche die regulatorischen Genbereiche von *thr* enthalten (*gthr*$^{\Delta VQ}$*-myc* und *gthr*RD*-myc*). Durch beide Transgene wird die Letalität von amorphen *thr*-Mutationen aufgehoben. Das bedeutet, dass THR$^{\Delta VQ}$-myc und THRRD-myc funktionsfähige THR-Varianten sind. Die Spaltung von THR ist also unter optimalen Bedingungen nicht essentiell.

Die Spaltung von THR wird jedoch essentiell, wenn die Kulturtemperatur von 25°C auf 18°C gesenkt wird. Unter diesen Bedingungen führt die Expression von THR$^{\Delta VQ}$-myc oder THRRD-myc zu embryonaler Letalität. Die Expression von THR-myc hat unter diesen Bedingungen keinen Effekt. Interessanterweise ist die Expression von THR$^{\Delta VQ}$-myc oder THRRD-myc auch dann letal, wenn gleichzeitig spaltbares THR-Protein vorhanden ist.

In Temperatur-Wechsel-Experimenten wurde die Entwicklungsphase bestimmt, in der die Expression von THR$^{\Delta VQ}$-myc und THRRD-myc Letalität hervorruft. Es stellte sich heraus, dass die Expression von nicht spaltbaren THR-Varianten nur während der frühen Phase der Embryogenese zu Letalität führt. Spätere Stadien der Embryogenese und die Larven-Entwicklung sind auch bei 18°C nicht betroffen (Teilarbeit C, Fig. 5A und Daten nicht gezeigt).

In *D. melanogaster* findet in den frühen Stadien der Embryogenese keine Transkription statt, und der Embryo ist auf Proteine und mRNA angewiesen, die durch die Mutter im Ei abgelegt werden (maternale Kontribution). Daher hängt die Abundanz der meisten Proteine in dieser Phase der Embryogenese nicht vom Genotyp des Embryos, sondern vom Genotyp der Mutter ab. Es wurde gefunden, dass in den Müttern zwei Kopien der Transgene für nicht spaltbares THR erforderlich sind, um in den Nachkommen Letalität hervorzurufen. Eine Kopie des *gthr*$^{\Delta VQ}$-*myc* Transgens in den Müttern bleibt ohne Wirkung auf das Überleben der Nachkommen (Teilarbeit C, Fig. 5A). Daraus folgt, dass die Letalität außer von der Temperatur auch von der Abundanz von nicht spaltbarem THR abhängig ist. Im Folgenden werden Embryonen, die von Müttern mit zwei Kopien der Transgene *gthr*$^{\Delta VQ}$*-myc* oder *gthr*RD*-myc* abstammen, der Übersichtlichkeit halber als THR$^{\Delta VQ}$- und THRRD-Embryonen bezeichnet.

Nachdem die temperatursensitive Phase in der Entwicklung von THR$^{\Delta VQ}$- und THRRD-Embryonen bestimmt war, wurde untersucht welche Schäden durch die Expression von nicht spaltbaren THR-Varianten hervorgerufen werden. Die temperatursensitive Entwicklungsphase zeichnet sich durch Prozesse aus, die in späteren Stadien nicht ablaufen. Zu Beginn der Embryogenese finden 13 schnelle Kernteilungszyklen statt. Die Kernteilungen sind nicht von Zytokinese begleitet und führen daher zu einem Synzytium. Im Verlauf der synzytialen Kernteilungen wandern die Zellkerne an die Peripherie des Embryos. Dort bilden sie schließlich eine Schicht von Zellkernen. Im Prozess der Zellularisierung werden diese Zellkerne mit Zellmembranen umgeben. Dadurch wird ein einschichtiges zelluläres Epithel gebildet, das zelluläre Blastoderm. THR$^{\Delta VQ}$- und THRRD-Embryonen weisen bei 18°C sowohl in den synzytialen Kernteilungen als auch in der Zellularisierung Defekte auf. Beide Prozesse sind jedoch in unterschiedlichem Ausmaß betroffen.

Die synzytialen Kernteilungen sind nur schwach betroffen. In fixierten Embryonen wurden vielgestaltige Abnormalitäten gefunden. Einzelne Kerne scheinen in der Proliferation gestört zu sein und eliminiert zu werden (Teilarbeit C). Die Elimination von Zellkernen scheint in synzytialen Embryonen einen allgemeinen Mechanismus darzustellen, um Kerne nach fehlerhaften Replikations- oder Teilungs-Ereignissen an der weiteren Proliferation zu hindern.

Ein ausgeprägter und starker Defekt wurde während der Zellularisierung bei 18°C gefunden. In mindestens 98% der THR$^{\Delta VQ}$- oder THRRD-Embryonen verläuft die Zellularisierung fehlerhaft (Teilarbeit C). An fixierten THR$^{\Delta VQ}$- und THRRD-Embryonen wurde gezeigt, dass die Zellularisierung nicht wie im Wildtyp zur Bildung eines Epithels führt, sondern viele Zellkerne im Innern des Embryos akkumulieren (Teilarbeit C, Fig. 5B,C). Um die Zellularisierung auch in lebenden Embryonen verfolgen zu können wurde in THR$^{\Delta VQ}$-Embryonen eine mit GFP markierte

Histon-Variante exprimiert. In diesen Embryonen wurde das Chromatin der Zellkerne durch zeitaufgelöste Mikroskopie verfolgt. Dabei wurde beobachtet, wie sich Zellkerne von der Peripherie des Embryos lösen und internalisiert werden. Dieser Vorgang setzt deutlich nach der letzten Kernteilung des synzytialen Embryos ein, etwa zu dem Zeitpunkt, an dem die Zellularisierung beginnt. Diese *in vivo* Analysen haben außerdem gezeigt, dass die Zellularisierung defekt ist, obwohl die vorhergehende Kernteilung scheinbar normal durchlaufen wird. Daher ist der Zellularisierungsdefekt in $THR^{\Delta VQ}$- und THR^{RD}-Embryonen vermutlich keine Folge von früheren Defekten (Daten nicht gezeigt).

Nachdem die Zellularisierung als der biologische Prozess mit den schwerwiegendsten Defekten in $THR^{\Delta VQ}$- und THR^{RD}-Embryonen identifiziert war, wurden diese Defekte auf zellulärer Ebene charakterisiert. Der Beginn der Zellularisierung ist durch die Invagination von Zellmembranen gekennzeichnet. Die Invagination beginnt am Kortex des Embryos, setzt sich ins Innere des Embryos fort, und schließt die Zellkerne dabei ein. Die Membran-Invagination kann durch Immunfluoreszenz-Färbung des *D. melanogaster* β-Catenin-Homologs Armadillo verfolgt werden (Teilarbeit C, Fig. 5D-F, siehe auch Hunter und Wieschaus, 2000). Eine entsprechende Markierung an $THR^{\Delta VQ}$-Embryonen legt nahe, dass der Beginn der Membran-Invagination verzögert ist, und gleichzeitig damit die Internalisierung der Zellkerne beginnt (Teilarbeit C, Fig. 5G-J). Ein weiterer Aspekt des Zellularisierungsdefekts konnte durch die Immunfluoreszenz-Färbungen von α-Tubulin und γ-Tubulin aufgedeckt werden (Teilarbeit C, Fig. 5K-R). Danach ist die Internalisierung der Kerne mit einem Verlust des Kontakts der Kerne zum Tubulin-Zytoskelett verbunden (Teilarbeit C, Pfeilspitzen in Fig. 5Q-R). Das Tubulin-Zytoskelett wird im Wildtyp ausgehend von einem am Kortex verankerten Zentrosomenpaar organisiert und umschließt normalerweise die jeweils darunterliegenden Kerne. Die Funktion der Zentrosomen scheint in $THR^{\Delta VQ}$-Embryonen ebenfalls betroffen zu sein. Die Zentrosomen zeigen eine reduzierte Assoziation mit γ-Tubulin und einen Defekt in der Zentrosomen-Separation (Teilarbeit C, Pfeile in Fig. 5O, vergleiche Fig. 5K).

Zusammengefasst hat die Untersuchung von nicht spaltbaren THR-Varianten gezeigt, dass die Spaltung von THR bei erniedrigter Temperatur essentiell ist. Diese essentielle Funktion beschränkt sich auf die frühe Phase der Embryonalentwicklung. Eine detaillierte Analyse hat gezeigt, dass besonders in der Zellularisierung drastische Defekte ausgelöst werden. Es konnte gezeigt werden, dass nicht spaltbares THR verantwortlich für Schäden in der Organisation des Tubulin-Zytoskeletts ist. Die Verzögerung der Membran-Invagination ist möglicherweise eine Folge dieser Schäden, denn es ist bekannt, dass die Invagination der Membranen abhängig von der Funktion des Tubulin-Zytoskeletts ist (Lecuit und Wie-

schaus, 2000). Diese Ergebnisse waren überraschend, da bislang keine Funktion von THR, PIM und SSE in der Zellularisierung oder der Organisation des Tubulin-Zytoskeletts bekannt war.

5.6 Regulatorische Funktion der THR-Spaltung

Die Expression von nicht spaltbarem THR könnte eine Fehlregulation der Separase zur Folge haben. Prinzipiell könnte der Zellularisierungsdefekt in $THR^{\Delta VQ}$-Embryonen durch eine erhöhte oder eine erniedrigte Separase-Aktivität ausgelöst werden. Wenn nicht spaltbares THR eine erhöhte Separase-Aktivität zur Folge hätte, dann sollte die experimentelle Erniedrigung der Separase-Aktivität zu einer Suppression des Zellularisierungsdefekts führen. Im umgekehrten Fall sollte eine Erniedrigung der Separase-Aktivität zu einer Verstärkung des Zellularisierungsdefekts führen.

Durch Einkreuzen einer *Sse*-Mutation konnte in $THR^{\Delta VQ}$-Embryonen die Menge der katalytischen SSE-Untereinheit der Separase um etwa die Hälfte verringert werden. Als Ergebnis daraus wird der Zellularisierungsdefekt fast vollständig unterdrückt (Teilarbeit C, Fig. 6B). Dieses Experiment gibt einen Hinweis darauf, dass der Zellularisierungsdefekt durch eine erhöhte Aktivität der Separase ausgelöst wird.

Um zweifelsfrei zu zeigen, dass der Zellularisierungsdefekt von der katalytischen Aktivität der Separase abhängig ist und nicht nur von der Menge an SSE-Protein, wurde ein weiteres Experiment durchgeführt. Dabei wurde in $THR^{\Delta VQ}$-Embryonen die Menge an endogenem SSE-Protein durch eine *Sse*-Mutation gesenkt und gleichzeitig funktionelles SSE-Protein (HA-SSE) oder katalytisch inaktives SSE-Protein ($HA\text{-}SSE^{C497S}$) durch geeignete Transgene überexprimiert. Durch die Expression der funktionsfähigen SSE-Untereinheit wurde der Zellularisierungsdefekt wiederhergestellt. Durch die Expression der katalytisch inaktiven SSE-Untereinheit wurde der Zellularisierungsdefekt nicht wiederhergestellt (Teilarbeit C, Fig. 6C). HA-SSE und $HA\text{-}SSE^{C497S}$ wurden in diesem Experiment gleich stark exprimiert. Daher kann geschlossen werden, dass spezifisch die katalytische Aktivität der SSE-Untereinheit erforderlich ist damit $THR^{\Delta VQ}$-myc die Zellularisierung stören kann. Der Zellularisierungsdefekt ist dementsprechend abhängig von Separase-Aktivität und auf eine erhöhte Aktivität der Separase zurückzuführen. Da die Expression von nicht spaltbarem THR demnach zu einer Überaktivierung der Separase führt, liegt die eigentliche Funktion der THR-Spaltung in der Inaktivierung der Separase.

5.7 Modell der Separase-Regulation durch THR-Spaltung

Die Ergebnisse dieser Teilarbeit können in einem Modell zusammengefasst werden, dessen Kernaussage die Selbstinaktivierung der *D. melanogaster* Separase durch die Spaltung der THR-Untereinheit ist (Abb. 6A).

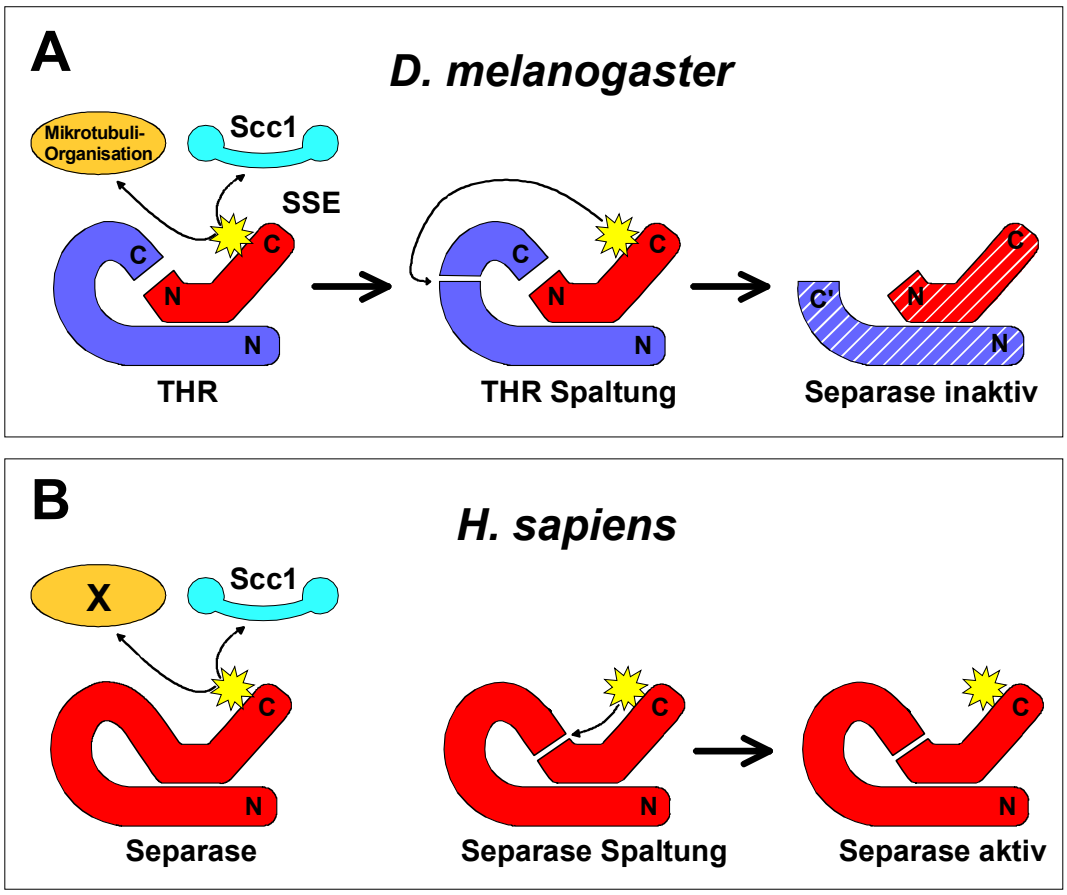

Abbildung 6: Modell für die Regulation der Separase-Aktivität durch Proteolyse.

(*A*) Der aktivierte Separase-Komplex ist in *D. melanogaster* für die Spaltung von Scc1 und anderer Substrate verantwortlich, die für die Regulation der Mikrotubuli-Organisation benötigt werden. Die Spaltung der THR-Untereinheit wird durch die SSE-Untereinheit katalysiert und führt zur Inaktivierung der Separase. Das C-terminale Spaltprodukt der THR-Untereinheit wird degradiert und es entsteht ein neuer C-Terminus von THR (C').
(*B*) Die aktivierte Separase aus *H. sapiens* besitzt neben Scc1 möglicherweise ebenfalls weitere Substrate (angedeutet durch X). Nach der autoproteolytischen Spaltung der humanen Separase bleiben die Spaltprodukte miteinander assoziiert und unverändert aktiv. Es ist unklar ob die Selbstspaltung der Separase vor oder nach der Spaltung anderer Substrate stattfindet. Daher sind in dieser Darstellung beide Vorgänge nicht durch einen Pfeil verbunden.

In einem *in vitro* Assay konnte gezeigt werden, dass auch die Separase aus *H. sapiens* autoproteolytisch gespalten wird (Waizenegger et al., 2000, siehe auch Abb. 5B). Es wurden Versuche unternommen analog zu diesem Assay die Spaltung der THR-Untereinheit *in vitro* durchzuführen. Aus unbekannten Gründen konnte in diesem Assay jedoch keine Spaltung der THR-Untereinheit nachgewiesen werden (Daten nicht gezeigt). Wie bereits erwähnt, konnte *in vitro* auch keine Spaltung von *D. melanogaster* Scc1 erreicht werden. Beide Resultate sind konsi-

stent damit, dass der Separase-Komplex aus *D. melanogaster in vitro* nicht durch die Degradation des Securins aktiviert werden konnte.

Bislang konnte nur im Menschen und in *D. melanogaster* gezeigt werden, dass die Separase autoproteolytisch gespalten wird. Für die Separasen aus *S. cerevisiae* und *S. pombe* liegen keine Hinweise auf eine mitotische Spaltung vor. Unter der Annahme, dass die THR-Untereinheit dem nicht konservierten N-Terminus der anderen Separasen entspricht, lässt sich die Position der Spaltstelle aus der humanen Separase auf ein hypothetisches THR-SSE-Fusionsprotein übertragen. Danach müsste die Spaltung nicht in der THR-Untereinheit, sondern innerhalb des N-Terminus der SSE-Untereinheit erfolgen. Die mitotische Stabilität von SSE wurde untersucht, aber es wurden keine Hinweise für eine Spaltung von SSE gefunden (Daten nicht gezeigt). Mittlerweile konnte demonstriert werden, dass die Spaltung der humanen Separase nicht für die Aktivierung der Separase benötigt wird, jedoch auch nicht unmittelbar zur Inaktivierung der Separase führt (Stemmann et al., 2001; Waizenegger et al., 2002). Da diese Ergebnisse aus einem *in vitro* System stammen, ist die physiologische Relevanz der Separase-Spaltung im Menschen immer noch unklar. Auch wenn in *D. melanogaster* direkte biochemische Evidenzen fehlen, belegen die hier dargestellten Ergebnisse, dass die THR-Untereinheit *in vivo* ein Substrat der Separase ist und diese Spaltung unter physiologischen Bedingungen zur Inaktivierung der Separase beiträgt.

Da die Inaktivierung der Separase autoproteolytisch ist, muss die Spaltung der THR-Untereinheit zeitlich reguliert sein. Nach der Aktivierung des Separase-Komplexes muss ein Zeitfenster existieren, in dem die Separase essentielle Substrate wie Scc1 spalten kann, bevor die Spaltung der THR-Untereinheit zur Inaktivierung der Separase führt. Es ist unklar wie diese sukzessive Spaltung verschiedener Substrate erreicht wird. Eine einfache Möglichkeit wäre, dass die Kinetik der unterschiedlichen Spaltungsreaktionen verschieden ist. Eine schnelle und effiziente Spaltung anderer Substrate, könnte in Kombination mit einer langsamen Spaltung der THR-Untereinheit, das erforderliche Zeitfenster von Separase-Aktivität erzeugen. Alternativ könnte die Spaltung von THR abhängig von der Proteolyse anderer Substrate sein, indem sie beispielsweise durch Spaltprodukte dieser Substrate reguliert wird.

Eine weitere Frage ist, warum die Spaltung der THR-Untereinheit zur Inaktivierung der Separase führt. Nach der Spaltung von THR entsteht ein N-terminales Spaltprodukt (Aminosäuren 1-1035) und ein C-terminales Spaltprodukt (Aminosäuren 1036-1379). Die Deletionsvarianten THR 1-930-myc und THR 1-1204-myc binden vergleichbar mit THR-myc an PIM und SSE, sie sind jedoch nicht funktionell (Teilarbeit B, Fig. 5C und Daten nicht gezeigt). Daraus folgt, dass der C-Terminus von THR eine essentielle Funktion hat, die unabhängig von der Bindung an PIM und SSE ist. Diese essentielle Funktion ist in dem Teil von THR lokalisiert,

welcher in das instabile C-terminale Spaltprodukt von THR übergeht. Die Domänen für die Interaktion mit PIM und SSE liegen dagegen im N-terminalen Spaltprodukt. Es ist daher anzunehmen, dass nach der Spaltung der THR-Untereinheit das C-terminale Spaltprodukt aus dem Separase-Komplex dissoziiert und damit eine essentielle Funktion der Separase verloren geht (Abb. 6A). Dieser Überlegung zufolge würde die Spaltung der THR-Untereinheit eine sehr schnelle Inaktivierung der Separase ermöglichen. Alternativ wäre denkbar, dass erst die Degradation des C-terminalen Spaltprodukts zur Inaktivierung der Separase führt. In jedem Fall scheint jedoch der Verlust des C-terminalen THR-Spaltprodukts, entweder durch Degradation oder Dissoziation, zur Inaktivierung der Separase zu führen. Es ist nicht bekannt welche Funktion der C-Terminus der THR-Untereinheit übernimmt. Diese Frage wird jedoch gegenwärtig bearbeitet.

Die Konsequenzen der Expression von nicht spaltbarem THR sind überraschend mild. Die THR-Spaltung ist selbst bei 18°C nur während der frühembryonalen Entwicklung essentiell. Es ist jedoch anzunehmen, dass auch während späteren Stadien der Entwicklung die Separase nach dem Austritt aus der Mitose inaktiviert werden muss. Als Folge von Separase-Aktivität während der Interphase sollte es zu einer ektopischen Spaltung von Scc1 kommen und damit zu Defekten in der Schwesterchromatiden-Kohäsion. In verschiedenen Organismen konnte gezeigt werden, dass der Verlust der Schwesterchromatiden-Kohäsion zu Defekten in der Mitose führt (Tanaka et al., 2000; Sonoda et al., 2001; Toyoda et al., 2002). Es ist daher wahrscheinlich, dass in *D. melanogaster* neben der Spaltung der THR-Untereinheit noch andere Mechanismen zur Inaktivierung der Separase existieren. Dazu zählt vermutlich die Bindung von neusynthetisiertem PIM an den Separase-Komplex, welches als Securin die Aktivität der Separase inhibieren kann. Die THR-Spaltung und die Bindung von PIM scheinen jedoch zwei funktionell verschiedene Wege zur Inhibition der Separase zu sein. Die Spaltung der THR-Untereinheit beginnt in der Mitose, zu einem Zeitpunkt an dem der APC/C die Degradation von PIM vermittelt. Die THR-Spaltung ist daher vermutlich für die negative Regulation der Separase in der Mitose erforderlich, während PIM diese Aufgabe in der Interphase erfüllt. Konsistent mit dieser Vermutung werden als Konsequenz der Expression von nicht spaltbarem THR mitotische Defekte während der schnellen synzytialen Kernteilungen gefunden. Diese Zyklen besitzen eine sehr kurze S-Phase und die Inaktivierung der Separase muss daher vermutlich schon in der Mitose erfolgen.

Ein überraschendes Resultat dieser Arbeit war, dass die Inaktivierung der Separase von Bedeutung für die Organisation des Tubulin-Zytoskeletts während der Zellularisierung ist. Dieses Ergebnis zeigt, dass die Separase-Aktivität in *D. melanogaster* auch in anderen Prozessen als der Schwesterchromatiden-Trennung reguliert werden muss. In *S. cerevisiae* wurde gezeigt, dass die Separase für Or-

ganisation der Spindel-Mikrotubuli in der Anaphase benötigt wird (Uhlmann et al., 2000; Jensen et al., 2001). Mit Slk19 konnte in *S. cerevisiae* ein Substrat der Separase identifiziert werden, das für die Stabilität der Spindel in der Anaphase benötigt wird (Sullivan et al., 2001). Slk19 scheint auf der Ebene der Primärstruktur allerdings außerhalb von *S. cerevisiae* keine Homologe zu besitzen. In höheren Eukaryoten fehlten bislang Hinweise darauf, dass durch Substrate der Separase die Dynamik des Tubulin-Zytoskeletts reguliert wird. Die Ergebnisse dieser Arbeit lassen jedoch vermuten, dass solche Substrate auch in höheren Eukaryoten existieren. Die Expression von nicht spaltbaren THR-Varianten könnte durch die ektopische Spaltung solcher Substrate die Defekte am Tubulin-Zytoskelett bewirken. Damit könnte sich ebenfalls die Temperatursensitivität des Zellularisierungsdefekts erklären lassen, denn Mikrotubuli-abhängige Prozesse scheinen häufig kälteempfindlich zu sein (Brinkley und Cartwright, 1975; Rieder, 1981). Es ist bislang unklar warum die Spaltung von THR vor allem während der Zellularisierung benötigt wird. Es wäre möglich, dass die Zellularisierung besondere Anforderungen an das Tubulin-Zytoskelett stellt, die in anderen Stadien der Entwicklung nicht auftreten. Andererseits wäre denkbar, dass speziell während der Zellularisierung der Separase-Komplex nicht effizient durch die Bindung von PIM inhibiert werden kann. Die Zellularisierung findet zwar in der Interphase statt, die *pim*-mRNA wird jedoch während der Zellularisierung zum Teil abgebaut und daher sinkt vermutlich auch die Menge an PIM (Stratmann und Lehner, 1996).

Zusammengenommen hat diese Arbeit zwei wesentliche Ergebnisse erbracht. Zum einen wurde gezeigt, dass die Separase in *D. melanogaster*, im Gegensatz zu den Separasen anderer Organismen, aus zwei unabhängigen Untereinheiten aufgebaut ist. Zum anderen wurde mit der Spaltung der THR-Untereinheit ein neuer Mechanismus zur Inaktivierung der Separase identifiziert. Dieser Mechanismus ist von besonderer Bedeutung in einem insektenspezifischen Prozess. Im Menschen erfolgt ebenfalls eine proteolytische Spaltung der Separase. Beide Prozesse finden in der Mitose statt und sind von Separase-Aktivität abhängig. Der Mechanismus der mitotischen Separase-Selbstspaltung scheint also zwischen Mensch und *D. melanogaster* prinzipiell konserviert zu sein. In funktioneller Hinsicht jedoch unterscheiden sich die beide Vorgänge. Im Gegensatz zu *D. melanogaster* hat die Spaltung der humanen Separase keinen direkten Einfluss auf die Aktivität der Separase. In Übereinstimmung mit diesem funktionellen Unterschied, ist das Ergebnis der Separase-Selbstspaltung im Menschen und in *D. melanogaster* auch auf struktureller Ebene verschieden. Die Selbstspaltung der humanen Separase erzeugt zwei Fragmente, die miteinander assoziiert bleiben (Waizenegger et al., 2002). In *D. melanogaster* entsteht ein C-terminales THR-Fragment, das vermutlich aus dem Separase-Komplex dissoziieren kann. Der C-Terminus von THR hat eine essentielle Funktion in der Schwesterchromatiden-

Trennung, und daher ist die Dissoziation des C-terminalen THR-Fragments wahrscheinlich ursächlich für die Inaktivierung der Separase. Das C-terminale THR-Fragment entsteht jedoch nur deshalb, weil THR eine eigenständige Separase-Untereinheit darstellt (Abb. 6A). Es ist daher eine attraktive Spekulation, dass durch die Aufteilung der Separase in zwei unabhängige Untereinheiten die Separase-Selbstspaltung in *D. melanogaster* eine veränderte Funktion übernehmen konnte. Die Ergebnisse dieser Arbeit legen nahe, dass diese Funktion in der schnellen, Securin-unabhängigen Inaktivierung der Separase liegt.

6 Literaturverzeichnis

Alexandru, G., F. Uhlmann, K. Mechtler, M.A. Poupart und K. Nasmyth. 2001. Phosphorylation of the cohesin subunit Scc1 by Polo/Cdc5 kinase regulates sister chromatid separation in yeast. *Cell* **105**: 459-472.

Amon, A. 1999. The spindle checkpoint. *Curr Opin Genet Dev* **9**: 69-75.

Brinkley, B.R. und J. Cartwright, Jr. 1975. Cold-labile and cold-stable microtubules in the mitotic spindle of mammalian cells. *Ann N Y Acad Sci* **253**: 428-439.

Chen, L., R. Puri, E.J. Lefkowitz und S.S. Kakar. 2000. Identification of the human pituitary tumor transforming gene (hPTTG) family: molecular structure, expression, and chromosomal localization. *Gene* **248**: 41-50.

Ciosk, R., W. Zachariae, C. Michaelis, A. Shevchenko, M. Mann und K. Nasmyth. 1998. An ESP1/PDS1 complex regulates loss of sister chromatid cohesion at the metaphase to anaphase transition in yeast. *Cell* **93**: 1067-1076.

Cohen-Fix, O., J.M. Peters, M.W. Kirschner und D. Koshland. 1996. Anaphase initiation in Saccharomyces cerevisiae is controlled by the APC-dependent degradation of the anaphase inhibitor Pds1p. *Genes Dev* **10**: 3081-3093.

D'Andrea, R.J., R. Stratmann, C.F. Lehner, U.P. John und R. Saint. 1993. The *three rows* gene of *Drosophila melanogaster* encodes a novel protein that is required for chromosome disjunction during mitosis. *Mol Biol Cell* **4**: 1161-1174.

Foe, V.E. und B.M. Alberts. 1983. Studies of nuclear and cytoplasmic behaviour during the five mitotic cycles that precede gastrulation in Drosophila embryogenesis. *J Cell Sci* **61**: 31-70.

Funabiki, H., K. Kumada und M. Yanagida. 1996a. Fission yeast Cut1 and Cut2 are essential for sister separation, concentrate along the metaphase spindle and form large complexes. *EMBO J* **15**: 6617-6628.

Funabiki, H., H. Yamano, K. Kumada, K. Nagao, T. Hunt und M. Yanagida. 1996b. Cut2 proteolysis required for sister-chromatid separation in fission yeast. *Nature* **381**: 438-441.

Glotzer, M., A.W. Murray und M.W. Kirschner. 1991. Cyclin is degraded by the ubiquitin pathway. *Nature* **349**: 132-138.

Haering, C.H., J. Lowe, A. Hochwagen und K. Nasmyth. 2002. Molecular Architecture of SMC Proteins and the Yeast Cohesin Complex. *Mol Cell* **9**: 773-88.

Hauf, S., I.C. Waizenegger und J.M. Peters. 2001. Cohesin cleavage by separase required for anaphase and cytokinesis in human cells. *Science* **293**: 1320-1323.

Hershko, A., D. Ganoth, J. Pehrson, R.E. Palazzo und L.H. Cohen. 1991. Methylated ubiquitin inhibits cyclin degradation in clam embryo extracts. *J Biol Chem* **266**: 16376-16379.

Holloway, S.L., M. Glotzer, R.W. King und A.W. Murray. 1993. Anaphase is initiated by proteolysis rather than by the inactivation of maturation promoting factor. *Cell* **73**: 1393-1402.

Hornig, N.C., P.P. Knowles, N.Q. McDonald und F. Uhlmann. 2002. The dual mechanism of separase regulation by securin. *Curr Biol* **12**: 973-82.

Hunter, C. und E. Wieschaus. 2000. Regulated expression of nullo is required for the formation of distinct apical and basal adherens junctions in the Drosophila blastoderm. *J Cell Biol* **150**: 391-401.

Irniger, S., S. Piatti, C. Michaelis und K. Nasmyth. 1995. Genes involved in sister chromatid separation are needed for B-type cyclin proteolysis in budding yeast. *Cell* **81**: 269-278.

Jallepalli, P.V., I.C. Waizenegger, F. Bunz, S. Langer, M.R. Speicher, J.M. Peters, K.W. Kinzler, B. Vogelstein und C. Lengauer. 2001. Securin is required for chromosomal stability in human cells. *Cell* **105**: 445-457.

Jensen, S., M. Segal, D.J. Clarke und S.I. Reed. 2001. A novel role of the budding yeast separin Esp1 in anaphase spindle elongation: evidence that proper spindle association of Esp1 is regulated by Pds1. *J Cell Biol* **152**: 27-40.

Karsenti, E. und I. Vernos. 2001. The mitotic spindle: a self-made machine. *Science* **294**: 543-7.

Kumada, K., T. Nakamura, K. Nagao, H. Funabiki, T. Nakagawa und M. Yanagida. 1998. Cut1 is loaded onto the spindle by binding to Cut2 and promotes anaphase spindle movement upon Cut2 proteolysis. *Curr Biol* **8**: 633-641.

Lecuit, T. und E. Wieschaus. 2000. Polarized insertion of new membrane from a cytoplasmic reservoir during cleavage of the Drosophila embryo. *J Cell Biol* **150**: 849-60.

Losada, A., M. Hirano und T. Hirano. 1998. Identification of Xenopus SMC protein complexes required for sister chromatid cohesion. *Genes Dev* **12**: 1986-97.

Mei, J., X. Huang und P. Zhang. 2001. Securin is not required for cellular viability, but is required for normal growth of mouse embryonic fibroblasts. *Curr Biol* **11**: 1197-1201.

Michaelis, C., R. Ciosk und K. Nasmyth. 1997. Cohesins: Chromosomal proteins that prevent premature separation of sister chromatids. *Cell* **91**: 35-45.

Nasmyth, K. 2002. Segregating sister genomes: the molecular biology of chromosome separation. *Science* **297**: 559-65.

Peters, J.M. 2002. The anaphase-promoting complex: proteolysis in mitosis and beyond. *Mol Cell* **9**: 931-43.

Philp, A.V., J.M. Axton, R.D.C. Saunders und D.M. Glover. 1993. Mutations in the *Drosophila melanogaster* gene *three rows* permit aspects of mitosis to continue in the absence of chromatid segregation. *J Cell Sci* **106**: 87-98.

Rao, H., F. Uhlmann, K. Nasmyth und A. Varshavsky. 2001. Degradation of a cohesin subunit by the N-end rule pathway is essential for chromosome stability. *Nature* **410**: 955-959.

Rieder, C.L. 1981. The structure of the cold-stable kinetochore fiber in metaphase PtK1 cells. *Chromosoma* **84**: 145-158.

Sonoda, E., T. Matsusaka, C. Morrison, P. Vagnarelli, O. Hoshi, T. Ushiki, K. Nojima, T. Fukagawa, I.C. Waizenegger, J.M. Peters, W.C. Earnshaw und S. Takeda. 2001. Scc1/Rad21/Mcd1 is required for sister chromatid cohesion and kinetochore function in vertebrate cells. *Dev Cell* **1**: 759-70.

Stemmann, O., H. Zou, S.A. Gerber, S.P. Gygi und M.W. Kirschner. 2001. Dual inhibition of sister chromatid separation at metaphase. *Cell* **107**: 715-726.

Stratmann, R. und C.F. Lehner. 1996. Separation of sister chromatids in mitosis requires the *Drosophila pimples* product, a protein degraded after the metaphase anaphase transition. *Cell* **84**: 25-35.

Sullivan, M., C. Lehane und F. Uhlmann. 2001. Orchestrating anaphase and mitotic exit: separase cleavage and localization of Slk19. *Nat Cell Biol* **3**: 771-777.

Sumara, I., E. Vorlaufer, C. Gieffers, B.H. Peters und J.M. Peters. 2000. Characterization of vertebrate cohesin complexes and their regulation in prophase. *J Cell Biol* **151**: 749-62.

Sumara, I., E. Vorlaufer, P.T. Stukenberg, O. Kelm, N. Redemann, E.A. Nigg und J.M. Peters. 2002. The dissociation of cohesin from chromosomes in prophase is regulated by Polo-like kinase. *Mol Cell* **9**: 515-25.

Surana, U., A. Amon, C. Dowzer, J. McGrew, B. Byers und K. Nasmyth. 1993. Destruction of the CDC28/CLB mitotic kinase is not required for the metaphase to anaphase transition in budding yeast. *EMBO Journal* **12**: 1969-1978.

Tanaka, T., J. Fuchs, J. Loidl und K. Nasmyth. 2000. Cohesin ensures bipolar attachment of microtubules to sister centromeres and resists their precocious separation. *Nat Cell Biol* **2**: 492-9.

Tomonaga, T., K. Nagao, Y. Kawasaki, K. Furuya, A. Murakami, J. Morishita, T. Yuasa, T. Sutani, S.E. Kearsey, F. Uhlmann, K. Nasmyth und M. Yanagida. 2000. Characterization of fission yeast cohesin: essential anaphase proteolysis of Rad21 phosphorylated in the S phase. *Genes Dev* **14**: 2757-2770.

Toth, A., R. Ciosk, F. Uhlmann, M. Galova, A. Schleiffer und K. Nasmyth. 1999. Yeast cohesin complex requires a conserved protein, Eco1p(Ctf7), to establish cohesion between sister chromatids during DNA replication. *Genes Dev* **13**: 320-33.

Toyoda, Y., K. Furuya, G. Goshima, K. Nagao, K. Takahashi und M. Yanagida. 2002. Requirement of chromatid cohesion proteins rad21/scc1 and mis4/scc2 for normal spindle-kinetochore interaction in fission yeast. *Curr Biol* **12**: 347-58.

Tugendreich, S., J. Tomkiel, W. Earnshaw und P. Hieter. 1995. CDC27Hs colocalizes with CDC16Hs to the centrosome and mitotic spindle and is essential for the metaphase to anaphase transition. *Cell* **81**: 261-268.

Uhlmann, F., F. Lottspeich und K. Nasmyth. 1999. Sister-chromatid separation at anaphase onset is promoted by cleavage of the cohesin subunit Scc1. *Nature* **400**: 37-42.

Uhlmann, F. und K. Nasmyth. 1998. Cohesion between sister chromatids must be established during DNA replication. *Curr Biol* **8**: 1095-101.

Uhlmann, F., D. Wernic, M.A. Poupart, E.V. Koonin und K. Nasmyth. 2000. Cleavage of cohesin by the CD clan protease separin triggers anaphase in yeast. *Cell* **103**: 375-86.

Varshavsky, A. 1996. The N-end rule: functions, mysteries, uses. *Proc Natl Acad Sci U S A* **93**: 12142-12149.

Waizenegger, I.C., J.F. Gimenez-Abian, D. Wernic und J.-M. Peters. 2002. Regulation of Human separase by securin binding and autocleavage. *Curr Biol* **12**: 1368-78.

Waizenegger, I.C., S. Hauf, A. Meinke und J.M. Peters. 2000. Two distinct pathways remove mammalian cohesin from chromosome arms in prophase and from centromeres in anaphase. *Cell* **103**: 399-410.

Wang, Z., R. Yu und S. Melmed. 2001. Mice lacking pituitary tumor transforming gene show testicular and splenic hypoplasia, thymic hyperplasia, thrombocytopenia, aberrant cell cycle progression, and premature centromere division. *Mol Endocrinol* **15**: 1870-1879.

Warren, W.D., E. Lin, T.V. Nheu, G.R. Hime und M.J. McKay. 2000a. Drad21, a Drosophila rad21 homologue expressed in S-phase cells. *Gene* **250**: 77-84.

Warren, W.D., S. Steffensen, E. Lin, P. Coelho, M. Loupart, N. Cobbe, J.Y. Lee, M.J. McKay, T. Orr-Weaver, M.M. Heck und C.E. Sunkel. 2000b. The Drosophila RAD21 cohesin persists at the centromere region in mitosis. *Curr Biol* **10**: 1463-6.

Yamamoto, A., V. Guacci und D. Koshland. 1996. Pds1p, an inhibitor for faithful execution of anaphase in the yeast Saccharomyces cerevisiae. *J Cell Biol* **133**: 85-97.

Zou, H., T.J. McGarry, T. Bernal und M.W. Kirschner. 1999. Identification of a vertebrate sister-chromatid separation inhibitor involved in transformation and tumorigenesis. *Science* **285**: 418-422.

7 Anhang

Teilarbeit A

Darstellung des Eigenanteils an Teilarbeit A

Teilarbeit B

Darstellung des Eigenanteils an Teilarbeit B

Teilarbeit C

Darstellung des Eigenanteils an Teilarbeit C

Erklärung

Teilarbeit A

Degradation of *Drosophila* PIM regulates sister chromatid separation during mitosis.

Oliver Leismann, Alf Herzig, Stefan Heidmann and Christian F. Lehner

Genes and Development 14, 2192-2205 (2000).

Darstellung des Eigenanteils in Teilarbeit A

Das Ergebnis meiner Arbeit ist der Nachweis eines Proteinkomplexes, der PIM und THR enthält (Fig. 1). Außerdem ist in dieser Teilarbeit THR-myc beschrieben, die von mir hergestellte und charakterisierte Epitop-markierte THR-Variante.

Die anderen Ergebnisse dieser Teilarbeit wurden von Oliver Leismann erhalten.

Die Teilarbeit wurde von allen Autoren gemeinsam verfasst.

Degradation of *Drosophila* PIM regulates sister chromatid separation during mitosis

Oliver Leismann, Alf Herzig, Stefan Heidmann, and Christian F. Lehner[1]

Department of Genetics, University of Bayreuth, 95440 Bayreuth, Germany

Drosophila Pimples (PIM) and Three rows (THR) are required for sister chromatid separation in mitosis. PIM accumulates during interphase and is degraded rapidly during mitosis. This degradation is dependent on a destruction box similar to that of B-type cyclins. Nondegradable PIM with a mutant destruction box can rescue sister chromatid separation in *pim* mutants but only when expressed at low levels. Higher levels of nondegradable PIM, as well as overexpression of wild-type PIM, inhibit sister chromatid separation. Moreover, cells arrested in mitosis before sister chromatid separation (by colcemid or by mutations in *fizzy/CDC20*) fail to degrade PIM. Thus, although not related by primary sequence, PIM has intriguing functional similarities to the securin proteins of budding yeast, fission yeast, and vertebrates. Whereas these securins are known to form a complex with separins, we show that PIM associates in vivo with THR, which does not contain the conserved separin domain.

[*Key Words*: Mitosis; sister chromatid separation; securin; separin; *pimples*; *three rows*]

Received March 10, 2000; revised version accepted July 5, 2000.

Pairs of sister chromatids are generated during the S phase of the eukaryotic cell division cycle. Sister chromatids remain paired throughout the G2 phase and during the initial phase of mitosis (prophase) while chromatin is condensed and the spindle is assembled. However, the cohesion between sister chromatids is ultimately destroyed at the metaphase–anaphase transition allowing their segregation to opposite poles. Considerable progress has been made recently in understanding the molecular basis of cohesion and separation of sister chromatids (for review, see Zachariae and Nasmyth 1999; Nasmyth et al. 2000). Cohesion is known to be dependent on the binding of the cohesin protein complex to nascent sister chromatids during S phase (Guacci et al. 1997; Michaelis et al. 1997; Losada et al. 1998; Uhlmann and Nasmyth 1998; Blat and Kleckner 1999; Tanaka et al. 1999; Toth et al. 1999; Watanabe and Nurse 1999). Separation of sister chromatids in budding yeast mitosis requires the proteolytic processing of the cohesin subunit Scc1p/Mcd1p during the metaphase–anaphase transition (Uhlmann et al. 1999). In vertebrates, cohesin complexes dissociate from chromosomes already during prophase concomitant with chromatin condensation and well before the onset of sister chromatid separation (Losada et al. 1998; Darwiche et al. 1999). Moreover, Scc1p cleavage during prophase is not detectable in *Drosophila* (S. Heidmann, unpubl.). However, it is not excluded that residual cohesin complexes might persist in particular in the centromeric region of vertebrate chromosomes. The final separation of sister chromatids in higher eukaryotes, therefore, might also result from Scc1p cleavage during the metaphase–anaphase transition.

This hypothesis of a conserved mechanism of sister chromatid separation in eukaryotes is supported by findings concerning the role of the separin and securin proteins (Nasmyth et al. 2000). The separins (Esp1p, Cut1, BimB) were implicated originally in mitosis based on genetic analyses in fungi. Homologous genes have been detected recently in plant and animal species. All these separins share a conserved carboxy-terminal domain, the separin domain. The budding yeast separin Esp1p is known to be required for Scc1p cleavage and sister chromatid separation (Uhlmann et al. 1999). Separins are thought to be activated only during the metaphase–anaphase transition. Premature activation of separins is prevented by securin proteins that accumulate during interphase and bind to the separins. The budding yeast securin Pds1p forms a complex with Esp1p (Ciosk et al. 1998). The fission yeast securin Cut2 binds to Cut1 (Funabiki et al. 1996a; Yanagida 2000). In vertebrates, the protein encoded by the pituitary tumor transforming gene (PTTG) associates with a protein containing the conserved separin domain (Zou et al. 1999). All these securins (Pds1p, Cut2, PTTG) share essentially no sequence similarity except for the presence of at least one destruction box, a nine amino acid consensus motif [RX(A or V or L)LGXXXN] originally defined in B-type cyclins. Securins are therefore degraded

[1]**Corresponding author.**
E-MAIL chle@uni-bayreuth.de; FAX 49-921-55-2710.
Article and publication are at www.genesdev.org/cgi/doi/10.1101/gad.176700.

rapidly during the metaphase–anaphase transition like mitotic cyclins. Securin proteins with mutations in the destruction box fail to be degraded and inhibit sister chromatid separation in yeast and in *Xenopus* extracts (Cohen-Fix et al. 1996; Funabiki et al. 1996b, 1997; Zou et al. 1999).

Mitotic proteolysis of destruction box proteins occurs after polyubiquitination resulting from the activation of a special ubiquitin ligase known as anaphase-promoting complex/cyclosome (APC/C). APC/C activation, therefore, is a crucial step in the regulation of the metaphase–anaphase transition (for review, see Zachariae and Nasmyth 1999). This activation process is not yet fully understood. However, it is clear that the WD-40 repeat proteins Fizzy/Cdc20p and Fizzy-related/Hct1p/Cdh1p play important roles in APC/C regulation. These proteins bind to the APC/C in different cell cycle phases and respond to different regulatory inputs. While *Drosophila* Fizzy-related is known to be essential for the degradation of mitotic cyclins in G1, Fizzy is required for cyclin degradation and sister chromatid separation during mitosis (Sigrist et al. 1995; Sigrist and Lehner 1997). The dependency of sister chromatid separation on Cdc20p function has been explained in budding yeast by the finding that Cdc20p is required for the degradation of the securin Pds1p (Visintin et al. 1997; Lim et al. 1998; Shirayama et al. 1999). Fizzy/Cdc20p is inactivated in the presence of unattached kinetochores and spindle damage by a mitotic checkpoint pathway which results in the binding of the inhibitor Mad2p to the Fizzy/Cdc20p–APC/C complex (Chen et al. 1996; Fang et al. 1998; Hwang et al. 1998; Kallio et al. 1998; Kim et al. 1998; Alexandru et al. 1999; Waters et al. 1999; Zachariae and Nasmyth 1999). This checkpoint pathway therefore assures that sister chromatid separation and exit from mitosis occur only when all chromosomes have acquired the correct bipolar orientation within a functional spindle.

With the exception of securins, all the components involved in the control of sister chromatid separation that have been introduced above are highly conserved in eukaryotes. Interestingly, we have identified previously two nonconserved *Drosophila* genes, *pimples* (*pim*) and *three rows* (*thr*), which are both required specifically for sister chromatid separation during mitosis (D'Andrea et al. 1993; Stratmann and Lehner 1996). We show that the Pimples protein (PIM) shares extensive functional similarities with securin proteins and in particular with Cut2 from fission yeast. Moreover, we demonstrate that PIM is found in a complex with Three rows protein (THR). Our results indicate that the regulation of sister chromatid separation in *Drosophila* involves securin-like proteins that associate with proteins lacking the evolutionary conserved separin domain.

Results

PIM and THR are present in a complex

Neither PIM nor THR share significant sequence similarities with known proteins, and their biochemical function is not known. However, the indistinguishable phenotypes resulting from null mutations in *pim* and *thr* suggested that the corresponding gene products might function in a complex. Therefore, we analyzed PIM–THR complex formation by coimmunoprecipitation. Extracts were prepared from embryos carrying transgenes (*gpim–myc* or *gthr–myc*) allowing expression of either PIM protein with a carboxy-terminal extension of six myc epitope copies or THR protein with a carboxy-terminal extension of 10 myc epitope copies under the control of the corresponding genomic promoters. These myc-tagged proteins are functional because the transgenes can rescue *pim* and *thr* mutants, respectively. Anti-myc immunoprecipitates of PIM–myc were found to contain THR (Fig. 1). Conversely, immunoprecipitates of THR–myc contained PIM (Fig. 1). Control immunoprecipitates of CDK1–myc contained Cyclin B, as expected, but did not contain PIM or THR (Fig. 1), indicating that coimmunoprecipitation of PIM and THR is specific. Our coimmunoprecipitation experiments also indicated that the PIM–THR complex does not contain multiple copies of PIM and THR. In case of complexes with multiple copies, PIM–myc and THR–myc immunoprecipitates would be expected to contain wild-type PIM and THR, respectively. However, the products expressed from the endogenous loci were not coimmunoprecipitated by the myc-tagged transgene products (Fig. 1).

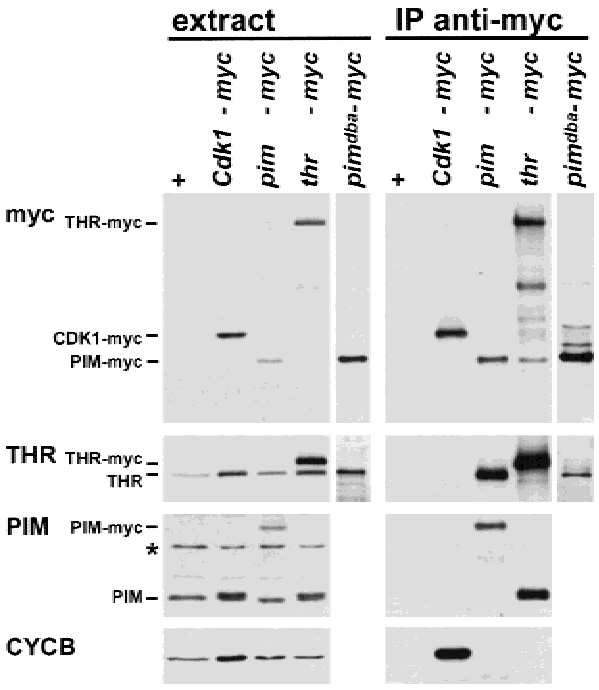

Figure 1. PIM and THR form a complex in vivo. Extracts (extract) prepared from embryos expressing either no transgene (+), or *Cdk1–myc* (*Cdk1–myc*), *gpim–myc* (*pim–myc*), *gthr–myc* (*thr–myc*), or pim^{dba}*–myc* (pim^{dba}*–myc*), as well as anti-myc immunoprecipitates isolated from these extracts (IP anti-myc), were analyzed by immunoblotting with antibodies against the myc epitope (myc), THR (THR), PIM (PIM), or Cyclin B (CYCB). (*) Crossreaction of the antibodies against PIM with an unknown protein.

Mitotic PIM degradation depends on a destruction box and is required for sister chromatid separation

By immunolabeling we have shown previously that PIM–myc is cleared from mitotic cells after the metaphase–anaphase transition similar to Cyclin B (Stratmann and Lehner 1996). The mitotic degradation of Cyclin B and other mitotic regulators is dependent on the presence of a destruction box motif in the amino-terminal region (Peters et al. 1998). *Drosophila* Cyclin B lacking this destruction box cannot be degraded during mitosis and blocks exit from mitosis (Rimmington et al. 1994; Sigrist et al. 1995; Fig. 2A–C). Although PIM does not have a motif that fits the RX(A or V or L)LGXXXN consensus sequence of mitotic destruction boxes (King et al. 1996; Peters et al. 1998; Zou et al. 1999), it contains the related sequence KKPLGNLDN. To determine whether this sequence variant can function as a destruction box, we expressed a mutant Cyclin B protein in *Drosophila* embryos that had this PIM motif instead of the Cyclin B destruction box. The PIM motif conferred mitotic instability indistinguishable from wild-type Cyclin B and did not result in a mitotic arrest (Fig. 2, cf. D–F with G–L). When the PIM motif was mutated from **KKPL**GNLD**N** to **A**KP**A**GNLD**A** (*dba*), it was no longer able to functionally replace the destruction box in Cyclin B (data not shown).

To determine whether the KKPLGNLDN sequence is required for PIM degradation during mitosis, we introduced the *dba* mutation into a *pim* transgene (*UAS–*

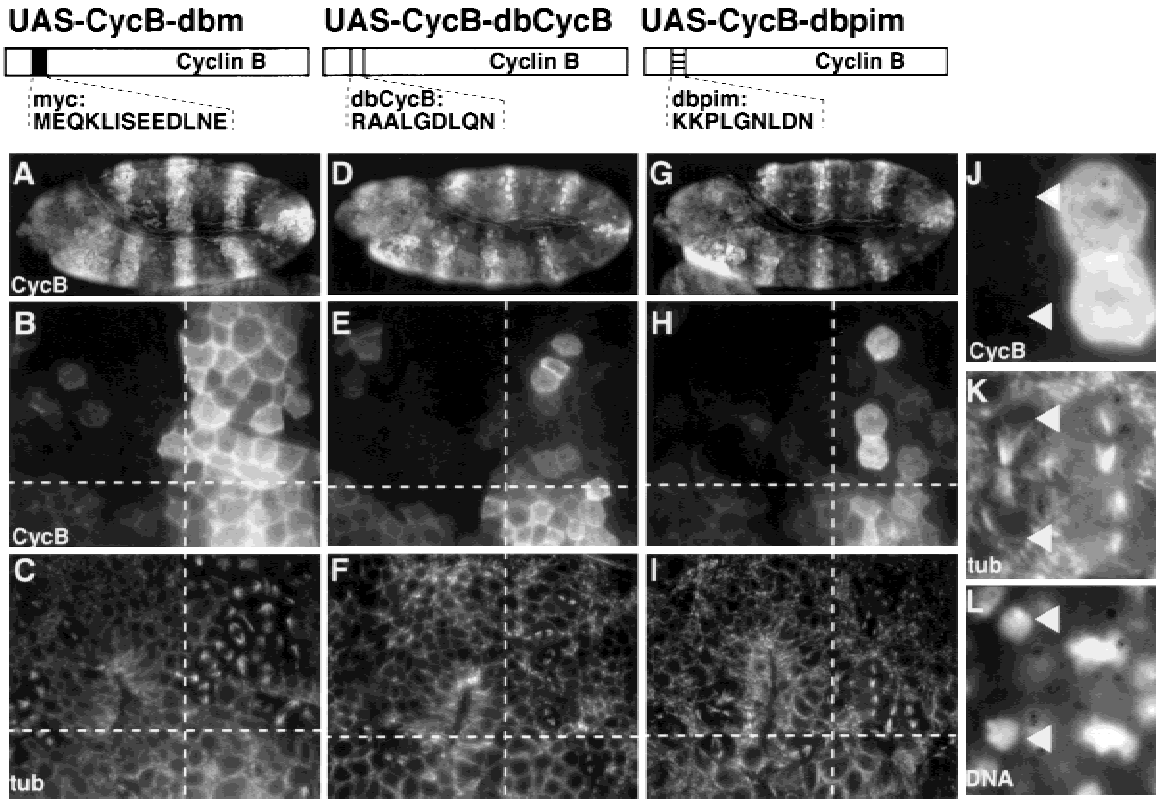

Figure 2. The PIM destruction box variant can replace the Cyclin B destruction box. *prd–GAL4,* which directs *UAS* target gene expression in alternating segments starting before mitosis 15 of *Drosophila* embryogenesis, was used to express either Cyclin B with the myc epitope in place of the destruction box (*UAS–CycB–dbm*; *A–C*), or Cyclin B with the endogenous destruction box (*UAS–CycB–dbCycB*; *D–F*), or Cyclin B with the PIM destruction box (*UAS–CycB–dbpim*; *G–L*). Embryos (*A*,*D*,*G*) were fixed during the stage of mitosis 15 and double-labeled with antibodies against Cyclin B (CycB; *A*,*B*,*D*,*E*,*G*,*H*,*J*), tubulin (tub; *C*,*F*,*I*,*K*) and a DNA stain (DNA; *L*). Higher magnification views of the embryonic epidermis (*B*,*C*,*E*,*F*,*H*,*I*) are shown with the regions of *UAS* target gene expression to the right of the dashed vertical lines. *UAS* target gene expression is absent from the regions on the left of the dashed vertical line. These regions express only endogenous Cyclin B and serve as internal control for progression through mitosis 15. Progression through mitosis 15 is accompanied by degradation of Cyclin B protein when carrying a functional degradation box and occurs in a segmentally repeated pattern (Foe et al. 1993) first in the dorsal epidermis (above the horizontal dashed line) and only later in the ventral epidermis (below the horizontal dashed line). At the stage shown, mitosis 15 is largely completed in the dorsal epidermis and just starting in the ventral epidermis. Nondegradable Cyclin B with the myc epitope in place of the destruction box blocks exit from mitosis and results in an enrichment of mitotic figures (*C*, *upper right*) in cells that are labeled by anti-Cyclin B (*B*, *upper right*). In contrast, Cyclin B with the PIM motif in place of the destruction box does not block exit from mitosis and is degraded during late mitosis as illustrated in the regions shown at even higher magnification (*J–L*). Arrowheads mark a telophase cell that is not labeled with anti-Cyclin B (*J*) while the neighboring metaphase cells (*right*) are strongly labeled. The structure of the different *UAS*-transgenes is schematically illustrated above the panels with the corresponding results.

pim^{dba}*–myc*). The mutant PIM^{dba}–myc protein product was found to be stable during mitosis, while wild-type PIM–myc expressed from an analogous transgene (*UAS–pim–myc*) was degraded normally (Fig. 3, cf. A,B with E,F).

PIM^{dba}–myc did not block the mitotic degradation of Cyclin A (data not shown) and Cyclin B (Fig. 3G) indicating that it does not inhibit the APC/C-dependent degradation pathway. Interestingly, however, PIM^{dba}–myc was found to block sister chromatid separation. In *UAS–pim*^{dba}*–myc*-expressing embryos, we observed only abnormal, decondensing metaphase plates in the regions without Cyclin B labeling (Fig. 3H, see arrows) instead of anaphase and telophase figures which are abundant in those regions of control embryos that have degraded Cyclin B and thus have progressed beyond the metaphase–anaphase transition (Fig. 3D, see arrowheads). Early mitotic figures (prophase and metaphase) were normal in *UAS–pim*^{dba}*–myc*-expressing embryos, and tubulin labeling revealed the presence of mitotic spindles (Fig. 4E; data not shown). The observation that congression of mitotic chromosomes into the metaphase plate occurred normally indicated that PIM^{dba}–myc does not interfere with spindle function.

The *nos–GAL4–GCN4–bcd3′UTR* transgene used in these experiments to drive *UAS–pim*^{dba}*–myc* expression resulted in a graded expression with a maximum at the anterior pole of the embryo. Whereas an apparently complete block of sister chromatid separation occurred in regions with high levels of expression (Fig. 3F–H), only a partial inhibition was observed in regions with lower expression levels. In these regions, aberrant anaphase and telophase figures with chromatin bridges were frequent (data not shown).

To confirm that high levels of *UAS–pim*^{dba}*–myc* expression abolished sister chromatid separation specifically and not other processes during cell cycle progression, we analyzed mitotic chromosomes from *UAS–pim*^{dba}*–myc* I.1; *UAS–pim*^{dba}*–myc* III.1/*da–GAL4* embryos after treatment with the microtubule destabilizing drug colcemid (demecolcine) during the stage of mitosis 16. In these embryos, sister chromatid separation appeared to be inhibited completely during mitosis 15 which follows after the onset of *da–GAL4*-driven *UAS*-transgene expression (data not shown). Thus, after nondisjunction of sister chromatids during mitosis 15 and re-replication during S phase 16, diplochromosomes would be expected to be present during the colcemid-arrested mitosis 16. In fact, whereas we observed only normal mitotic chromosomes in control embryos (Fig. 3I), mitotic cells with a normal number of chromosomes that had twice as many arms than normal chromosomes were present in the *UAS–pim*^{dba}*–myc*-expressing embryos (Fig. 3J). The presence of these diplochromosomes demonstrates that *UAS–pim*^{dba}*–myc* expression specifically blocks sister chromatid separation.

The finding that sister chromatid separation was inhibited by the nondegradable PIM^{dba}–myc protein suggested that this process is dependent on mitotic PIM degradation. High levels of wild-type PIM resulting from overexpression, therefore, might inhibit sister chromatid separation equally. In fact, sister chromatid separation

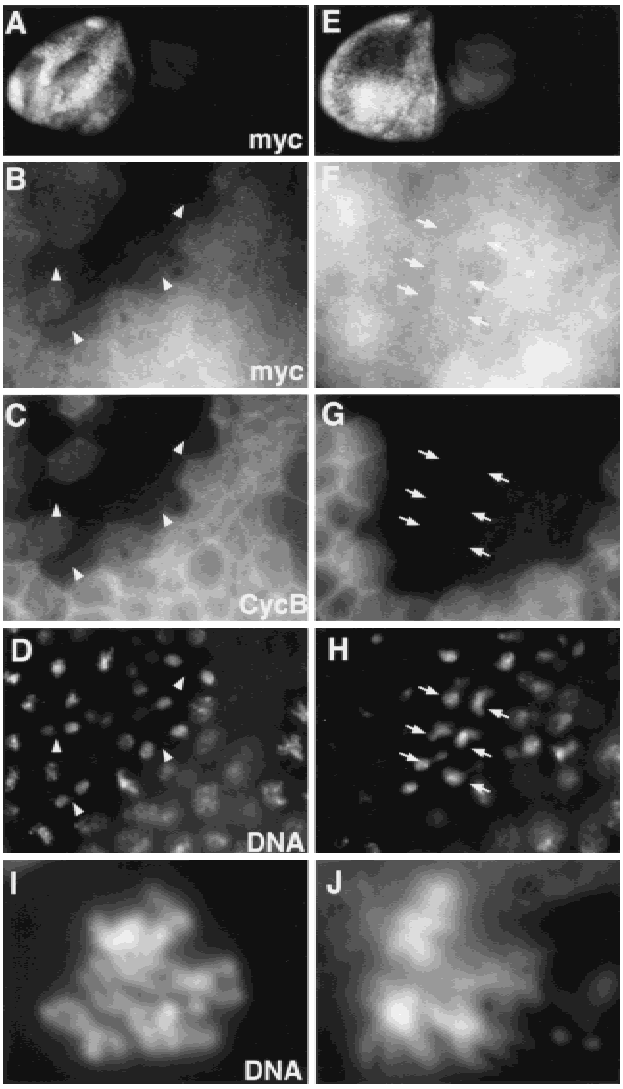

Figure 3. PIM with mutations in the destruction box motif is stable in mitosis and inhibits sister chromatid separation. *nos–GAL4–GCN4–bcd3′UTR* was used to express either wild-type PIM with carboxy-terminal myc epitopes (*UAS–pim–myc*; *A–D*) or PIM with carboxy-terminal myc epitopes and a mutant destruction box (*UAS–pim*^{dba}*–myc*; *E–H*) in the anterior region of gastrulating embryos. Embryos (*A*,*E*) were fixed and labeled with antibodies against the myc epitope (myc; *A*,*B*,*E*,*F*), Cyclin B (CycB; *C*,*G*) and a DNA stain (DNA; *D*,*H*). Arrowheads in the high magnification views of a head region indicate normal anaphase and telophase figures (*B–D*), while arrows mark abnormal "metaphase" plates with decondensing chromosomes (*E–H*) in regions that lack anti-Cyclin B labeling and thus have progressed beyond the metaphase–anaphase transition. *UAS–pim*^{dba}*–myc* I.1; *UAS–pim*^{dba}*–myc* III.1 embryos for control (*I*) and *UAS–pim*^{dba}*–myc* I.1/+; *UAS–pim*^{dba}*–myc* III.1/*da–GAL4* embryos (*J*), in which mitosis 15 is the first division affected by the expression of nondegradable PIM, were incubated in colcemid at the stage of mitosis 16 before preparation of mitotic chromosome spreads stained for DNA. Diplo-chromosomes (*J*) indicating the failure of sister chromatid separation during mitosis 15 were not observed in controls (*I*).

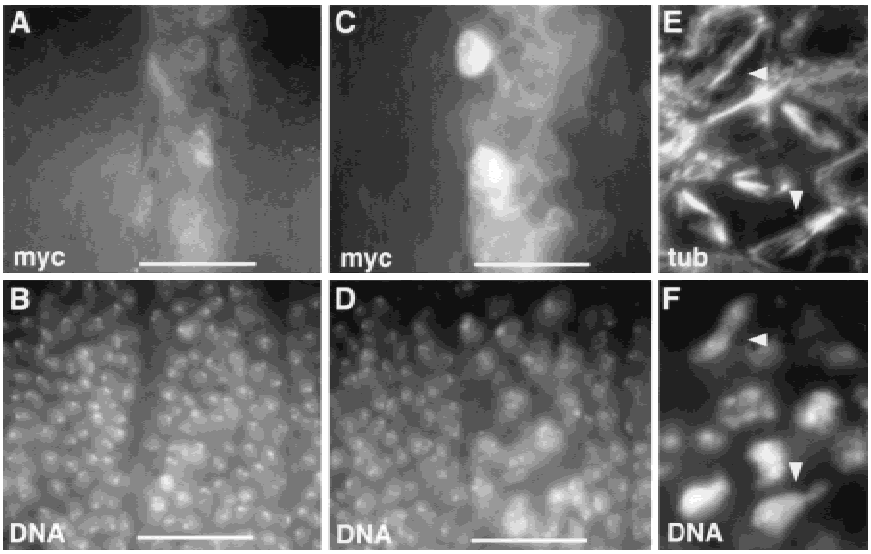

Figure 4. Overexpression of wild-type PIM inhibits sister chromatid separation. *prd–GAL4* (*A–D*) or *da–GAL4* (*E,F*) was used for overexpression of wild-type PIM with carboxy-terminal myc epitopes from either one (*A,B*) or two (*C–F*) *UAS–pim–myc* transgene copies. Embryos were fixed either after mitosis 16 (*A–D*) or during mitosis 16 (*E,F*) and labeled with antibodies against the myc epitope (myc; *A,C*), tubulin (tub; *E*) and with a DNA stain (DNA; *B,D,F*). Overexpression from one *UAS–pim–myc* copy does not affect progression through the sixteenth embryonic division. The normal nuclear density is therefore observed in the *prd–GAL4*-expressing segments (*A,B*, white horizontal bars). In contrast, overexpression from two *UAS–pim–myc* copies results in inhibition of sister chromatid separation during mitosis 16. Arrowheads in *E* and *F* indicate cells during telophase of mitosis 16 with unseparated chromosomes. As a consequence, cytokinesis fails as well, but exit from mitosis 16 occurs normally. This failure of sister chromatid separation and cytokinesis is evidenced by the lower density of interphase nuclei in the *prd–GAL4*-expressing segments (*C,D*, white bars) after mitosis 16.

failed when two copies of the *UAS–pim–myc* transgene were expressed during the embryonic mitoses using the *da–GAL4* or *prd–GAL4* transgenes (Fig. 4C–F). Expression of one *UAS–pim–myc* copy did not inhibit sister chromatid separation (Fig. 4A,B). Quantitative immunoblotting experiments indicated that ubiquitous expression of two *UAS–pim–myc* copies with *da–GAL4* resulted in about five-fold higher levels of expression compared to wild type (data not shown). Although this level of overexpression inhibited sister chromatid separation, it did not interfere with mitotic cyclin destruction. Moreover, *UAS–pim–myc* overexpression in endoreduplicating salivary gland cells throughout late embryogenesis and larval development had no effect, whereas it resulted in severe phenotypic abnormalities in mitotically proliferating imaginal disc cells (data not shown). Overexpression of wild-type *pim*, therefore, is not generally cytotoxic and inhibits sister chromatid separation specifically.

Interestingly, the phenotype resulting from *UAS–pim^{dba}–myc* and *UAS–pim–myc* overexpression is identical to the phenotype observed in mutant embryos lacking *pim* function (Stratmann and Lehner 1996). It appears, therefore, that both the accumulation of PIM during interphase as well as the subsequent degradation during mitosis are important for sister chromatid separation.

PIM degradation is regulated by the spindle checkpoint

Mitotic degradation of Cyclins A, B, and B3 requires Fizzy/Cdc20p, an activator of APC/C-dependent ubiquitination (Dawson et al. 1995; Sigrist et al. 1995). To evaluate whether Fizzy is also involved in PIM degradation during mitosis, we analyzed the consequences of *UAS–pim–myc* expression in *fizzy* mutants. The maternal *fizzy* contribution present in *fizzy* mutants is sufficient for progression through all of the 16 embryonic divisions in the dorsal epidermis when *UAS–pim–myc* is not expressed (Sigrist et al. 1995). However, when *UAS–pim–myc* was expressed, sister chromatid separation was found to be inhibited in the dorsal epidermis of *fizzy* mutants during mitosis 16, while exit from this mitosis 16 still occurred. Importantly, in contrast to the results observed in wild-type embryos (Fig. 4A,B), expression of just one *UAS–pim–myc* copy was already sufficient for inhibition of sister chromatid separation in the dorsal region of *fizzy* mutants (Fig. 5A,B) and resulted in a phenotype that was only observed in wild-type embryos when two *UAS–pim–myc* copies were expressed (Fig. 4C,D).

In the ventral region of *fizzy* homozygotes, the maternal *fizzy* contribution is not sufficient to allow completion of mitosis 16. Therefore, a large fraction of ventral cells become arrested during metaphase 16 in *fizzy* mutants (Dawson et al. 1995; Sigrist et al. 1995). When *UAS–pim–myc* was expressed in *fizzy* mutants, we observed very strong anti-myc labeling in the arrested cells of the ventral region (Fig. 5C). This labeling was much more intense than in the dorsal *UAS–pim–myc* expressing cells that were not arrested (Fig. 5A). The persistence of PIM–myc during metaphase arrest resulting from lack of *fizzy* function was also observed when expression was directed at lower levels by transgenes under the control of the *pim*$^{+}$ regulatory region (data not shown). Moreover, immunoblotting experiments confirmed that the endogenous PIM protein is also stabilized in *fizzy* homozygotes (Fig. 5E). We conclude, therefore, that *fizzy* is required for PIM degradation during mitosis.

Spindle defects result in a mitotic checkpoint arrest during which sister chromatids do not separate, possibly because PIM is not degraded. To evaluate whether PIM is

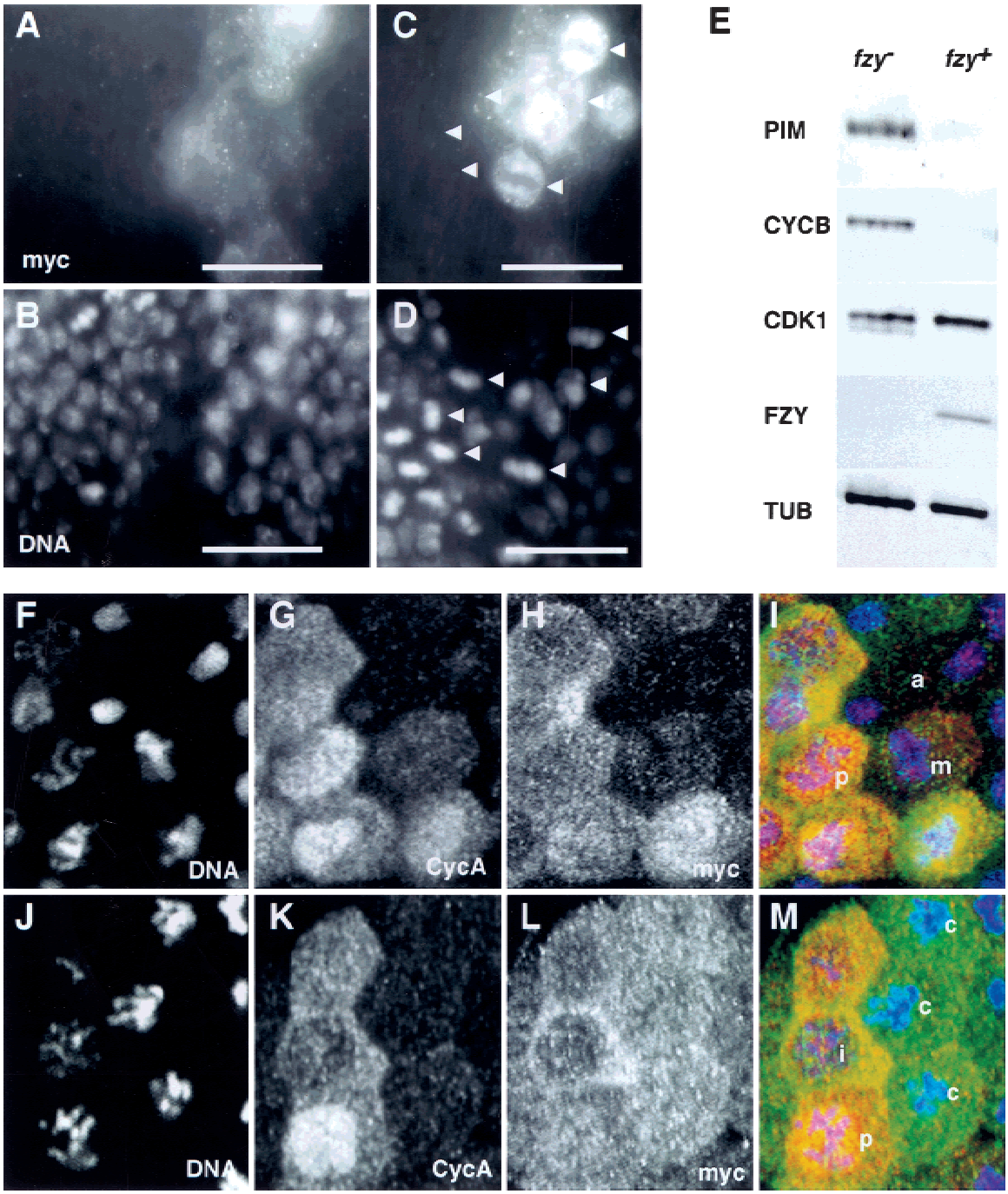

Figure 5. PIM persists during the mitotic arrest caused by colcemid or lack of Fizzy. (*A–D*) *prd–GAL4* was used to express one *UAS–pim–myc* copy in *fizzy* mutant embryos. Embryos were fixed at a stage where mitosis 16 is completed during wild-type development and labeled with anti-myc (*A*,*C*), a DNA stain (*B*,*D*), and anti-β-galactosidase for the identification of *fizzy* homozygotes (data not shown). High magnification views of the dorsal epidermis (*A*,*B*) illustrate that one *UAS–pim–myc* copy is sufficient to inhibit sister chromatid separation during mitosis 16 in *fizzy* mutants, leading to the reduced nuclear density in the *prd–GAL4*-expressing regions (white bar). High magnification views of the ventral epidermis (*C*,*D*) illustrate the persistence of PIM–myc in cells arrested in metaphase 16 because of lack of Fizzy (arrowheads), leading to the intense anti-myc labeling in the arrested cells within the *prd–GAL4*-expressing region (white bar). (*E*) Progeny from *fizzy*/*CyO* parents was aged to the stage where mitosis 16 is completed during wild-type development. *fizzy* homozygous embryos (*fzy*$^{-}$) were sorted from sibling embryos (*fzy*$^{+}$) and analyzed by immunoblotting with antibodies against PIM (PIM), Cyclin B (CYCB), Cdk1 (CDK1), FZY (FZY), and tubulin (TUB). (*F–M*) *nos–GAL4–GCN4–bcd3′ UTR* was used to express PIM with carboxy-terminal myc epitopes (*UAS–pim–myc*). Embryos at the stage of mitosis 14 were permeabilized and incubated for 25 min either in the absence (*F–I*) or presence (*J–M*) of colcemid before fixation and labeling with antibodies against the myc epitope (myc; *H*,*L*), Cyclin A (CycA; *G*,*K*) and a DNA stain (DNA; *F*,*J*). The merged panels (*I*,*M*) show labeling of DNA in blue, Cyclin A in red, and PIM–myc in green. (i) Interphase; (p) prophase; (m) metaphase; (a) anaphase; (c) colcemid-arrested cells.

stable during a mitotic checkpoint arrest, we treated *UAS–pim–myc*-expressing embryos with colcemid (Fig. 5J–M) and used mock-treated embryos as control (Fig. 5F–I). These embryos were subsequently labeled with a DNA stain (Fig. 5F,J) to identify arrested cells and with anti-myc antibodies (Fig. 5H,L) to monitor the presence of PIM–myc. We also labeled the embryos with an antibody against Cyclin A (Fig. 5G,K) which is known to be degraded in colcemid-arrested cells in contrast to Cyclin B (Whitfield et al. 1990). PIM–myc remained clearly detectable in mitotic domains of arrested cells with condensed chromosomes and without Cyclin A labeling (Fig. 5L,M, see cells labeled "c"). These observations demonstrate that PIM is not degraded in cells arrested by the spindle checkpoint pathway.

Sister chromatid separation in the presence of low levels of nondegradable PIM

The PIM persistence in cells arrested by colcemid or lack of *fizzy*, as well as the inhibition of sister chromatid separation resulting from *UAS–pim^{dba}–myc* and *UAS–pim–myc* expression, were consistent with the notion that sister chromatid separation is strictly dependent on PIM degradation during mitosis. However, the experiments with *UAS–pim^{dba}–myc* and *UAS–pim–myc* involved overexpression. To analyze the effects of physiological levels of PIM^{dba}–myc, we constructed a transgene with the *pim^{+}* regulatory region directing PIM^{dba}–myc expression (*gpim^{dba}–myc*). Interestingly, we were able to establish transgenic lines indicating that expression of a single *gpim^{dba}–myc* copy is tolerated in a *pim^{+}* background. However, when present in two copies, transgene insertions resulted in complete lethality (five out of eight lines) or severe morphological abnormalities (rough eyes, notched wings, sterility) in rare escapers (three out of eight lines). The analysis of heterozygous combinations of different transgene insertions indicated that these phenotypes were not caused by transgene insertion position effects. The phenotypes indicated clearly that PIM^{dba}–myc is highly toxic.

The fact that we were able to isolate transgenic lines with *gpim^{dba}–myc* insertions suggested that sister chromatid separation is not absolutely dependent on complete PIM degradation during each mitosis. However, *gpim^{dba}–myc* expression might occur only at very low levels as a result of a selection against insertions generating normal expression levels during transgene establishment. Moreover, wild-type PIM might compete with PIM^{dba}–myc and thereby protect cells. Therefore, we addressed *gpim^{dba}–myc* expression levels in immunoblotting experiments (Fig. 6) and analyzed the consequences of *gpim^{dba}–myc* expression in *pim* mutants (Fig. 7).

The insertion *gpim^{dba}–myc* II.5, which resulted in lethality when homozygous, was found to result in expression levels that were only ~25% lower as those of the endogenous locus (Fig. 6). In these experiments, protein products resulting from early zygotic expression during < 2 embryonic cell cycles were compared (see Materials and Methods). Comparison of protein levels that had accumulated during this brief phase was chosen as the difference in PIM–myc and PIM^{dba}–myc levels is likely to increase with every cell cycle due to the differential stability during mitosis. Moreover, the maternal *pim^{+}* contribution is known to be exhausted in *pim* mutants at this stage (Stratmann and Lehner 1996; see also Fig. 7A–C). Thus the consequences of *gpim^{dba}–myc* expression on progression through mitosis in the absence of wild-type *pim^{+}* were also analyzed at this stage (Fig. 7D–F). For this analysis, *gpim^{dba}–myc* II.5 was recombined with a mutant *pim* allele (*pim^{1}*) which abolishes expression from the endogenous locus (data not shown). Analysis of mitosis 15 in *pim^{1}/pim^{1}*, *gpim^{dba}–myc* embryos (Fig. 7D–F) and in *pim^{1}*, *gpim^{dba}–myc/pim^{1}*, *gpim^{dba}–myc* embryos (data not shown) indicated that sister chromatid separation occurred almost normally. Moreover, the same observations were also made during mitosis 16. As in wild-type embryos, anaphase and telophase figures were observed readily in these embryos in cells lacking Cyclin B labeling (Fig. 7D–F). However, a significant fraction of anaphase and telophase figures (~10%) had chromatin bridges (Fig. 7D, see asterisk) suggesting that sister chromatid separation was not always normal. Moreover, *gpim^{dba}–myc* failed to rescue the development of *pim^{1}* homozygotes to the adult stage, whereas the lethality associated with *pim^{1}* is prevented by *gpim–myc*. Nevertheless, the very significant rescue of sister chromatid separation during the embryonic divisions obtained with *gpim^{dba}–myc* in *pim^{1}* mutants, demonstrated that PIM^{dba}–myc can still provide some positive function required for sister chromatid separation. In addition, coimmunoprecipitation experiments indicated that PIM^{dba}–

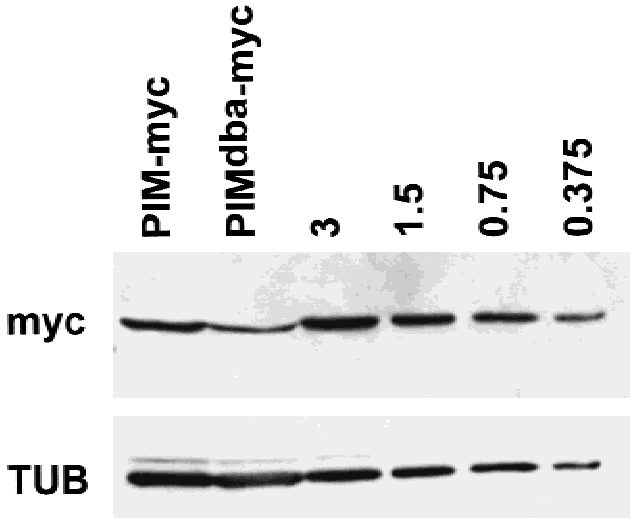

Figure 6. Analysis of PIM^{dba}–myc expression levels. Extracts from embryos with either the *gpim–myc* (PIM–myc) or the *gpim^{dba}–myc* (PIM^{dba}–myc) transgene were analyzed by immunoblotting with antibodies against the myc epitope (myc) or tubulin (TUB), which served as a loading control. In addition, to allow quantitative comparisons, we also analyzed an extract from embryos with a 3× higher *gpim–myc* transgene dose (3) as well as twofold serial dilutions of this extract (1.5; 0.75; 0.375).

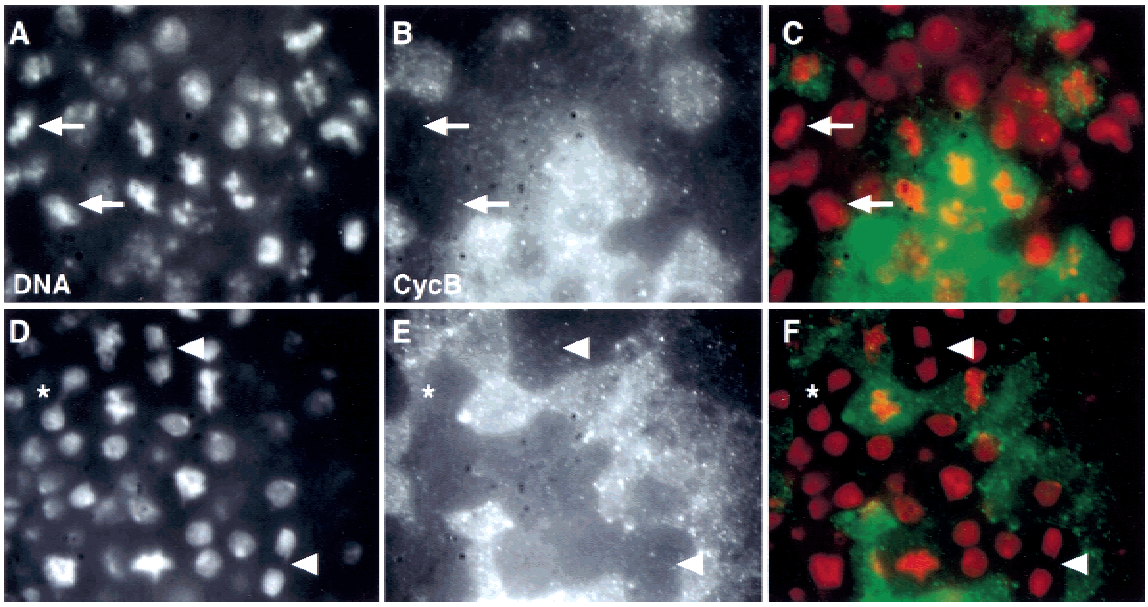

Figure 7. Low levels of PIM^{dba}–myc expression allow sister chromatid separation in *pim* mutants. *pim*^{1}/ *pim*^{1} (*A–C*) or *pim*^{1}/ *pim*^{1}, *gpim*^{dba}*–myc* (*D–F*) embryos at the stage of mitosis 15 were labeled with a DNA stain (DNA; *A*,*D*) and antibodies against Cyclin B (CycB; *B*,*E*). Regions of the dorsal epidermis are shown. In the merged panels (*C*,*F*) DNA labeling is shown in red and Cyclin B in green. Arrows in *A–C* indicate cells that have failed to separate sister chromatids even though they have progressed beyond the metaphase–anaphase transition as evidenced by lack of anti-Cyclin B labeling. Arrowheads in *D–F* indicate cells that have separated sister chromatids successfully after the metaphase–anaphase transition. (⋆, *D–F*) Cell with an anaphase bridge.

myc is associated with THR (Fig. 1). The *dba* mutation therefore appears to interfere specifically with mitotic degradation. The observation that sister chromatid separation is not inhibited in the presence of near physiological levels of nondegradable PIM^{dba}–myc argues strongly that sister chromatid separation is likely to be controlled by other mechanisms operating in addition to PIM degradation.

Discussion

PIM is degraded during the metaphase–anaphase transition. This mitotic degradation of PIM is dependent on a destruction box motif that deviates at the first invariant position of the hitherto established destruction box consensus. While all previously characterized destruction boxes start with an arginine (King et al. 1996; Peters et al. 1998), we find a lysine in the PIM motif. However, this PIM variant can replace the destruction box of Cyclin B. Moreover, we find that Fizzy, an activator of the APC/C that is required for the degradation of mitotic cyclins (Dawson et al. 1995; Sigrist et al. 1995), is also required for PIM degradation. We assume, therefore, that PIM is degraded by the proteasome after APC/C-dependent polyubiquitination just like the mitotic cyclins.

PIM degradation during mitosis appears to be an important step for sister chromatid separation. Overexpression of wild-type PIM and nondegradable PIM results in a complete inhibition of sister chromatid separation. We have shown previously that sister chromatid separation is equally defective in the absence of PIM (Stratmann and Lehner 1996). PIM therefore can act as both an activator and an inhibitor of sister chromatid separation.

Inhibitors of sister chromatid separation which are degraded during the metaphase–anaphase transition by the APC/C pathway, and which function to a variable extent as activators of sister chromatid separation, have been described previously in yeast and vertebrates (Cohen-Fix et al. 1996; Funabiki et al. 1996b; Zou et al. 1999). These securin proteins (*S. cerevisiae* Pds1p, *S. pombe* Cut2, vertebrate PTTG) have an additional property in common. They all bind to proteins containing a conserved carboxy-terminal separin domain (*S. cerevisiae* Esp1p, *S. pombe* Cut1, vertebrate Esp1p). The separin proteins play a crucial role for sister chromatid separation. The functional characterization of budding yeast separin Esp1p has suggested that it may function as a protease which cleaves a cohesin subunit and thereby causes the dissolution of sister chromatid cohesion at the metaphase–anaphase transition (Uhlmann et al. 1999; Nasmyth et al. 2000). In addition, separin proteins might also be involved in the regulation of spindle function (Yanagida 2000). Premature activation of separin activity is restricted by the securin proteins (Ciosk et al. 1998; Kumada et al. 1998; Uhlmann et al. 1999).

We do not know whether PIM binds to a protein with a separin domain. The *Drosophila* genome sequence predicts the existence of a protein with a separin domain (Gadfly gene number CG 10583). Interestingly, this *Drosophila* separin homolog exhibits less sequence conservation than all the other known separin proteins from fungi, plants, nematodes, and vertebrates. The *Dro-*

sophila protein is highly divergent in one of the conserved motifs within the carboxy-terminal separin domain and has a relatively small amino-terminal domain (H. Jäger, S. Heidmann and C.F. Lehner, unpubl.). The amino-terminal regions of separin proteins generally show very little sequence conservation, but the fission yeast securin has been shown to bind to this nonconserved region. Although the separin proteins share at least a related carboxy-terminal domain, securin proteins do not display significant sequence similarity. The only conserved feature of the securins is the distribution of charged residues. The amino-terminal region is highly basic and the carboxy-terminal region highly acidic. This charge distribution is also present in PIM. It is therefore entirely possible that PIM represents a securin protein involved in the regulation of a *Drosophila* separin.

Although we do not yet know whether PIM binds to a separin protein, we can clearly demonstrate that PIM associates with THR in vivo. Like PIM, THR is also required for sister chromatid separation and shows no significant similarity to known proteins (D'Andrea et al. 1993). A further detailed characterization of the PIM–THR complex is underway including an analysis of its relationship to separin complexes. Three main hypotheses will have to be addressed:

1. The separin gene might have broken apart during the evolution of *Drosophila melanogaster* resulting in the *thr* gene encoding the nonconserved amino-terminal region and a distinct gene encoding the conserved carboxy-terminal separin domain which might also be part of the PIM–THR complex. The PIM–THR complex might therefore be largely equivalent to the securin/separin complex.
2. Instead of playing the role of the amino-terminal separin region, THR might be a novel separin-associated protein. Unknown separin-associated proteins in addition to the known securins were revealed by affinity purification in *Xenopus* (Zou et al. 1999) but not in budding yeast (Ciosk et al. 1998).
3. The PIM–THR complex might be distinct from securin/separin complexes. We emphasize that the role of higher eukaryote separin proteins have not yet been studied in detail and that the vertebrate homolog of the budding yeast cohesin subunit Scc1p dissociates from chromatin already during prophase, presumably as a requirement for chromatin condensation (Nasmyth et al. 2000). It remains a possibility therefore, that additional mechanisms have evolved in higher eukaryotes to maintain sister chromatid cohesion until the metaphase–anaphase transition, in particular in the centromeric region. The PIM–THR complex might be involved in the dissolution of this residual cohesion maintained in the centromeric region of higher eukaryote mitotic chromosomes. Maintenance of cohesion in the centromeric region is also of particular importance during the first meiotic division and a gene specifically required for this maintenance has been identified in *Drosophila*. Interestingly, this gene (*Mei-S332*) has no obvious homologs in other species, and it has been proposed to be involved in maintaining cohesion not only during the first meiotic division but also during mitotic divisions (Tang et al. 1998).

Apart from their shared functions (inhibition of sister chromatid separation, separin binding, APC/C substrate) the securins Pds1p, Cut2, and PTTG differ with regard to their role as positive regulators of sister chromatid separation and their involvement in checkpoint mechanisms. The following comparisons indicate that PIM is functionally most similar to fission yeast Cut2. Both proteins provide a positive and essential function. They are absolutely required for sister chromatid separation (Uzawa et al. 1990; Stratmann and Lehner 1996). In contrast, budding yeast Pds1p is clearly not required for sister chromatid separation in unperturbed cells (Yamamoto et al. 1996a; Alexandru et al. 1999). Pds1p is only essential at high temperatures and in the presence of DNA damage, lagging chromosomes and spindle damage. Moreover, while Cut2 appears to function only in mitotic checkpoint control, Pds1p has been implicated in both DNA damage and mitotic checkpoint pathways (Yamamoto et al. 1996a,b; Cohen-Fix and Koshland 1997, 1999; Alexandru et al. 1999; Tinker-Kulberg and Morgan 1999). Overexpression of nondegradable mutant Pds1p inhibits both sister chromatid separation and exit from mitosis in budding yeast (Cohen-Fix and Koshland 1999; Tinker-Kulberg and Morgan 1999). In contrast, only the former process appears to be blocked by nondegradable mutant Cut2 in fission yeast (Funabiki et al. 1996b). This differential involvement in checkpoint regulation might reflect a fundamental physiological difference between budding and fission yeast. DNA damage causes fission yeast (and animal cells) primarily to block entry into mitosis by preventing Cdk1 activation. In contrast, DNA damage inhibits the metaphase–anaphase transition in budding yeast and Pds1p is of major importance for this DNA damage checkpoint arrest. It is not known whether PIM and vertebrate PTTG are involved in a DNA damage checkpoint pathway. However, based on the effects caused by the expression of nondegradable mutant proteins, PIM and vertebrate PTTG appear to be more similar to Cut2 than to Pds1p. Nondegradable PTTG and PIM inhibit only sister chromatid separation but not the degradation of mitotic cyclins and exit from mitosis (Zou et al. 1999; this paper).

The mitotic checkpoint pathway which delays the metaphase–anaphase transition in the presence of unattached kinetochores prevents the activation of APC/C by Fizzy/Cdc20p (Zachariae and Nasmyth 1999). As a consequence, mitotic cyclins and securins persist in the arrested cells. In budding yeast, the persistence of Pds1p has been demonstrated to be required for the inhibition of sister chromatid separation by elegant and conclusive genetic experiments involving cells lacking *PDS1* (Yamamoto et al. 1996b; Zachariae et al. 1998; Alexandru et al. 1999). Although not proven, the persistence of fission yeast Cut2 and vertebrate PTTG in checkpoint arrested cells is also thought to be responsible for the inhibition

of sister chromatid separation. We show that PIM persists in mitotic checkpoint-arrested cells as well. As in the case of Cut2, however, the essential positive role of PIM in sister chromatid separation makes it impossible to demonstrate that this PIM persistence is responsible for the inhibition of sister chromatid separation in the same elegant way realized in budding yeast. It is clear, however, that PIM levels are of crucial importance for sister chromatid separation. Our results demonstrate that modest overexpression of nondegradable PIM leads to a complete inhibition of sister chromatid separation. Moreover, higher but still relatively modest levels of wild-type PIM overexpression (~fivefold) inhibit as well. In this context, we consider it very likely that overexpression of the vertebrate securin PTTG results in chromosome instability, explaining its oncogenic potential (Pei and Melmed 1997; Zhang et al. 1999).

Even though our findings demonstrate clearly the importance of PIM degradation, they cannot answer the question whether PIM protein persistence is responsible for the inhibition of sister chromatid separation in cells arrested by the spindle checkpoint. In this case, one would expect physiological levels of nondegradable PIM to inhibit sister chromatid separation completely. However, most cells with near physiological levels of mutant, nondegradable PIM protein (~75% of wild type) instead of normal PIM appear to separate sister chromatids without major problems. Although not excluded, it appears unlikely, therefore, that the persistence of PIM protein during a mitotic checkpoint arrest is solely responsible for the block of sister chromatid separation. PIM persistence might be only one of several measures that cooperatively prevent premature sister chromatid separation in the presence of spindle damage. However, we emphasize that it remains to be shown that the myc epitopes present at the carboxyl terminus of the nondegradable PIM protein expressed in our experiments do not reduce the anaphase inhibitor function of PIM.

The almost normal progression through mitosis in the presence of near physiological levels of nondegradable PIM suggests that the onset of sister chromatid separation is not determined exclusively by the kinetics of PIM degradation. We have not detected an increase in the fraction of cells with metaphase plates in the presence of nondegradable PIM and careful examination by confocal microscopy did not reveal any residual partial degradation of the mutant PIM protein. The notion that the timing of sister chromatid separation during mitosis can be controlled by pathways that are independent of PIM degradation is also supported by the observation that expression of nondegradable Cyclin A clearly delays the metaphase–anaphase transition (Sigrist et al. 1995) even though it does not appear to result in a delay of PIM degradation (O. Leismann and C.F. Lehner, unpubl.). The timing of sister chromatid separation under normal conditions in budding yeast, when spindle or DNA damage checkpoints are not activated, is also not controlled by Pds1p degradation, because it occurs with normal kinetics in cells lacking Pds1p (Alexandru et al. 1999).

We conclude that PIM levels that are controlled by mitotic degradation are of crucial importance for sister chromatid separation. PIM therefore shares extensive similarities with securin proteins. Although its role in the regulation of *Drosophila* separin remains to be analyzed, it is clear that it associates with THR, a protein that is equally important for sister chromatid separation and that does not contain a separin domain.

Materials and methods

Drosophila *stocks*

The alleles fzy^1, fzy^3, and pim^1 were used in our experiments (Nüsslein-Volhard et al. 1984; Dawson et al. 1993; Stratmann and Lehner 1996). Second site lethal mutation present on the original pim^1 chromosome were removed by meiotic recombination. The lethality resulting from homozygosity of the pim^1 chromosome which was used in this study was completely prevented by a pim^+ transgene (Stratmann and Lehner 1996), indicating the absence of other lethal mutations except for the mutation in *pim*.

For expression of *UAS* transgenes, we used the following *GAL4* transgenes: *prd–GAL4* (Brand and Perrimon 1993), *da–GAL4* G32 (Wodarz et al. 1995), *arm–GAL4* (Sanson et al. 1996), F4, which results in expression in salivary glands (Weiss et al. 1998), and *nos–GAL4–GCN4–bcd3′UTR* (kindly provided by N. Dostatni, LGPD, IBDM, Marseille, France). A nos^+ promoter directs transcription of the *nos–GAL4–GCN4–bcd3′ UTR* transgene during oogenesis. The 3′ UTR from *bcd* which is present in the resulting transcripts leads to mRNA localization to the anterior end of the egg. The GAL4–GCN4 fusion protein translated from this mRNA, therefore, forms a concentration gradient with maximal concentrations at the anterior pole and results in graded expression of *UAS* target genes starting during cellularization in cell cycle 14 of embryogenesis.

The *UAS–CycB* (Weiss et al. 1998) and *UAS–Cdk1–myc* (Meyer et al. 2000) lines have been described previously. The *UAS–Cdk1–myc* transgene allows Gal4p-dependent expression of functional *Drosophila* Cdk1 with a carboxy-terminal extension consisting of six myc epitope copies. *UAS–CycA–Δ170* (TF73) was kindly provided by Frank Sprenger (University of Cologne, Germany). The *UAS–CycA–Δ170* transgene allows expression of *Drosophila* Cyclin A-lacking amino acids 1–170 which contains the signals required for mitotic destruction (Sigrist et al. 1995; Sprenger et al. 1997).

Lines with *UAS–CycB* transgenes allowing expression of *Drosophila* Cyclin B with alterations in the destruction box region were obtained after P element-mediated germline transformation with pUAST (Brand and Perrimon 1993) constructs following standard procedures. In an initial step of the generation of these constructs, we deleted the region encoding the destruction box in a *Drosophila* Cyclin B cDNA (Lehner and O'Farrell 1990) by inverse polymerase chain reaction (PCR) using the primers 5′-CATGGTACCTTTTGTTGTTGCCTCCATGG-3′ and 5′-GACGGTACCCGCGGCATAAGTCGTCCC-3′. Ligation of the amplification product after digestion with *Kpn*I resulted in a mutant cDNA plasmid that contained a *Kpn*I restriction site instead of the destruction box. A double-stranded oligonucleotide encoding the myc epitope (MEQKLISEEDLNE) with compatible ends was inserted into this *Kpn*I site for the construction of the *UAS–CycB–dbm* transgene. The compatible ends resulted in two additional codons on either side of the myc sequence. The mutant cDNA, therefore, coded for GT MEQKLISEEDLNE RT in place of the destruction box (RAALGDLQN). For the construction of the *UAS–CycB–dbpim* transgene, we

inserted a different oligonucleotide encoding the PIM destruction box with compatible ends (GT **K**KP**L**GNLD**N** GT). An oligonucleotide encoding a mutant PIM destruction box (GT **A**KP**A**GNLD**A** GT) was used for the construction of *UAS–CycB–dbapim*. For control experiments, we also inserted an oligonucleotide restoring the Cyclin B destruction box flanked by the extra amino acids resulting from the compatible ends on either side (GT RAALGDLQN GT) to yield *UAS–CycB–dbCycB*. The Cyclin B cDNA fragments with the different destruction box regions were excised with *Xho*I and *Xba*I and inserted into the corresponding sites of pUAST.

To analyze the toxicity of Cyclin B containing either a myc epitope tag, or the PIM destruction box, or the mutant PIM destruction box instead of the normal Cyclin B destruction box, we expressed the appropriate transgenes (*UAS–CycB–dbm* III.1, *UAS–CycB–dbm* III.2, *UAS–CycB–dbpim* II.1, *UAS–CycB–dbpim* II.2, *UAS–CycB–dbapim* II.1, *UAS–CycB–dbapim* II.2, *UAS–CycB–dbCycB* II.1, *UAS–CycB–dbCycB* III.1, *UAS–CycB* II.2, *UAS–CycB* III.3) ubiquitously using *da–GAL4* G32. *UAS–CycB–dbm* and *UAS–CycB–dbapim* expression resulted in complete embryonic lethality in these experiments. In contrast, *UAS–CycB–dbpim*, *UAS–CycB–dbCycB*, and *UAS–CycB* did not affect embryonic viability.

Lines with transgenes resulting in the expression of PIM protein with a carboxy-terminal extension of six myc epitopes under the control of the pim^+ regulatory region (*gpim–myc*) have been described previously (Stratmann and Lehner 1996). For the construction of $gpim^{dba}$*–myc* transgenes, in which the pim^+ regulatory region directed expression of myc-tagged PIM protein with a mutant destruction box (**A**KP**A**GNLD**A**), we started with the removal of an *Xba*I–*Bgl*II fragment encompassing the pim^+ coding region from pKS + *gpim–myc*, a cloning intermediate that had been used already for the construction of *gpim–myc*. Insertion of an *Xba*I–*Bgl*II replacement fragment including the mutant destruction box region resulted in pKS + $gpim^{dba}$*–myc*. For the construction of this replacement fragment, we amplified a first PCR fragment using primer 1 (5′-CCATCTCTAGAAAAGTGCCGC-3′) and primer 2 (5′-ACC**TGC**CGGTTT**GGC**CAATACGGAATTTG-TAGG-3′) from pKS + *gpim–myc*. In addition, using primer 3 (5′-ATTG**GCC**AAACCG**GCA**GGTAACCTTGAC**GCT**GTGA-TGCACCAAACTCCT-3′) and primer 4 (5′-GATCTAAAAT-AGAAGATCTGAATT-3′) we amplified a second PCR fragment from pKS + *gpim–myc*. The intended mutations in the destruction box were introduced by primers 2 and 3 (bold print). The two PCR fragments were digested with *Bgl*I and ligated. The final replacement fragment was obtained after digestion of the resulting ligation product with *Xba*I and *Bgl*II. In a final step, the insert was excised from pKS + $gpim^{dba}$*–myc* using *Not*I and *Kpn*I and inserted into the corresponding sites of pCaSpeR 4 (Pirrotta 1988).

The pUAST construct used for the generation of lines allowing Gal4p-dependent expression of PIM protein with a carboxy-terminal extension of six myc epitopes (*UAS–pim–myc*) contained an insert fragment obtained from pKS + *gpim–myc* by PCR. Primer 5 (5′- GGACGGCCGAAGTGCCGCTCGTTT-3′) and primer 6 (5′-GCATCTAGAAGTTTTTATAGTTGCTT-TAATTC-3′) were used for amplification. The resulting fragment was digested with *Eag*I and *Xba*I and inserted into the corresponding sites of pUAST. For the construction of *UAS–*pim^{dba}*–myc*, we inserted a different *Eag*I–*Xba*I fragment including the mutant destruction box region into pUAST. For the generation of this fragment, we amplified a first fragment from pKS + *gpim–myc* with primers 5 and 2. In addition, using primers 3 and 6 we amplified a second PCR fragment from pKS + *gpim–myc*. The two PCR fragments were digested with *Bgl*I and ligated. The final insert fragment was obtained after digestion of the resulting ligation product with *Eag*I and *Xba*I.

Lines allowing expression of THR protein with a carboxy-terminal extension of 10 myc epitopes (*gthr–myc*) were obtained using a pCaSpeR 4 construct. In a first construction phase, we introduced restriction sites immediately downstream of the initiation codon (*Sal*I) and immediately upstream of the stop codon (*Nco*I) into a 9.2-kb genomic *Xba*I/*Xho*I fragment that contains all of the sequences required for thr^+ function (M. Sadler, S. Heidmann, and C. Lehner, unpubl.). An *Nco*I/*Afl*III PCR fragment encoding 10 myc epitope copies was inserted into the *Nco*I site. The modified *Xba*I/*Xho*I fragment was subsequently transferred into the corresponding sites of pCaSpeR 4 and used to establish the *gthr–myc* lines.

Antibodies

We used mouse monoclonal antibodies against a myc epitope (Evan et al. 1985), the PSTAIRE epitope present in Cdk1 (Yamashita et al. 1991), β-galactosidase (Promega), α-tubulin (Amersham), and *Drosophila* Cyclin B (Knoblich and Lehner 1993). In addition, we used rabbit polyclonal antibodies against *Drosophila* Cyclin A (Lehner and O'Farrell 1989), Cyclin B (Jacobs et al. 1998), FZY (Sigrist et al. 1995), PIM (Stratmann and Lehner 1996), and THR. The rabbit antiserum against THR was induced with a 45-kD hexahistidine tagged carboxy-terminal fragment that was expressed in bacteria and purified using Ni^{2+}–NTA affinity chromatography (Qiagen).

Immunoprecipitation

For the coimmunoprecipitation experiments, we collected eggs from either w^1, or *arm–GAL4*, *UAS–Cdk1–myc* II.2, or *gpim–myc* 3A, or *gthr–myc* III.1 flies. In addition, we collected eggs from a cross of *da–GAL4* females with *UAS–*pim^{dba}*–myc* III.1 males. Eggs were collected for 3 hr on apple juice agar plates and aged for 3 hr at 25°C before extract preparation. Extracts were prepared by homogenization in lysis buffer (50 mM HEPES at pH 7.5, 60 mM NaCl, 3 mM $MgCl_2$ 1 mM $CaCl_2$, 0.2% Triton X-100, 0.2% Nonidet NP-40, 10% glycerol, 1 mM DTT, 2 mM Pefabloc, 2 mM Benzamidin, 10 μg/ml Aprotinin, 2 μg/ml Pepstatin A, 10 μg/ml Leupeptin). For immunoprecipitation from the cleared homogenates, we used the anti-myc antibody cross-linked (Harlow and Lane 1988) to Protein A–Sepharose 6MB beads (Pharmacia). The immunoprecipitates were analyzed by immunoblotting using ECL (Amersham). Analysis of the immunoprecipitates by silver staining indicated the presence of many nonspecifically precipitated proteins obscuring the specifically coimmunoprecipitated proteins.

Immunolabeling

Fixation of embryos and immunolabeling was performed as described previously (Lehner and O'Farrell 1989). Secondary antibodies against rabbit or mouse IgG were conjugated to Alexa488 (Molecular Probes), Cy3, or Cy5 (Dianova). DNA was labeled by propidium iodide for analysis by confocal microscopy (Leica TCS-SP) or by Hoechst 33258 for conventional fluorescence microscopy (Zeiss Axiophot equipped with a Photometrics Nu200A cooled CCD camera).

For the analysis of the mitotic degradation of Cyclin B with various destruction boxes, we collected embryos for immunolabeling experiments from crosses of *prd–GAL4* females with either *UAS–CycB–dbm* III.2, or *UAS–CycB–dbpim* II.1, or *UAS–CycB–dbCycB* II.1, or *UAS–CycB–dbapim* II.1. Eggs were collected for 4 hr and aged for 4 hr at 25°C before fixation and labeling.

For the comparison of the mitotic degradation of PIM–myc and PIM^{dba}–myc, we collected embryos from crosses of *nos–GAL4–GCN4–bcd3′UTR* females and either *UAS–pim–myc* III.3 or *UAS–pim^{dba}–myc* I.1 males. Eggs were collected for 2 hr and aged for 2 hr at 25°C before fixation and immunolabeling.

For the inhibition of sister chromatid separation during mitosis 15 and cytological analysis of chromosomes in the subsequent mitosis 16, we crossed *da–GAL4* G32 females to *UAS–pim^{dba}–myc* I.1; *UAS–pim^{dba}–myc* III.1 males. Eggs were collected for 1 hr and aged for 6 hr at 25°C before permeabilization and colcemid treatment (Sigrist et al. 1995). Mitotic chromosome spreads were prepared from these embryos as described previously (Sigrist et al. 1995).

The consequences of *pim* overexpression were analyzed in progeny collected from crosses of *prd–GAL4* females with either *UAS–pim–myc* III.3 or *UAS–pim–myc* II.2; *UAS pim–myc* III.3 males.

To analyze *UAS–pim–myc* expression in *fizzy* mutant embryos, we collected eggs from a cross of *fzy^3/CyO, P[w+, ftz–lacZ]*; *prd–GAL4/+* females with *fzy^3/CyO, P[w+, ftz–lacZ]*; *UAS–pim–myc* III.3/+ males. Embryos homozygous for *fzy^3* could be identified because they were lacking anti-β-galactosidase labeling.

To analyze PIM behavior during spindle checkpoint arrest, we collected eggs from a cross of *nos–GAL4–GCN4–bcd3′UTR* females and *UAS–pim–myc* III.3 males. Eggs were collected for 30 min and aged for 165 min at 25°C. After chorion removal in 5% sodium hypochlorite (50% Klorix, Palmolive), we incubated the embryos in a 1:1 mixture of octane and Schneider's *Drosophila* cell culture medium containing 10 μM demecolcine (Sigma) for 25 min at room temperature on a rotating wheel. For fixation, the cell culture medium was replaced by phosphate buffered saline containing 4% formaldehyde and further processing for immunolabeling was as described previously (Lehner et al. 1991).

To analyze the function of nondegradable PIM in *pim* mutants, we constructed a *pim^1* chromosome with the *gpim^{dba}–myc* II.5 insertion by meiotic recombination. We collected eggs from parents carrying this chromosome over *CyO* [*gpim^{dba}–myc* II.5, *pim^1/CyO, P(w+, ftz–lacZ)*]. In addition, we also analyzed progeny from a cross of *gpim^{dba}–myc* II.5, *pim^1/CyO, P[w+, ftz–lacZ]* females and *pim^1/CyO, P[w+, ftz–lacZ]* males. Moreover, for control experiments we collected eggs from *pim^1/CyO, P[w+, ftz–lacZ]* flies and from *pim^1/CyO, P[w+, ftz–lacZ]*; *gpim–myc* III.1 flies. Progeny homozygous for *pim^1* could be identified because they were lacking anti-β-galactosidase labeling.

Immunoblotting

Eggs collected from *fzy^1/CyO* flies were aged to stage 12 and fixed as described previously (Edgar et al. 1994). After DNA labeling, homozygous *fzy^1* embryos were sorted from sibling embryos using an inverted epifluorescence microscope (Zeiss Axiovert). Extracts were prepared from pooled embryos and analyzed by immunoblotting as described previously (Edgar et al. 1994).

To analyze *pim* transgene expression levels by immunoblotting with anti-myc, we crossed *pim^1/CyO, P[w+, ftz–lacZ]* virgin females with *gpim^{dba}–myc* II.5, *pim^1/CyO P[w+, ftz–lacZ]* males. In parallel, we crossed females of the same genotype also with males carrying either only the *gpim–myc* III.1 transgene insertion [*pim^1/CyO, P(w+, ftz–lacZ)*; *gpim–myc* III.1/+] or multiple *gpim–myc* transgene insertions [*gpim–myc* I.1/Y; *pim^1/CyO, P(w+, ftz–lacZ)*; *gpim–myc* III.3/*gpim–myc* III.3]. Progeny from these crosses were collected for 30 min on apple juice agar plates and aged for 4 hr at 25°C before preparation of total embryo extracts in SDS–gel sample buffer. The embryos used for extract preparation, therefore, were between 4 and 4.5 hr old, i.e., at the stage when the fifteenth round of embryonic mitoses starts. The embryos contained only zygotically expressed transgene products, because all transgenes were of paternal origin. Zygotic *pim$^+$* expression starts during cycle 14 of embryogenesis and reaches significant levels only during cycle 15. Zygotic expression of *gpim–myc* directed by the *pim$^+$* regulatory region present in our transgenes results in levels comparable to those expressed from the endogenous *pim$^+$* gene (data not shown). The fraction of unfertilized eggs was controlled after DNA labeling and microscopic inspection of eggs collected immediately after the eggs used for the immunoblotting experiments.

The quantification of PIMdba–myc levels relative to PIM–myc levels by immunoblotting with anti-myc antibodies instead of using anti-PIM antibodies and comparing transgene product levels relative to the endogenous *pim$^+$* gene products was chosen because the reactivity of our anti-PIM antibodies was found to be strongly decreased by the carboxy-terminal myc epitope extension present in the transgene products. Moreover, it is not possible to distinguish the early zygotic from the maternal expression of the endogenous *pim$^+$* gene when using the anti-PIM antibodies.

Acknowledgments

We acknowledge the contribution of Carola Weise, Malte Siedler, and Andreas Weiss in the initial PIM–THR coimmunoprecipitation experiments, the initial characterization of the *thr* genomic region, and the generation of the *UAS–CycBdbm* lines, respectively. We thank Rob Saint for *thr* cDNA and genomic clones, and Frank Sprenger for the *UAS–CycA–Δ170* lines. This work was supported by grants from the Deutsche Forschungsgemeinschaft (DFG Le 987/2-1 and 3-1).

The publication costs of this article were defrayed in part by payment of page charges. This article must therefore be hereby marked "advertisement" in accordance with 18 USC section 1734 solely to indicate this fact.

References

Alexandru, G., Zachariae, W., Schleiffer, A., and Nasmyth, K. 1999. Sister chromatid separation and chromosome re-duplication are regulated by different mechanisms in response to spindle damage. *EMBO J.* **18:** 2707–2721.

Blat, Y. and Kleckner, N. 1999. Cohesins bind to preferential sites along yeast chromosome III, with differential regulation along arms versus the centric region. *Cell* **98:** 249–259.

Brand, A.H. and Perrimon, N. 1993. Targeted gene expression as a means of altering cell fates and generating dominant phenotypes. *Development* **118:** 401–415.

Chen, R.H., Waters, J.C., Salmon, E.D., and Murray, A.W. 1996. Association of spindle assembly checkpoint component XMAD2 with unattached kinetochores. *Science* **274:** 242–246.

Ciosk, R., Zachariae, W., Michaelis, C., Shevchenko, A., Mann, M., and Nasmyth, K. 1998. An ESP1/PDS1 complex regulates loss of sister chromatid cohesion at the metaphase to anaphase transition in yeast. *Cell* **93:** 1067–1076.

Cohen-Fix, O. and Koshland, D. 1997. The anaphase inhibitor of *Saccharomyces cerevisiae* Pds1p is a target of the DNA damage checkpoint pathway. *Proc. Natl. Acad. Sci.* **94:** 14361–

14366.
———. 1999. Pds1p of budding yeast has dual roles: Inhibition of anaphase initiation and regulation of mitotic exit. *Genes & Dev.* **13:** 1950–1959.
Cohen-Fix, O., Peters, J.M., Kirschner, M.W., and Koshland, D. 1996. Anaphase initiation in *Saccharomyces cerevisiae* is controlled by the APC-dependent degradation of the anaphase inhibitor Pds1p. *Genes & Dev.* **10:** 3081–3093.
D'Andrea, R.J., Stratmann, R., Lehner, C.F., John, U.P., and Saint, R. 1993. The *three rows* gene of *Drosophila melanogaster* encodes a novel protein that is required for chromosome disjunction during mitosis. *Mol. Biol. Cell* **4:** 1161–1174.
Darwiche, N., Freeman, L.A., and Strunnikov, A. 1999. Characterization of the components of the putative mammalian sister chromatid cohesion complex. *Gene* **233:** 39–47.
Dawson, I.A., Roth, S., Akam, M., and Artavanis-Tsakonas, S. 1993. Mutations of the *fizzy* locus cause metaphase arrest in *Drosophila melanogaster* embryos. *Development* **117:** 359–376.
Dawson, I.A., Roth, S., and Artavanis-Tsakonas, S. 1995. The *Drosophila* cell cycle gene *fizzy* is required for normal degradation of cyclins A and B during mitosis and has homology to the CDC20 gene of *Saccharomyces cerevisiae*. *J. Cell Biol.* **129:** 725–737.
Edgar, B.A., Sprenger, F., Duronio, R.J., Leopold, P., and O'Farrell, P.H. 1994. Distinct molecular mechanisms regulate cell cycle timing at successive stages of *Drosophila* embryogenesis. *Genes & Dev.* **8:** 440–452.
Evan, G.I., Lewis, G.K., Ramsay, G., and Bishop, J.M. 1985. Isolation of monoclonal antibodies specific for human c-myc proto-oncogene product. *Mol. Cell. Biol.* **5:** 3610–3616.
Fang, G., Yu, H., and Kirschner, M.W. 1998. The checkpoint protein MAD2 and the mitotic regulator CDC20 form a ternary complex with the anaphase-promoting complex to control anaphase initiation. *Genes & Dev.* **12:** 1871–1883.
Foe, V.E., Odell, G.M., and Edgar, B.A. 1993. Mitosis and morphogenesis in the *Drosophila* embryo: Point and counterpoint. In *The development of* Drosophila melanogaster. (ed. M. Bate and A. Martinez Arias), pp. 149–300. Cold Spring Harbor Laboratory Press, Cold Spring Harbor, NY.
Funabiki, H., Kumada, K., and Yanagida, M. 1996a. Fission yeast Cut1 and Cut2 are essential for sister separation, concentrate along the metaphase spindle and form large complexes. *EMBO J.* **15:** 6617–6628.
Funabiki, H., Yamano, H., Kumada, K., Nagao, K., Hunt, T., and Yanagida, M. 1996b. Cut2 proteolysis required for sister-chromatid separation in fission yeast. *Nature* **381:** 438–441.
Funabiki, H., Yamano, H., Nagao, K., Tanaka, H., Yasuda, H., Hunt, T., and Yanagida, M. 1997. Fission yeast Cut2 required for anaphase has two destruction boxes. *EMBO J.* **16:** 5977–5987.
Guacci, V., Koshland, D., and Strunnikov, A. 1997. A direct link between sister chromatid cohesion and chromosome condensation revealed through the analysis of MCD1 in *S. cerevisiae*. *Cell* **91:** 47–57.
Harlow, E. and Lane, D. 1988. Antibodies. A laboratory manual. Cold Spring Harbor Laboratory Press, Cold Spring Harbor, NY.
Hwang, L.H., Lau, L.F., Smith, D.L., Mistrot, C.A., Hardwick, K.G., Hwang, E.S., Amon, A., and Murray, A.W. 1998. Budding yeast Cdc20: A target of the spindle checkpoint. *Science* **279:** 1041–1044.
Jacobs, H.W., Knoblich, J.A., and Lehner, C.F. 1998. Drosophila Cyclin B3 is required for female fertility and is dispensable for mitosis like Cyclin B. *Genes & Dev.* **12:** 3741–3751.
Kallio, M., Weinstein, J., Daum, J.R., Burke, D.J., and Gorbsky, G.J. 1998. Mammalian p55CDC mediates association of the spindle checkpoint protein Mad2 with the cyclosome/anaphase-promoting complex, and is involved in regulating anaphase onset and late mitotic events. *J. Cell Biol.* **141:** 1393–1406.
Kim, S.H., Lin, D.P., Matsumoto, S., Kitazono, A., and Matsumoto, T. 1998. Fission yeast Slp1: An effector of the Mad2-dependent spindle checkpoint. *Science* **279:** 1045–1047.
King, R.W., Glotzer, M., and Kirschner, M.W. 1996. Mutagenic analysis of the destruction signal of mitotic cyclins and structural characterization of ubiquitinated intermediates. *Mol. Biol. Cell* **7:** 1343–1357.
Knoblich, J.A. and Lehner, C.F. 1993. Synergistic action of *Drosophila* cyclin A and cyclin B during the G2-M transition. *EMBO J.* **12:** 65–74.
Kumada, K., Nakamura, T., Nagao, K., Funabiki, H., Nakagawa, T., and Yanagida, M. 1998. Cut1 is loaded onto the spindle by binding to Cut2 and promotes anaphase spindle movement upon Cut2 proteolysis. *Curr. Biol.* **8:** 633–641.
Lehner, C.F. and O'Farrell, P.H. 1989. Expression and function of *Drosophila* cyclin A during embryonic cell cycle progression. *Cell* **56:** 957–968.
———. 1990. The roles of *Drosophila* cyclin A and cyclin B in mitotic control. *Cell* **61:** 535–547.
Lehner, C.F., Yakubovich, N., and O'Farrell, P.H. 1991. Exploring the role of *Drosophila* cyclin A in the regulation of S-phase. *Cold Spring Harb. Symp. Quant. Biol.* **56:** 465–475.
Lim, H.H., Goh, P.Y., and Surana, U. 1998. Cdc20 is essential for the cyclosome-mediated proteolysis of both Pds1 and Clb2 during M phase in budding yeast. *Curr. Biol.* **8:** 231–234.
Losada, A., Hirano, M., and Hirano, T. 1998. Identification of Xenopus SMC protein complexes required for sister chromatid cohesion. *Genes & Dev.* **12:** 1986–1997.
Meyer, C.A., Jacobs, H.W., Datar, S.A., Du, W., Edgar, B.A., and Lehner, C.F. 2000. *Drosophila* Cdk4 is required for normal growth and dispensable for cell cycle progression. EMBO J. (in press).
Michaelis, C., Ciosk, R., and Nasmyth, K. 1997. Cohesins: Chromosomal proteins that prevent premature separation of sister chromatids. *Cell* **91:** 35–45.
Nasmyth, K., Peters, J.M., and Uhlmann, F. 2000. Splitting the chromosomes: Cutting the ties that bind sister chromatids. *Science* **288:** 1379–1385.
Nüsslein-Volhard, C., Wieschaus, E., and Kluding, H. 1984. Mutations affecting the pattern of the larval cuticle in *Drosophila melanogaster*. I. Zygotic loci on the second chromosome. *Roux's Arch. Dev. Biol.* **193:** 267–282.
Pei, L. and Melmed, S. 1997. Isolation and characterization of a pituitary tumor-transforming gene (PTTG). *Mol. Endocrinol.* **11:** 433–441.
Peters, J.M., King, R.W., and Deshaies, R.J. 1998. Cell cycle control by ubiquitin-dependent proteolysis. In *Ubiquitin and the biology of the cell* (ed. R. Peters et al.), pp. 345–387. Plenum Press, New York, NY.
Pirrotta, V. 1988. Vectors for P-element transformation in *Drosophila*. In *Vectors. A survey of cloning vectors and their uses* (ed. R.L. Rodriguez and D.T. Denhardt), pp. 437–456. Butterworths, Boston, MA and London, UK.
Rimmington, G., Dalby, B., and Glover, D.M. 1994. Expression of N-terminally truncated cyclin-B in the *Drosophila* larval brain leads to mitotic delay at late anaphase. *J. Cell Sci.* **107:** 2729–2738.
Sanson, B., White, P., and Vincent, J.P. 1996. Uncoupling cadherin-based adhesion from wingless signalling in *Dro-*

sophila. *Nature* **383:** 627–630.
Shirayama, M., Toth, A., Galova, M., and Nasmyth, K. 1999. APC(Cdc20) promotes exit from mitosis by destroying the anaphase inhibitor Pds1 and cyclin Clb5. *Nature* **402:** 203–207.
Sigrist, S.J. and Lehner, C.F. 1997. Drosophila *fizzy-related* down-regulates mitotic cyclins and is required for cell proliferation arrest and entry into endocycles. *Cell* **90:** 671–681.
Sigrist, S., Jacobs, H., Stratmann, R., and Lehner, C.F. 1995. Exit from mitosis is regulated by *Drosophila fizzy* and the sequential destruction of cyclins A, B and B3. *EMBO J.* **14:** 4827–4838.
Sprenger, F., Yakubovich, N., and O'Farrell, P.H. 1997. S phase function of *Drosophila* cyclin A and its downregulation in G1 phase. *Curr. Biol.* **7:** 488–499.
Stratmann, R. and Lehner, C.F. 1996. Separation of sister chromatids in mitosis requires the *Drosophila* pimples product, a protein degraded after the metaphase anaphase transition. *Cell* **84:** 25–35.
Tanaka, T., Cosma, M.P., Wirth, K., and Nasmyth, K. 1999. Identification of cohesin association sites at centromeres and along chromosome arms. *Cell* **98:** 847–858.
Tang, T.T.L., Bickel, S.E., Young, L.M., and Orr-Weaver, T.L. 1998. Maintenance of sister-chromatid cohesion at the centromere by the *Drosophila* MEI-S332 protein. *Genes & Dev.* **12:** 3843–3856.
Tinker-Kulberg, R.L. and Morgan, D.O. 1999. Pds1 and Esp1 control both anaphase and mitotic exit in normal cells and after DNA damage. *Genes & Dev.* **13:** 1936–1949.
Toth, A., Ciosk, R., Uhlmann, F., Galova, M., Schleiffer, A., and Nasmyth, K. 1999. Yeast cohesin complex requires a conserved protein, Eco1p(Ctf7), to establish cohesion between sister chromatids during DNA replication. *Genes & Dev.* **13:** 320–333.
Uhlmann, F. and Nasmyth, K. 1998. Cohesion between sister chromatids must be established during DNA replication. *Curr. Biol.* **8:** 1095–1101.
Uhlmann, F., Lottspeich, F., and Nasmyth, K. 1999. Sister-chromatid separation at anaphase onset is promoted by cleavage of the cohesin subunit Scc1. *Nature* **400:** 37–42.
Uzawa, S., Samejima, I., Hirano, T., Tanaka, K., and Yanagida, M. 1990. The fission yeast cut1+ gene regulates spindle pole body duplication and has homology to the budding yeast ESP1 gene. *Cell* **62:** 913–925.
Visintin, R., Prinz, S., and Amon, A. 1997. CDC20 and CDH1: A family of substrate-specific activators of APC-dependent proteolysis. *Science* **278:** 460–463.
Watanabe, Y. and Nurse, P. 1999. Cohesin Rec8 is required for reductional chromosome segregation at meiosis. *Nature* **400:** 461–464.
Waters, J.C., Chen, R.H., Murray, A.W., Gorbsky, G.J., Salmon, E.D., and Nicklas, R.B. 1999. Mad2 binding by phosphorylated kinetochores links error detection and checkpoint action in mitosis. *Curr. Biol.* **9:** 649–652.
Weiss, A., Herzig, A., Jacobs, H., and Lehner, C.F. 1998. Continuous Cyclin E expression inhibits progression through endoreduplication cycles in *Drosophila*. *Curr. Biol.* **8:** 239–242.
Whitfield, W.G.F., Gonzalez, C., Maldonado-Codina, G., and Glover, D.M. 1990. The A-type and B-type cyclins of *Drosophila* are accumulated and destroyed in temporally distinct events that define separable phases of the G2-M transition. *EMBO J.* **9:** 2563–2572.
Wodarz, A., Hinz, U., Engelbert, M., and Knust, E. 1995. Expression of crumbs confers apical character on plasma membrane domains of ectodermal epithelia of *Drosophila*. *Cell* **82:** 67–76.
Yamamoto, A., Guacci, V., and Koshland, D. 1996a. Pds1p, an inhibitor for faithful execution of anaphase in the yeast Saccharomyces cerevisiae. *J. Cell Biol.* **133:** 85–97.
———. 1996b. Pds1p, an inhibitor of anaphase in budding yeast, plays a critical role in the APC and checkpoint pathway(s). *J. Cell Biol.* **133:** 99–110.
Yamashita, M., Yoshikuni, M., Hirai, T., Fukada, S., and Nagahama, Y. 1991. A monoclonal antibody against the PSTAIR sequence of p34cdc2, catalytic subunit of maturation-promoting factor and key regulator of the cell cycle. *Dev. Growth Differ.* **33:** 617–624.
Yanagida, M. 2000. Cell cycle mechanisms of sister chromatid separation; Roles of Cut1/separin and Cut2/securin. *Genes Cells* **5:** 1–8.
Zachariae, W. and Nasmyth, K. 1999. Whose end is destruction: Cell division and the anaphase-promoting complex. *Genes & Dev.* **13:** 2039–2058.
Zachariae, W., Shevchenko, A., Andrews, P.D., Ciosk, R., Galova, M., Stark, M.J.R., Mann, M., and Nasmyth, K. 1998. Mass spectrometric analysis of the Anaphase-Promoting Complex from yeast: Identification of a subunit related to cullins. *Science* **279:** 1216–1219.
Zhang, X., Horwitz, G.A., Heaney, A.P., Nakashima, M., Prezant, T.R., Bronstein, M.D., and Melmed, S. 1999. Pituitary tumor transforming gene (PTTG) expression in pituitary adenomas. *J. Clin. Endocrinol. Metab.* **84:** 761–767.
Zou, H., McGarry, T.J., Bernal, T., and Kirschner, M.W. 1999. Identification of a vertebrate sister-chromatid separation inhibitor involved in transformation and tumorigenesis. *Science* **285:** 418–422.

Teilarbeit B

Drosophila Separase is required for sister chromatid separation and binds to PIM and THR.

Hubert Jäger*, Alf Herzig*, Christian F. Lehner and Stefan Heidmann

Genes and Development 15, 2572-2584 (2001)

* beide Autoren haben im selben Maß zu dieser Arbeit beigetragen

Darstellung des Eigenanteils in Teilarbeit B

Ein Ergebnis meiner Arbeit ist die Charakterisierung der Interaktions-Domänen zwischen THR, PIM und SSE (Fig. 3). Diese Experimente wurden von mir und von Jörg Höflich unter meiner Anleitung durchgeführt. Weitere Ergebnisse meiner Arbeit sind die Herstellung und Charakterisierung von THR-Deletionsvarianten, Interaktionsstudien mit diesen Deletions-Varianten und der Nachweis eines heterotrimeren Komplexes aus THR, PIM und SSE (Fig. 5). Die Ergebnisse meiner Arbeit haben zu dem Modell des Separase-Komplexes aus *D. melanogaster* geführt (Fig. 6).

Die Klonierung und Charakterisierung des *Sse*-Gens (Fig. 1 und Fig. 2), die Herstellung von Sse-Transgenen, sowie die initiale Untersuchung der Komplexbildung von SSE mit THR und PIM (Fig. 4) wurden von Hubert Jäger durchgeführt.

Diese Teilarbeit wurde von allen Autoren gemeinsam verfasst.

Drosophila Separase is required for sister chromatid separation and binds to PIM and THR

Hubert Jäger,[1] Alf Herzig,[1] Christian F. Lehner, and Stefan Heidmann[2]

Department of Genetics, University of Bayreuth, 95440 Bayreuth, Germany

***Drosophila* PIM and THR are required for sister chromatid separation in mitosis and associate in vivo. Neither of these two proteins shares significant sequence similarity with known proteins. However, PIM has functional similarities with securin proteins. Like securin, PIM is degraded at the metaphase-to-anaphase transition and this degradation is required for sister chromatid separation. Securin binds and inhibits separase, a conserved cysteine endoprotease. Proteolysis of securin at the metaphase-to-anaphase transition activates separase, which degrades a conserved cohesin subunit, thereby allowing sister chromatid separation. To address whether PIM regulates separase activity or functions with THR in a distinct pathway, we have characterized a *Drosophila* separase homolog (SSE). SSE is an unusual member of the separase family. SSE is only about one-third the size of other separases and has a diverged endoprotease domain. However, our genetic analyses show that SSE is essential and required for sister chromatid separation during mitosis. Moreover, we show that SSE associates with both PIM and THR. Although our work shows that separase is required for sister chromatid separation in higher eukaryotes, in addition, it also indicates that the regulatory proteins have diverged to a surprising degree, particularly in *Drosophila*.**

[*Key Words*: Mitosis; sister chromatid separation; securin; separase; *pimples*; *three rows*]

Received May 4, 2001; revised version accepted August 10, 2001.

A distinct hallmark of eukaryotes is their use of a microtubule-based spindle to segregate their genetic information onto two daughter cells during cell division. This mechanism necessitates regulated sister chromatid cohesion. Sister chromatids have to remain in association after DNA replication so that they can be recognized as such and oriented in the mitotic spindle during prometaphase. However, after their correct bipolar orientation in the mitotic spindle, cohesion has to be resolved so that sister chromatids can be segregated to opposite poles during anaphase.

Because regulated sister chromatid cohesion is an essential element of eukaryotic cell divisions, its molecular basis is expected to be conserved. Most of our current mechanistic understanding of how sister chromatid cohesion is established during S phase, maintained until the end of metaphase, and resolved at the onset of anaphase, has been obtained with yeast (for recent reviews, see Dej and Orr-Weaver 2000; Hirano 2000; Koshland and Guacci 2000; Nasmyth et al. 2000; Yanagida 2000).

In budding yeast, the cohesin protein complex is assembled on chromatin during S phase and is required for holding sister chromatids together until the end of metaphase (Guacci et al. 1997; Michaelis et al. 1997; Uhlmann and Nasmyth 1998; Skibbens et al. 1999; Uhlmann et al. 2000). At the metaphase-to-anaphase transition, the Scc1p/Mcd1p subunit of the cohesin complex is proteolytically cleaved, which allows sister chromatid segregation during anaphase. The Esp1p protease, which is responsible for Scc1p cleavage, is kept inactive until metaphase by an inhibitory subunit, the Pds1p anaphase inhibitor. The timely activation of Esp1p at the onset of anaphase results from degradation of Pds1p by the anaphase-promoting complex/cyclosome (APC/C)-dependent pathway (Ciosk et al. 1998). The APC/C acts as an ubiquitin ligase that is regulated by the spindle assembly checkpoint (for review, see Zachariae and Nasmyth 1999).

Observations in other species support the notion that the mechanisms controlling sister chromatid cohesion are evolutionarily conserved. In particular, analyses in fission yeast and initial studies in vertebrates have given analogous results as described above for budding yeast. Proteins homologous to Scc1p have been shown to become cleaved at the metaphase-to-anaphase transition (Tomonaga et al. 2000; Waizenegger et al. 2000). Moreover, the Esp1p-like proteases (named separases) are all regulated by inhibitory protein subunits (named securins), which are degraded by the APC/C pathway at

[1]These authors contributed equally to this work.
[2]Corresponding author.
E-MAIL stefan.heidmann@uni-bayreuth.de; FAX 49-921-55-2710.
Article and publication are at http://www.genesdev.org/cgi/doi/10.1101/gad.207301.

the end of metaphase (Funabiki et al. 1996; Zou et al. 1999).

Beyond these similarities, however, higher eukaryotes have evolved specific regulatory variations and additions. The majority of the cohesin complexes is dissociated from vertebrate chromosomes already during prophase and independent of separase activity (Losada et al. 1998; Sumara et al. 2000). This early dissociation of cohesin during prophase might be required to allow chromosome condensation, which is far more extensive in higher eukaryotes than in budding yeast. The minor amount of cohesin, which remains on chromosomes until the onset of anaphase, appears to be concentrated in the centromeric region (Waizenegger et al. 2000; Warren et al. 2000). In *Drosophila*, the protein MEI-S332 has been suggested to mediate this maintenance of cohesin specifically in the centromeric region (Tang et al. 1998). Whereas the dissociation of these remaining cohesin complexes from HeLa chromosomes has been shown to be accompanied by Scc1p cleavage that can be induced in vitro by immunoprecipitated activated separase (Waizenegger et al. 2000), a separase requirement for sister chromatid separation in higher eukaryotes has not yet been demonstrated directly. Moreover, the securin proteins that have been identified in budding yeast (Pds1p), fission yeast (Cut2p), and vertebrates (PTTG) do not share significant sequence similarity except for the presence of D-boxes, which target the proteins for APC/C-dependent mitotic degradation. This mitotic destruction appears to be required for sister separation in vertebrates also (Zou et al. 1999). However, it remains a possibility that securins have evolved to regulate proteins in addition to separase.

Our analysis of the two *Drosophila* genes, *three rows* (*thr*) and *pimples* (*pim*), which do not share significant similarity with known genes, has indicated that at least in *Drosophila*, sister chromatid separation involves distinct, nonconserved components also. Loss of *pim* and *thr* function completely blocks the separation of sister chromatids, primarily within the centromeric region, but it does not inhibit cell cycle progression (D'Andrea et al. 1993; Philp et al. 1993; Stratmann and Lehner 1996). After each cell cycle, therefore, a doubled number of chromosome arms emanating from a common centromeric region is displayed in these mutants during mitosis. The indistinguishable mutant phenotypes argued for a common function. Consistently, PIM and THR have been found to form a complex in vivo (Leismann et al. 2000).

Despite the lack of significant sequence similarities with known proteins, PIM has been shown to have clear functional similarities with securin proteins. PIM is degraded during mitosis via the APC/C pathway, and a nondegradable PIM mutant as well as high levels of wild-type PIM inhibit sister chromatid separation during mitosis (Leismann et al. 2000). Therefore, PIM might also bind and regulate a *Drosophila* separase. However, PIM is known to bind to THR, which clearly does not have the structural features of separases. PIM and THR, therefore, might either both regulate a *Drosophila* separase or function in a distinct pathway. To address this issue, we have identified and characterized a *Drosophila* separase.

Here, we report that PIM and THR both bind to the *Drosophila* separase homolog SSE, which is required for sister chromatid separation. Interestingly, the *Drosophila* SSE sequence is highly diverged, lacking some features conserved in homologs from trypanosomatids to vertebrates. Our results show, therefore, that the decisive role of separase in the control of sister chromatid separation has been conserved during evolution of higher eukaryotes. Nevertheless, the surprising degree of divergence of separase and regulatory proteins indicates that regulation is highly evolved, particularly in *Drosophila*.

Results

Drosophila *SSE is a distant separase family member*

To evaluate whether PIM binds to a separase, we first searched in the genome sequence for a *Drosophila* homolog. We identified a single gene (*CG10583*) with significant similarity to the known separase genes. Comparison of our cDNA and genomic sequences revealed the structure of this gene, which will be designated as *Separase* (*Sse*) (Fig. 1A). The predicted protein product (SSE) has 634 amino acids and a calculated molecular mass of 72.9 kD.

Thus, SSE appears to be much smaller than separase homologs from other organisms, which range in size between 150 and 230 kD. Several findings support our size prediction. The *Sse* upstream region has virtually no coding potential and three stop codons are present in frame upstream of and close to the presumptive translational start in several independent cDNAs. One of these short cDNAs prevents the phenotype resulting from a complete loss of *Sse* function when expressed in *Sse* mutants (see below). Moreover, antibodies against SSE detect a protein with an apparent molecular mass of ~75 kD (see below).

The sequence similarity of separase homologs is restricted to the C-terminal part. This domain includes two invariant residues, an histidine and a cysteine, surrounded by regions typically found in cysteine proteases of the CD clan (Uhlmann et al. 2000). This presumptive catalytic dyad is also present in SSE. However, two additional sequence blocks within this C-terminal domain, which are highly conserved among separase family members, are divergent in SSE (Fig. 1B). As a consequence, SSE is the most distant member in the separase family tree (Fig. 1C).

SSE is required for sister chromatid separation

To assess *Sse* function, we generated mutant alleles. Starting with a P-element insertion within a neighboring gene (*CG17334*), we isolated a small deficiency [*Df(3L)SseA*] by male recombination (Fig. 1A). A molecular breakpoint analysis indicated that this deficiency deletes *Sse* and parts of the neighboring genes, *CG17334*

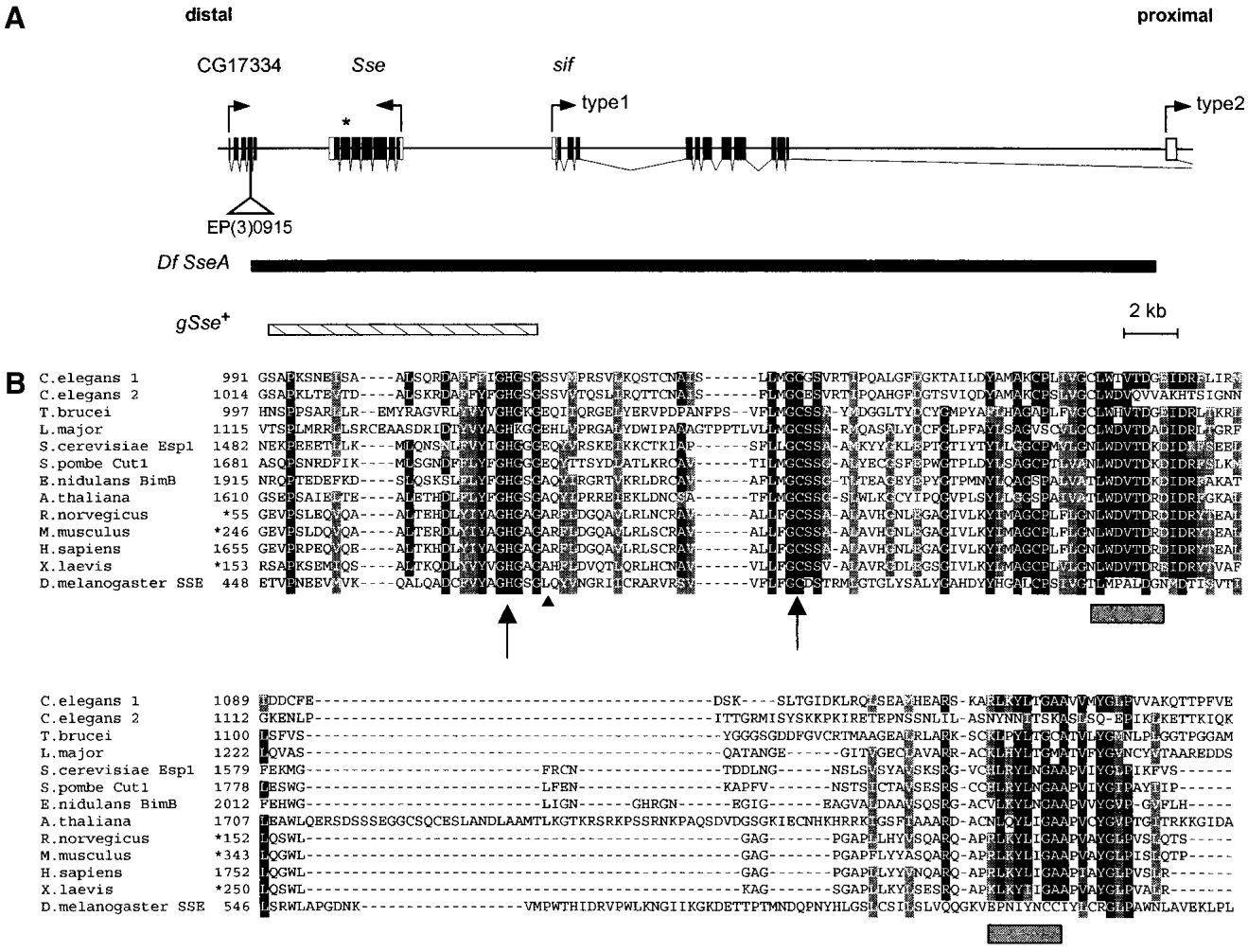

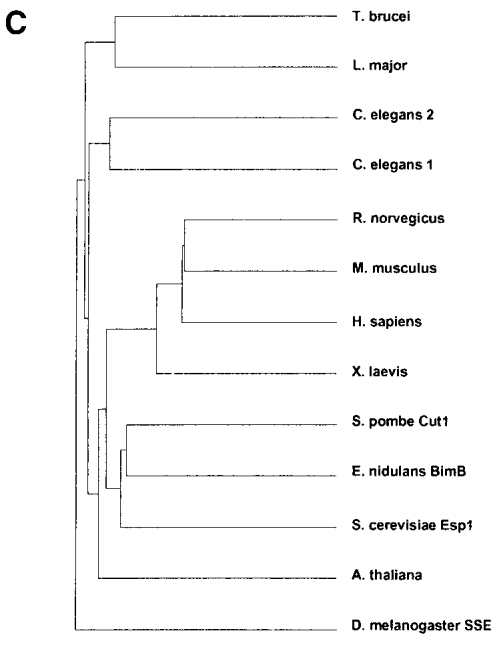

Figure 1. The separase homolog of *D. melanogaster*. (*A*) Genomic organization of the *Sse* locus with the adjacent genes, *still life* (*sif*) and *CG17334*. Boxes indicate exon sequences. Open and solid boxes denote untranslated and translated regions, respectively. Arrows indicate the orientation of transcription. A triangle marks the insertion site of the P-element EP(3)0915. The extent of the deficiency *Df (3L)SseA* isolated as male recombinant after mobilizing EP(3)0915 is shown by a black bar. The genomic *Sse* rescue fragment (*gSse*) is indicated by a hatched bar. An asterisk marks the position of the 4-bp deletion in Sse^{13m}. (*B*) Sequence alignment of the C-terminal regions of various separase homologs. *C. elegans* 1 and *C. elegans* 2 extend for 116 and 104 amino acids beyond the shown region, respectively. Arrows indicate the invariant histidine and cysteine residues representing the catalytic dyad of CD-clan proteases. Hatched rectangles denote regions poorly conserved in *D. melanogaster* SSE. The arrowhead points to the position of the 4-bp deletion in the allele Sse^{13m}. Asterisks indicate cases in which only partial sequences were available. (*C*) Dendrogram of clustering relationships among the sequences shown in *B*.

and *sif*. Interestingly, this deficiency failed to complement the recessive lethal mutation *l(3)13m-281*. This mutation has been shown to affect mitotically proliferating cells in a way that might be expected for a mutation in *Sse* (Gatti and Baker 1989; see below). Sequence analysis of the *Sse* region isolated from the *l(3)13m-281* chromosome revealed a deletion of four bases between the positions encoding the invariant histidine and cysteine residues, resulting in a frame shift followed by a premature translational stop (Fig. 1B). The product encoded by *l(3)13m-281*, therefore, is expected to lack part of the conserved C-terminal separase domain, including the invariant cysteine residue believed to be involved in catalysis. Thus, *l(3)13m-281* is presumably a null allele of *Sse* and will be designated as Sse^{13m} in the following.

Previous phenotypic analyses (Gatti and Baker 1989) had indicated that Sse^{13m} homozygotes die at the larval-pupal boundary. In Sse^{13m} larvae at third instar wandering stage, imaginal discs were found to be abnormally small and the mitotic index in the brains to be strongly reduced. Moreover, the few mitotic figures observed in larval brain squashes were reported to contain endoreduplicated chromosomes with bundles of two, four, or eight times the normal number of sister chromatid arms. Our phenotypic analyses with Sse^{13m}/*Df(3L)SseA* and *Df(3L)SseA*/*Df(3L)SseA* larvae confirmed these findings. These larvae showed identical phenotypes to Sse^{13m} homozygotes.

In embryos, we were unable to detect mitotic abnormalities in *Sse* mutants, suggesting that the maternal *Sse* contribution is sufficient to allow normal cell divisions throughout embryogenesis. However, in brains of Sse^{13m}/*Df(3L)SseA* early second instar larvae, the number of phosphorylated histone H3 (PH3)-positive cells (234 in 7 brains) was reduced to ~40% of the number of PH3-positive cells in sibling brains (238 in 3 brains). PH3 is an excellent marker for cells during the early mitotic stages until anaphase. Whereas mutants and siblings showed very similar fractions of prophase and metaphase figures in these PH3-positive cells, anaphase figures were almost completely absent from mutant brains (1 anaphase figure in 234 PH3-positive cells compared with 20 anaphase figures in 238 PH3-positive cells of sibling brains). We conclude, therefore, that the maternal *Sse* contribution is no longer sufficient to support normal anaphase when mitotic proliferation of postembryonic brain neuroblasts resumes during the second instar stage, although entry into mitosis still occurs. If *Sse* mutants specifically fail in separating sister chromatids, a rapid accumulation of chromosomes with twice the number of normal arms (diplo-chromosomes), as well as more extensively endoreduplicated chromosomes, is expected. Analysis of squash preparations of second instar larval brains fully confirmed this expectation. A total of 95% of the mitotic cells contained either diplo-chromosomes (Fig. 2K) or more extensively endoreduplicated chromosomes (Fig. 2L), whereas none of the mitotic cells of siblings contained endoreduplicated chromosomes (Fig. 2M). In addition to the presence of endoreduplicated chromosomes, mitotic figures in mutants frequently contained aneuploid numbers of chromosomes. However, we never observed polyploid figures with normal chromosomes, indicating that *Sse* mutants have no primary defect in cytokinesis.

In third instar wandering stage larvae, *Sse* mutant brains contained very few PH3-positive cells (<5% of the number of PH3-positive cells in sibling brains; Fig. 2; data not shown). The PH3-positive cells were abnormally large and had very high levels of DNA (Fig. 2C,D). We could not detect any normal anaphase and telophase figures in mutants, and squashes revealed highly abnormal and severely endoreduplicated chromosomes, as described previously (Gatti and Baker 1989). The progressive depletion of mitotic cells with increasing age suggests that most of the mitotically proliferating neuroblasts eventually die in *Sse* mutants, presumably as a consequence of hyper- and aneuploidy.

To show that the endoreduplicated unseparated chromosomes in Sse^{13m} larvae result from the loss of Sse^{+} function and not from linked second-site mutations, we performed rescue experiments. One copy of the *gSse* transgene with a 10-kb genomic DNA fragment encompassing only the *Sse* gene (Fig. 1A) rescued the phenotype of Sse^{13m} homozygotes to full viability and fertility. Moreover, the cytological defects of Sse^{13m} mutants could be prevented by a combination of *da–GAL4* and *UAS–HA–Sse* (Fig. 2B,E–J). All our findings show that *Sse* is an essential gene required for sister chromatid separation during mitosis. Moreover, the *Sse* gene product is likely to function as a cysteine protease, as we found that *da–GAL4* mediated expression of *UAS–HA–*Sse^{C497S}, in which the codon for the putative catalytic cysteine residue was mutated into a serine codon was unable to rescue *Sse* mutants.

SSE forms complexes with PIM and THR

To investigate whether the putative *Drosophila* securin PIM can bind to SSE, we used the yeast two-hybrid system. We observed a strong interaction of PIM and SSE (Fig. 3). Interestingly, we found that a mutant PIM protein with a small internal deletion (amino acids 110–114) failed to bind to SSE. This deletion was identified in pim^2, a *Drosophila* allele that results in an amorphic phenotype (Stratmann and Lehner 1996). Whereas PIM^2 failed to interact with SSE, it bound to a THR fragment (amino acids 1–933) just like wild-type PIM. The deletion of amino acids 110–114 therefore abolishes specifically the binding to SSE and does not result in destabilization or complete misfolding of the mutant PIM^2 protein. We conclude that the interaction of PIM and SSE is likely to be functionally significant.

The behavior of PIM^2 suggested that different domains of PIM mediate the binding to SSE and THR. To evaluate this notion, we analyzed PIM fragments in additional two-hybrid experiments. Like other securin proteins, PIM is composed of a basic N-terminal and an acidic C-terminal domain. The N-terminal domain was found to interact with SSE, whereas an interaction with THR 1–933 was barely detectable (Fig. 3). Conversely, the C-

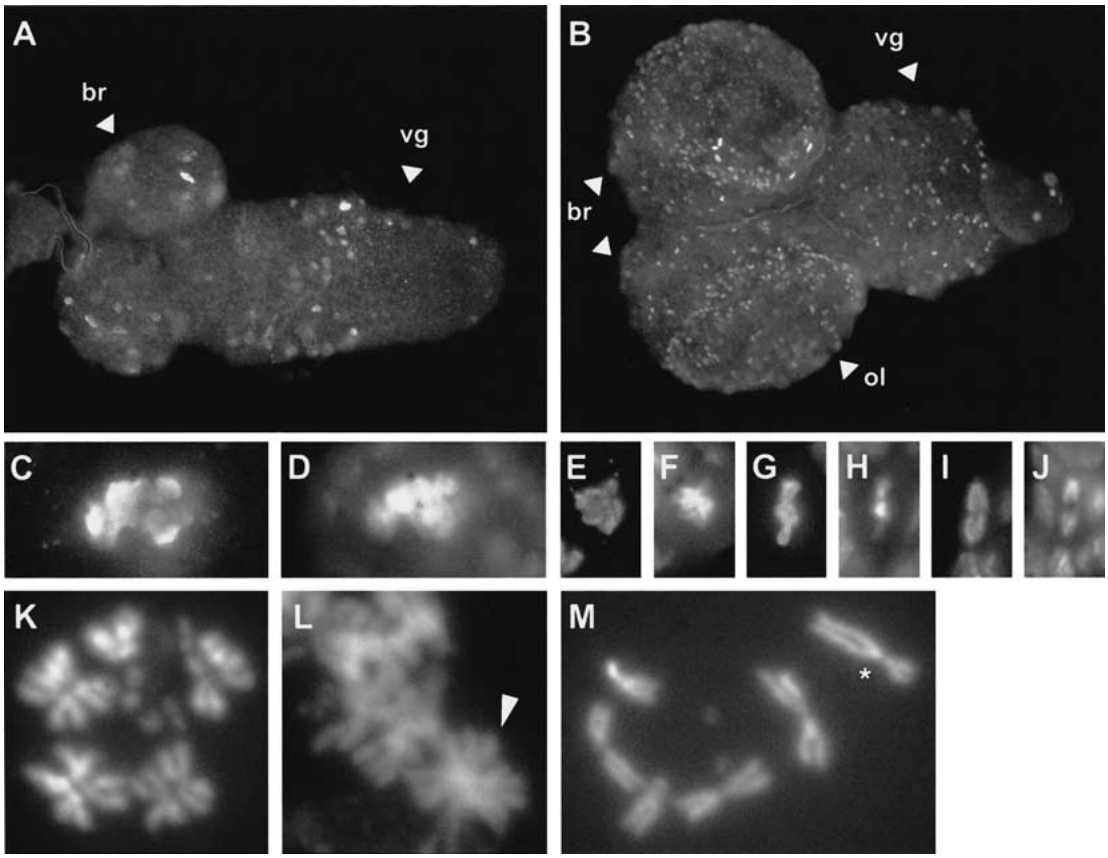

Figure 2. Mutations in *Sse* affect mitotic cells. Whole brains (*A*,*B*) from third instar larvae with the genotype $Sse^{13m}/Df(3L)SseA$ (*A*) or *UAS–HA–Sse* I.1/+; $Sse^{13m}/Df(3L)SseA$, *da–GAL4* (*B*) were immunostained for DNA (*D*,*F*,*H*,*J*) and PH3 (*A–C*,*E*,*G*,*I*). In mutant brains of third instar larvae, the PH3-positive cells contained large masses of condensed DNA (*C*,*D*) and anaphase figures could not be observed, whereas in the brains of larvae rescued by the HA-tagged Sse^{+} transgene prophase cells (*E*,*F*), metaphase cells (*G*,*H*) and cells in anaphase (*I*,*J*) could be detected. Squashes of brains from second instar larvae with the genotype $Sse^{13m}/Df(3L)SseA$ (*K*,*L*) or of brains from balanced siblings (*M*) were stained with Hoechst 33258 to visualize DNA. Diplo-chromosomes (*K*) and a quadruple-chromosome (*L*, arrowhead) are visible. The asterisk indicates the balancer chromosome *TM3*, *Ser*, *Act5c–GFP* in *M*. (br) Brain; (vg) ventral ganglion; (ol) optic lobe.

terminal domain interacted with THR 1–933, but not with SSE. These results strongly indicate that SSE and THR bind to different PIM domains.

Experiments with SSE fragments indicated that PIM binds to the N-terminal regions of SSE (Fig. 3). The interaction of PIM with full-length SSE or with a SSE fragment comprising amino acids 1–467 appeared to be stronger than with a shorter SSE fragment (amino acids 1–247). We assume that region 1–247 of SSE is sufficient for PIM binding, but the region 248–467 of SSE further strengthens this interaction. Clearly, the conserved C-terminal region of SSE is not required for the interaction with PIM.

Experiments with THR fragments indicated that PIM binds to the N-terminal region of THR. Region 1–476 of THR was found to be sufficient for PIM binding (Fig. 3). We note that we were unable to observe an interaction between PIM and the full-length THR protein. The considerable size of full-length THR 1–1379 might preclude expression of sufficiently high levels and/or entry into the nucleus.

Finally, we tested for a direct interaction between THR and SSE. The THR fragment 1–933 was found to interact with full-length SSE, SSE 1–247, and SSE 1–467. These results therefore raise the possibility that THR and PIM bind to the same region of SSE and thus might be competing in vivo. Moreover, the interactions between THR and SSE appeared to be weaker than the interactions between PIM and SSE, as in the former case, only one of the two reporter genes was activated. We were not able to define the region in THR that mediates SSE binding in more detail, because the shorter constructs THR 1–476, THR 208–933, and THR 477–933 failed to bind to SSE (data not shown).

Taken together, the results of our two-hybrid experiments show that all three proteins, PIM, THR, and SSE can interact independently with each other.

To confirm that PIM, THR, and SSE interact in vivo, we performed coimmunoprecipitation experiments. Two antibodies against SSE were raised and affinity purified. In embryo extracts, these antibodies detected a prominent band at 75 kD, which comigrated with SSE

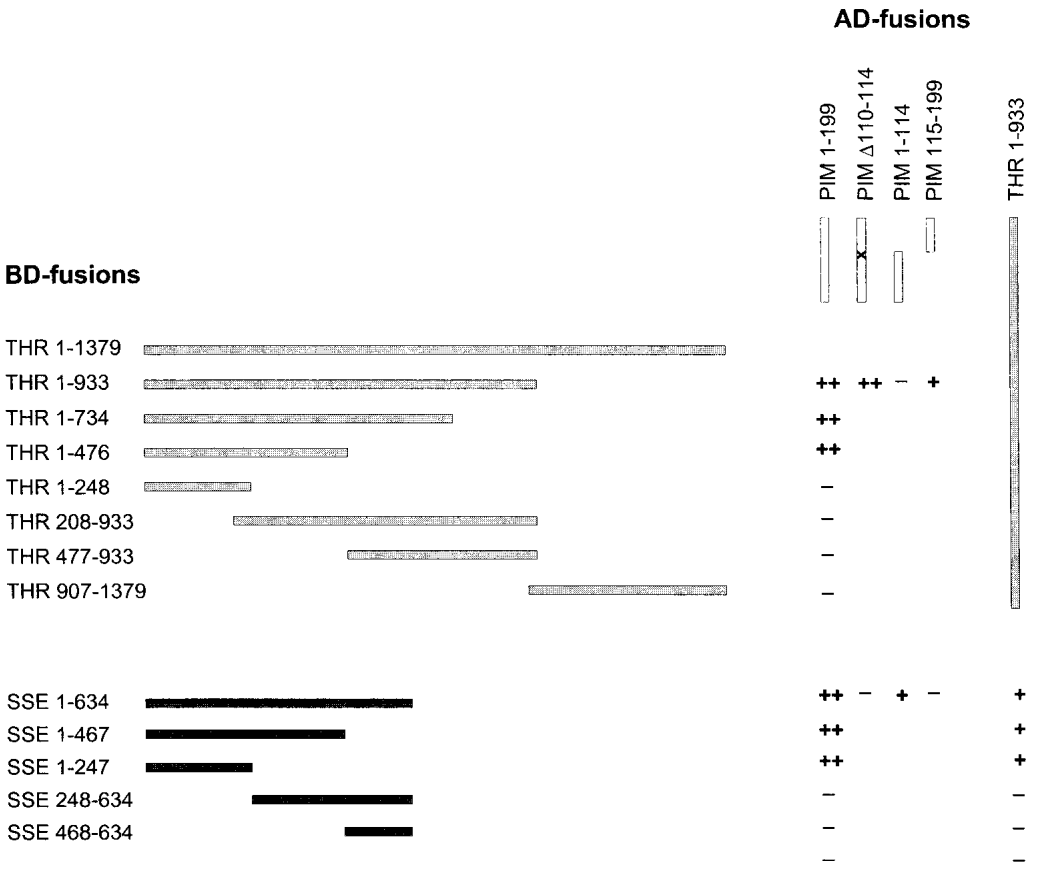

Figure 3. Interactions of PIM, THR, and SSE in the yeast two-hybrid system. Various deletion constructs of PIM (open bars), THR (light gray bars), and SSE (dark gray bars) were constructed as translational fusions with the GAL4 activation domain (AD-fusions) or with the GAL4 DNA-binding domain (BD-fusions). Interactions were scored as ++, if both GAL4 responsive reporter genes were activated by the respective combination and as – if no marker gene was activated. Activation of one reporter gene was scored as +.

translated in vitro (data not shown). This band was also detected in immunoprecipitates that were isolated with an anti-myc antibody from extracts of embryos expressing PIM or THR fused with myc epitope tags (Fig. 4A). Control experiments indicated that coimmunoprecipitation of SSE with PIM–myc and THR–myc is specific. This specific association was also observed when the antibodies against SSE were used for immunoprecipitation followed by immunoblotting with anti-myc (Fig. 4B). Taken together, these results clearly show that SSE associates in vivo with PIM and THR.

The interaction between THR and SSE observed in the yeast two-hybrid experiments was weak, raising the possibility that it might not be sufficiently strong to allow formation of THR–SSE complexes in vivo. PIM might therefore be required to bring THR and SSE together. To evaluate whether THR–SSE complexes can be formed in the absence of PIM in vivo, we expressed *gUAS–thr–myc* and *UAS–HA–Sse* in late embryos when endogenous PIM and THR levels are very low (D'Andrea et al. 1993; Stratmann and Lehner 1996; H. Jäger, A. Herzig, C.F. Lehner, and S. Heidmann, unpubl.). After precipitation of HA–SSE with an anti-HA antibody, we detected THR–myc as well as minor amounts of PIM in the immunoprecipitates (Fig. 5A). Quantitative immunoblotting revealed that THR–myc was present in an at least fivefold molar excess over PIM in these immunoprecipitates (Fig. 5A). Because THR does not form oligomers (Leismann et al. 2000), we conclude that THR and SSE can associate in the absence of PIM.

To investigate whether PIM is able to bind to SSE in the absence of THR in vivo, we performed a complementary experiment by expressing *UAS–HA–Sse* and *UAS–pim–myc* in late embryos (Fig. 5B). Surprisingly, in contrast to the results of the yeast two-hybrid experiments, only minor amounts of PIM–myc could be coprecipitated with SSE (Fig. 5B, lanes SP). However, simultaneous coexpression of *gUAS–thr–myc*, *UAS–HA–Sse*, and *UAS–pim–myc* resulted in the recovery of significant PIM levels (Fig. 5B, lanes SPT). We estimate that <10% of PIM is precipitated in the absence of THR when compared with the amount precipitated in the presence of THR. Significantly, PIM^2–myc does not form a stable complex with HA–SSE, even in the presence of THR (Fig. 5B, lanes SP2T). These results indicate that PIM, THR, and SSE form a trimeric complex in vivo, and that SSE is not sufficient to recruit PIM in the absence of THR. This notion was supported by the behavior of a THR deletion

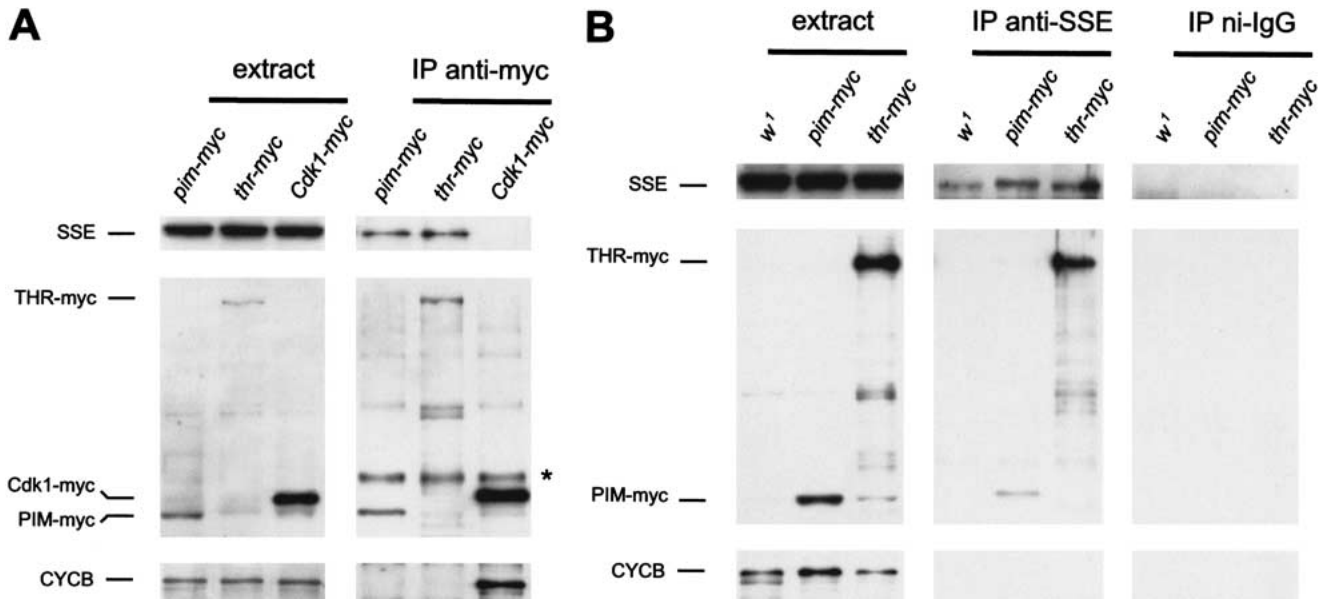

Figure 4. SSE forms complexes with PIM and THR in vivo. Extracts (extract) were prepared from embryos expressing either no transgene (w^1), *gpim–myc* (*pim–myc*), *gthr–myc* (*thr–myc*), or *Cdk1–myc* (*Cdk1–myc*). These extracts, as well as anti-myc (IP anti-myc) (*A*) or anti-SSE (IP anti-SSE) and rabbit nonimmune IgG (IP ni-IgG) (*B*) immunoprecipitates isolated from these extracts, were analyzed by immunoblotting with antibodies against SSE (*top*), the myc-epitope (*middle*), or Cyclin B (*bottom*). (*) Signal caused by IgG heavy chains of the anti-myc antibodies.

mutant (THR 445–1379–myc), which was lacking the region required for the two-hybrid interaction with PIM. When this mutant protein was expressed from a transgene under the control of the normal *thr* regulatory region and immunoprecipitated from embryo extracts, we detected almost no coimmunoprecipitation of PIM (Fig. 5C, lane 6). However, SSE was readily detected in the immunoprecipitates, confirming that THR and SSE can form a complex without PIM. Quantitative immunoblotting experiments indicated that SSE associates with THR 445–1379–myc with at least 50% efficiency when compared with its binding to full-length THR, whereas binding of PIM to THR 445–1379–myc was reduced to <5% (data not shown). On the basis of the results of our two-hybrid experiments, in which SSE interacts strongly with PIM, the SSE present in the THR 445–1379–myc immunoprecipitates would be expected to result in coimmunoprecipitation of PIM as well. However, the absence of PIM in the immunoprecipitates suggests that PIM cannot join SSE and THR in a trimeric complex when it is not bound by THR. Control experiments with THR–myc versions that contained the N-terminal PIM-binding region showed that coimmunoprecipitation of PIM along with SSE can be readily detected in these cases (Fig. 5C, lanes 3,4).

THR 1–478–myc did not form complexes with PIM in vivo, whereas THR 1–476 and PIM associate in our yeast two-hybrid experiments (Fig. 3). This discrepancy might result from different positions of the fused tags. Whereas in the two-hybrid experiments, the GAL4-binding domain was fused to the N terminus, the 10 myc epitope tags were fused to the C terminus of the THR fragment analyzed in *Drosophila* embryos. The C-terminal myc tags, therefore, might interfere with PIM binding to THR 1–478–myc.

The C-terminal fragment THR 932–1379–myc did not bind PIM or SSE, as expected from the yeast two-hybrid analysis. This fragment was present at very low levels in the embryo extracts as determined for four independent transgenic lines. This low abundance is presumably due to protein instability, as all genomic THR constructs contained identical 5′- and 3′-noncoding regulatory sequences. We also did not detect coimmunoprecipitation of PIM or SSE when loading was adjusted to compensate for the low abundance of THR 932–1379–myc (data not shown).

In summary, the behavior of THR fragments expressed in embryos during the proliferative stages extended our findings resulting from yeast two-hybrid experiments. We observe that the THR–SSE interaction is not necessarily mediated by PIM. Furthermore, our results show that the binding of PIM to SSE requires THR, strongly suggesting the existence of trimeric PIM–THR–SSE complexes in vivo.

Discussion

Our study shows that *Drosophila* Separase (SSE) is required for sister chromatid separation during mitosis, as shown previously in lower eukaryotes. However, we also show that this essential protease and its regulatory subunits have evolved rapidly, particularly in *Drosophila*, presumably to allow for more sophisticated regulation.

Drosophila SSE contains a C-terminal region with significant similarity to a cysteine endoprotease domain,

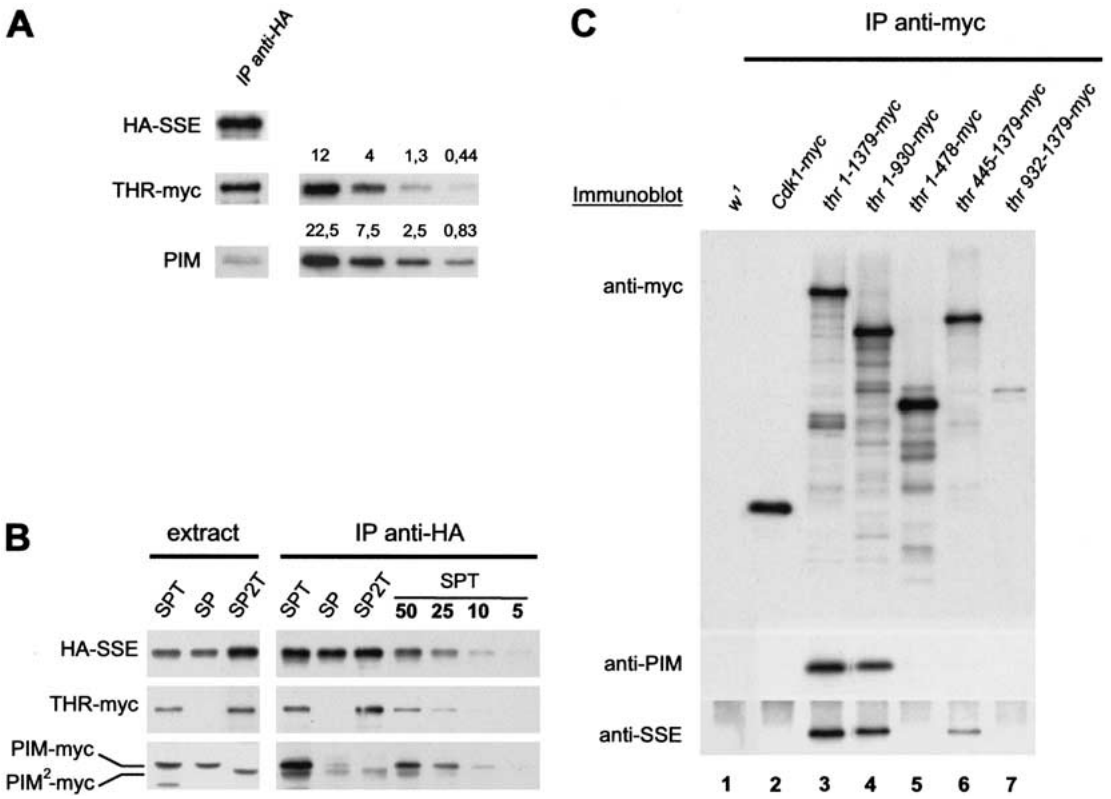

Figure 5. PIM, THR, and SSE form a trimeric complex. (*A*) An extract was prepared from embryos 12–15 h after egg deposition expressing *UAS–thr–myc* and *UAS–HA–Sse* under the control of *da–GAL4*, and was used for anti-HA immunoprecipitation. The precipitate was analyzed by immunoblotting with anti-HA (HA–SSE), anti-THR (THR–myc), and anti-PIM (PIM) antibodies (*left*). For quantitation, a dilution series of a mixture containing bacterially expressed full-length PIM and a THR fragment was loaded on the same gels (*right*). The corresponding *left* and *right* panels show identical exposures of the same blot. The amount of the proteins is given in fmole. (*B*) Extracts were prepared and analyzed as in *A* from embryos coexpressing either *UAS–HA–Sse*, *UAS–pim–myc* and *gUAS–thr–myc* (SPT), *UAS–HA–Sse* and *UAS–pim–myc* (SP), or *UAS–HA–Sse*, *UAS–pim*^{2}*–myc* and *gUAS–thr–myc* (SP2T). For quantification of precipitated proteins, a dilution series of the anti-HA immunoprecipitate from the SPT extract was loaded onto the same gel. The numbers represent percentage values. (*C*) Extracts were prepared from embryos expressing either no transgene (*w*^{1}), *Cdk1–myc* (*Cdk1–myc*), *gthr–myc* (*thr 1–1379–myc*), *thr 1–930–myc* (*thr 1–930–myc*), *gthr 1–478–myc* (*thr 1–478–myc*), *gthr 445–1379–myc* (*thr 445–1379–myc*), or *gthr 932–1379–myc* (*thr 932–1379–myc*), and were used for the isolation of anti-myc immunoprecipitates, which were analyzed by immunoblotting with antibodies against the myc-epitope (*top*), PIM (*middle*), or SSE (*bottom*).

which is found in the C-terminal region of all separases. Whereas this SSE region includes an invariant histidine as well as the putative catalytic cysteine residue that we show to be required for function, it diverges significantly from the other separases in two additional conserved sequence blocks. One of these blocks is functionally important in budding yeast and has been proposed to represent a Ca^{2+}-binding motif (Uzawa et al. 1990; Jensen et al. 2001). The *Drosophila* SSE sequence does not contain this Ca^{2+}-binding motif. If separase activity is regulated by binding of Ca^{2+} to the conserved region in the C terminus, then *Drosophila* SSE activity may be regulated by Ca^{2+} binding to (an) accessory protein(s). Another striking difference is the smaller size of SSE when compared with other separases. However, our genetic analysis clearly shows that SSE is required for sister chromatid separation.

Mutants, which cannot express functional *Sse* zygotically, complete embryogenesis presumably using the maternal *Sse* contribution. During the larval stages, however, the mitotically proliferating imaginal cells are specifically affected in these mutants. Our cytological analysis of larval brains confirmed the findings first described by Gatti and Baker (1989) for the mutant *l(3)13m-281*, which we show here to reflect a complete loss of zygotic *Sse* function. Mitotic cells in *Sse* mutant larvae contain endoreduplicated chromosomes with supernumerary arms all connected primarily in a centromeric region. Such chromosomes are also observed in embryos with mutations in the genes *pim* or *thr*, which are required for sister chromatid separation (D'Andrea et al. 1993; Stratmann and Lehner 1996), and which encode proteins that bind to SSE.

It is conceivable that in *pim* and *thr* mutants, SSE is destabilized, resulting in the failure to separate sister chromatids, which would explain the requirement of PIM and THR function for sister chromatid separation. However, Western blot analyses of extracts prepared

from *pim* and *thr* mutant embryos show that SSE is still present in these mutants. We favor the possibility that in these mutants a regulatory function is affected, resulting in the absence of SSE activity.

The *pim*, *thr*, and *Sse* mutant phenotypes argue that SSE activity is required primarily for sister chromatid separation within the centromeric region. In contrast, entry into mitosis, including assembly of a mitotic spindle, chromosome condensation, and congression into a metaphase plate do not appear to depend on SSE activity. Moreover, the degradation of mitotic cyclins and exit from mitosis (chromosome decondensation, spindle disassembly, nuclear envelope formation) appear to occur with normal kinetics, even though sister chromatids fail to be separated and segregated to the spindle poles (D'Andrea et al. 1993; Philp et al. 1993; Stratmann and Lehner 1996). The defects in these mutants, therefore, do not appear to be detected by an efficient checkpoint mechanism comparable with the mitotic exit network of budding yeast (Cohen-Fix and Koshland 1999; Tinker-Kulberg and Morgan 1999). Cytokinesis is also attempted in *pim* and *thr* mutants, but cannot be completed. Whether the failure to complete cytokinesis is simply a consequence of the presence of nonseparated chromosomes within the equatorial plane or whether SSE activity is directly involved in cytokinesis, is not known and difficult to resolve. Another unresolved and difficult issue at present is the potential involvement of SSE activity in the control of anaphase spindle dynamics, which is suggested by analyses in yeast (Kumada et al. 1998; Uhlmann et al. 2000; Jensen et al. 2001).

The early onset of phenotypic abnormalities in *pim* and *thr* mutants reflects the rapid disappearance of maternally contributed wild-type products. This disappearance is rapid because PIM and THR are both partially degraded during exit from mitosis (Stratmann and Lehner 1996; Leismann et al. 2000; A. Herzig, C.F. Lehner, and S. Heidmann, unpubl.). In contrast, the late onset of phenotypic abnormalities in *Sse* mutants indicates that SSE is a stable protein. In fact, we have been unable to detect SSE degradation during mitosis by immunoblotting experiments. Unfortunately, our antibodies do not allow SSE detection by immunofluorescence, which might be more sensitive and could also provide information on subcellular localization. Nevertheless, our present evidence strongly argues against the idea that SSE activity is regulated by SSE degradation. Partial cleavage of human separase has been observed during exit from mitosis, but its significance is not yet known (Waizenegger et al. 2000). This mitotic cleavage of human separase occurs upstream of the conserved endoprotease domain and might therefore represent a mode of regulation that is not conserved.

During the divisions of *Drosophila* embryogenesis, we have not only failed to detect cleavage of SSE but also of the *Drosophila* homolog of the yeast cohesin subunit Scc1p (A. Herzig, C.F. Lehner, and S. Heidmann, unpubl.). As in vertebrate cells, most of the *Drosophila* Scc1p homolog has also been shown to dissociate from chromosomes already during prophase (Warren et al. 2000). However, some can be visualized in the centromeric region of metaphase chromosomes until the onset of anaphase. We assume that cleavage by SSE is responsible for the subsequent disappearance of this centromeric pool and that the sensitivity of our immunoblotting experiments is insufficient to detect the cleavage of this minor fraction. So far, it has been impossible to show SSE protease activity directly.

The fact that the majority of Scc1 is clearly not cleaved during mitosis in higher eukaryotes indicates that the regulation of SSE activity within the cell is presumably complex and targeted to the centromeric region. Although much further work remains to be done to understand SSE regulation in detail, some insights can be derived from our analysis of the interactions of SSE with PIM and THR (Fig. 6). We show that PIM associates with SSE in vivo. This result further supports the role of PIM as a *Drosophila* securin. According to two-hybrid experiments, PIM binds to the N-terminal region of SSE. The yeast securins also interact with the N-terminal regions of the separases (Kumada et al. 1998; Jensen et al. 2001). Surprisingly, however, neither the securins nor the N-terminal separase regions display sequence conservation (Uzawa et al. 1990; Zou et al. 1999). Equally surprising is the finding that THR is required for the association of PIM with SSE. Moreover, for efficient complex formation, PIM also requires to contact SSE, because PIM^2 is not efficiently incorporated in a trimeric complex, despite its ability to bind to THR. We assume therefore that a trimeric PIM–THR–SSE complex, as schematically illustrated in Figure 6, is formed during interphase and present during entry into mitosis.

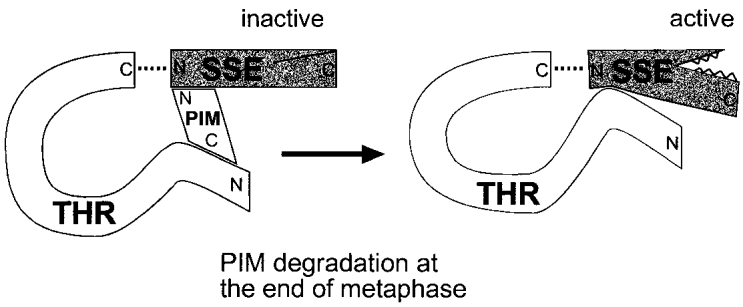

Figure 6. A model for the PIM–THR—SSE complex. In interphase cells, a trimeric complex composed of PIM (white), THR (light gray), and SSE (dark gray) is assembled, in which SSE is kept inactive. At the end of metaphase, PIM is degraded in an APC-dependent manner. This enables an activating contact between THR and SSE, allowing SSE to cleave its target, the *Drosophila* Scc1p cohesin subunit homolog, resulting in sister chromatid separation. The C terminus of THR is shown in association with the N terminus of SSE (broken lines) to illustrate the possibility that THR corresponds to the N terminus of separases from other organisms.

Although the analysis of the binding site for PIM in SSE is difficult in vivo because of the dependency on THR, our two-hybrid experiments indicate that PIM and THR might bind to the same region within SSE. Our model of the trimeric complex takes this into account by showing that PIM, and not THR, contacts SSE at its N terminus, and THR can only bind to this region of SSE after PIM has been degraded. However, PIM and THR interact with each other by use of binding sites that are distinct from those that contact SSE. SSE activity might be inhibited in the trimeric complexes because PIM prevents THR from providing an activating contact to SSE by competitive binding within the same SSE region. The mitotic degradation of PIM might then give way to the activating THR–SSE interaction, resulting in SSE activity at the onset of anaphase (Fig. 6).

We note some discrepancies between our two-hybrid results and those obtained in vivo by coimmunoprecipitation. Particularly, the strong interaction between PIM and SSE observed in yeast contrasts with the low abundance of PIM in SSE immunoprecipitates when almost no THR is present. We speculate that additional levels of regulation of complex formation may be present in the *Drosophila* embryo, which are lacking in yeast. Nevertheless, the PIM–SSE complex formation observed in yeast is likely to reflect a significant interaction, as PIM^2 does not associate with SSE in yeast, as it fails to do in the embryo.

We have speculated previously that an ancient separase gene might have broken into two genes during the evolution of *Drosophila* (Leismann et al. 2000). Accordingly, THR might correspond to the nonconserved N terminus and SSE to the conserved C-terminal endoprotease domain of the other separase proteins. This hypothesis predicts that the longer separase proteins might have two binding sites for securin. The published interaction studies do not rigorously exclude this possibility. The fact that the C-terminal acidic region of the *Drosophila* securin PIM interacts with THR, whereas the C-terminal acidic regions of yeast securins interact with the N-terminal nonconserved separase regions (Kumada et al. 1998; Jensen et al. 2001) is consistent with this hypothesis.

We emphasize that our suggestions (Fig. 6) are speculative. Moreover, important issues are not resolved by these hypotheses. For instance, they do not address why PIM is required for sister chromatid separation. PIM might be responsible for targeting SSE to specific subcellular locations, just like the yeast securins are required for spindle association or nuclear localization of the associated separases (Kumada et al. 1998; Jensen et al. 2001). Furthermore, if in fact a complex pathway controls SSE activation, the inactivation process is also an important issue that needs to be addressed. The requirement for an especially efficient SSE inactivation during the extremely rapid syncytial division cycles at the onset of embryogenesis might explain the particular high divergence of SSE and its regulators in *Drosophila*. This mechanism of regulation might be typical for insects and SSE might therefore be an interesting target for insecticide compounds.

Materials and methods

Fly stocks

For expression of UAS transgenes, we used *da–GAL4* G32 (Wodarz et al. 1995) and *arm–GAL4* (Sanson et al. 1996). *UAS–Cdk1–myc* and *UAS–pim–myc*, as well as *gpim–myc* and *gthr–myc* lines, which allow expression of myc-tagged products under the control of the normal genomic regulatory regions, have been described previously (Stratmann and Lehner 1996; Leismann et al. 2000). All of the myc-tagged products are capable of rescuing complete loss-of-function mutations in the corresponding genes.

UAS–HA–Sse lines were obtained after P-element-mediated germ-line transformation with a pUASP (Rørth 1998) construct following standard procedures. A fragment encoding six HA epitopes was amplified by PCR from the plasmid pWZV90 (Knop et al. 1999) and inserted into an *Age*I site downstream of the translational start codon of an *Sse* cDNA. Several *Sse* cDNAs were isolated from a *Drosophila* embryo cDNA library (Brown and Kafatos 1988) by use of radioactively labeled primers derived from genomic sequences determined by the Berkeley *Drosophila* Genome Project (BDGP) and identified by BLAST searches using separase sequences from other species. The sequence of these cDNAs confirmed the exon/intron structure predicted by the sequence of a single expressed sequence tag (LD08709) identified by the BDGP and the sequence (CT29682) predicted by the BDGP from the genomic sequence for the *Sse* gene (*CG10583*). For the generation of *UAS–HA–*Sse^{C497S} lines, we used an analogous construct in which a single codon was mutated using the QuikChange site-directed mutagenesis kit (Stratagene). The details of these and of the following plasmid constructions are available on request. PCR products for generation of expression constructs (bacterial, yeast, and fly) were obtained by use of *Pfu* polymerase (Stratagene), and sequenced.

Lines carrying *gSse* were generated by use of the germ-line transformation vector pP{w^{+mc}, 3×P3-EYFPaf} (Horn and Wimmer 2000), a 10-kb genomic Sse^{+} fragment assembled from a PCR fragment containing 5.4 kb of upstream regulatory sequences amplified from genomic DNA, a restriction fragment containing the complete coding sequences, and 2.3 kb of downstream sequences derived from a clone isolated from a *Drosophila* genomic lambda DASH library.

Lines allowing Gal4-dependent expression of *thr* fused to 10 myc epitopes at the C terminus (*gUAS–thr–myc*) were obtained with a modified *gthr–myc* construct (Leismann et al. 2000). Briefly, a PCR fragment encompassing the five UAS_{GAL4} sites and the *Hsp70* basal promoter was amplified from pUAST (Brand and Perrimon 1993) and cloned upstream of the *thr* translational initiation codon. Lines allowing Gal4-dependent expression of *pim* fused to six myc epitopes at the C terminus (*UAS–pim–myc*) have been described previously (Leismann et al. 2000). For the construction of the *UAS–*pim^2*–myc* transgene, we replaced a *Sex*AI/*Hin*dIII restriction fragment in *pim–myc* with a corresponding fragment that was excised from plasmid $pim^2 1 \times 1$, containing a 15-bp in-frame deletion coding for amino acids 110–114 of PIM.

Various lines (*gthr 1–478–myc*, *gthr 1–930–myc*, *gthr 445–1379–myc*, *gthr 932–1379–myc*) expressing truncated THR proteins fused C-terminally to 10 copies of the myc epitope were also generated with modified *gthr–myc* constructs. In the case of *gthr 1–930–myc*, we obtained only a single line, which did not express the transgene, presumably because of the toxicity of the transgene product. Therefore, using pUAST, we generated *UAS–thr 1–930–myc*, allowing conditional Gal4-dependent expression.

Deficiencies deleting *Sse* were isolated as male recombinants as described (Preston and Engels 1996; Preston et al. 1996) after mobilizing the P-element EP(3)0915 inserted in *CG17334*. This adjacent gene, downstream of *Sse*, encodes a potential cold-shock protein with similarity to the heterochronic *lin-28* gene product of *Caenorhabditis elegans*. EP(3)0915 homozygotes are viable and fertile without visible phenotypes, suggesting that *CG17334* is not an essential gene. Virgin EP(3)0915 females were crossed to *+/CyO*, *Δ2–3; ve st e/TM3*, *Ser* males. Of the progeny, 250 *+/CyO*, *Δ2–3; EP(3)0915/ve st e* male individuals were crossed to 500 *ve st e* virgin females. A total of 40,000 progeny were scored for recombination of the markers *ve* and *e* flanking *EP(3)0915*. A total of 71 out of 233 recombinants were ve^{+} *e*, indicating a recombination event at the right end of *EP(3)0915* (Preston et al. 1996). Six of the seventy-one recombinant chromosomes were lethal when homozygous or hemizygous over *Df(3L)ZN47*, which deletes a large region on the left arm of the third chromosome, including *Sse*. Animals carrying any of the six recombinant chromosomes were viable when transheterozygous with the lethal P-element insertion *l(3)02331* located ~110 kb proximal to the *EP(3)0915* insertion. Recombinants isolated after mobilization of P elements in the male germ line often have chromosomal deletions on one side of the P-element insertion, which is usually retained (Preston et al. 1996). For a molecular characterization of the recombinants by sequence analysis, therefore, we recovered DNA from five lines by plasmid rescue. Four of the lines were found to have deficiencies deleting more than 100 kb, and one line, *Df(3L)SseA*, carried a smaller deletion of 34 kb. This deletion encompasses part of *CG17334,* the complete *Sse* gene and part of *still life* (*sif*). Individuals homozygous for a *sif* null mutation are viable (Sone et al. 2000). The absence of the *Sse* coding region in *Df(3L)SseA* was further confirmed by PCR analysis of genomic DNA obtained from homozygous deficient larvae.

The EMS induced recessive lethal mutation *l(3)13m-281*, designated here as Sse^{13m}, was kindly provided by M. Gatti (University La Sapienza, Rome). Standard genetic complementation tests indicated that Sse^{13m} does not complement *Df(3L)SseA* and *Df(3L)ZN47*, whereas it did complement the deficiencies *Df(3L)h-i22* and *Df(3L)Scf-R6*, which delete regions in which Sse^{13m} originally had been mapped by meiotic recombination. To characterize the *Sse* sequence present on the Sse^{13m} chromosome, we amplified the coding region by PCR and sequenced the cloned products from three independent amplification reactions. In all three cases, a 4-bp deletion in exon 6 was detected 7 bp downstream of the triplet encoding the essential histidine residue of the presumptive separase catalytic dyad. The predicted C-terminal sequence encoded by Sse^{13m} starting from the essential histidine, is, therefore, HGSGSTSMVA.

Sequence comparison

TBLASTN searches of the nr and htgs databases of GenBank, of *Drosophila* sequences deposited at the BDGP Blast server, and of the assembled cDNA sequences available at The Institute of Genomic Research (TIGR; http://www.tigr.org/tdb/tgi.shtml) by using, as query, the C-terminal regions of human and fungal separase proteins. A multiple sequence alignment of the C-terminal regions of the various separase homologs was performed by using CLUSTALW (http://www2.ebi.ac.uk/clustalw/) with default parameters. A shaded display was obtained by using Boxshade version 3.21. A tree was drawn using the PILEUP program of the GCG program package with default parameters.

The sources for the sequence comparison were as follows: *C. elegans* 1 (AAF60651), *C. elegans* 2 (T27859), *Trypanosoma brucei* (CAB95528), *Leishmania major* (conceptual translation of a region of AL499620, position 1003853–1007689), *Saccharomyces cerevisiae* Esp1 (S64403), *Schizosaccharomyces pombe* Cut1 (A35694), *Emericella nidulans* BimB (P33144), and *Homo sapiens* (BAA11482). The partial sequences of *Mus musculus*, *Rattus norvegicus* and *Xenopus laevis* separases are conceptual translations of assembled cDNAs obtained from the TIGR Gene Index website (see above) and have the accession numbers TC120478, TC143396, and TC5660, respectively. The *Arabidopsis thaliana* separase homolog (CAA19812) is a hypothetical protein sequence deduced from genomic sequence. However, this protein sequence lacks the highly conserved cysteine residue and surrounding invariant residues. Assuming an alternative splice acceptor of an intron located in this region, the sequence GAQYIPRREIEKLDNCSATFLMGCSSGSLWLKGCYIP QGVPLSYLL can be inserted in frame at position 1635 of CAA19812, thus restoring the conserved region.

Yeast two-hybrid experiments

Protein–protein interactions were analyzed using the Matchmaker Two-Hybrid system and the yeast strain AH109 (Clontech). Interactions were scored by analysis of growth of transformants on medium selecting for the activation of the *HIS3* or *ADE2* genes. To evaluate the strength of interactions, we supplemented plates lacking histidine with varying amounts of 3-aminotriazole (3-AT). For control experiments, we used plasmids encoding the SV40 T-Antigen fused to the GAL4 activation domain (pGADT7-T) or p53 fused to the GAL4 DNA-binding domain (pGBKT7-p53).

The initial THR deletion constructs were cloned as fusions with the Gal4p DNA-binding domain into pGBKT7 (Clontech). To obtain fusions of THR fragments with the Gal4 activation domain, the respective deletion constructs were excised as *Nco*I–*Bam*HI fragments from the individual pGBKT7–THR constructs and cloned into pGADT7.

The *pim* coding region was cloned in frame into the vector pGADT7. From the resulting construct pGADT7–PIM, we constructed pGADT7–PIM^2 using the QuikChange mutagenesis kit to delete the 15 nucleotides coding for amino acids 110–114 (FPNEK). pGADT7–PIM 1–114 was constructed by subcloning a PCR fragment. In pGAD–PIM 115–199, the C-terminal part of the PIM coding region was fused at its C terminus to the Gal4p activation domain, in contrast to all our other pGADT7 constructs in which the Gal4p activation domain is N-terminal. The *Sse* constructs were generated with pGBKT7 and appropriate PCR fragments.

Immunoprecipitation, immunoblotting, and immunolabeling

Antibodies against phospho-histone H3 (Upstate Biotechnology) and secondary antibodies (Jackson Immunoresearch) were obtained commercially. The antibodies against the human c-myc epitope (mAb 9E10; Evan et al. 1985), the HA epitope (mAb 12CA5; Niman et al. 1983), *Drosophila* Cyclin B (Knoblich and Lehner 1993), PIM (Stratmann and Lehner 1996), and THR (Leismann et al. 2000) have been described previously. An additional rabbit antiserum against PIM was raised and used for immunoblotting in a dilution 1:3000 without further purification.

For the generation of antibodies against SSE, we expressed an N-terminal SSE region (amino acids 1–281) with a hexahistidine tag in bacteria using a pQE30 (QIAGEN) construct. The fusion protein was purified by Ni^{2+} affinity chromatography and used for the immunization of two rabbits. The immune sera were

affinity purified using antigen immobilized on BrCN-activated sepharose (Sigma).

For the coimmunoprecipitation experiments shown in Figure 4, we collected eggs from either w^1, or *UAS–Cdk1–myc* II.2/*CyO*; *arm–GAL4*, or *gpim–myc* 3A, or *gthr–myc* III.1 flies for 3 h on apple juice agar plates and aged them for 3 h at 25°C before extract preparation. After dechorionization, the embryos were homogenized in 4 vol of lysis buffer (50 mM HEPES at pH 7.5, 60 mM NaCl, 3 mM $MgCl_2$, 1 mM $CaCl_2$, 0.2% Triton X-100, 0.2% Nonidet NP-40, 10% glycerol, 1 mM DTT, 2 mM Pefabloc, 2 mM Benzamidin, 10 µg/mL Aprotinin, 2 µg/mL Pepstatin A, 10 µg/mL Leupeptin). The extracts were cleared by centrifugation and the supernatants were used for immunoprecipitation with the anti-myc antibody, nonimmune IgG from rabbits (Jackson Immunoresearch), immunopurified anti-SSE antibody bound to Protein A-Sepharose 6MB beads (Amersham Pharmacia Biotech), or CL4B beads (Sigma). The immunoprecipitates were analyzed by immunoblotting by use of horseradish peroxidase-coupled secondary antibodies followed by ECL detection (Amersham Pharmacia Biotech).

For the coimmunoprecipitation experiment shown in Figure 5C, eggs were collected from either w^1, or *UAS–Cdk1–myc* II.2/*CyO*; *arm–GAL4*, or *gthr–myc* III.1, or *thr 1–478–myc* III.1, or *thr 445–1379–myc* III.1, or *thr 932–1379–myc* III.1 flies, or from a cross of *UAS–thr 1–930–myc* III.1 and *da–GAL4* flies. For the analysis of complex formation of THR, PIM, and SSE in late embryos (Fig. 5A,B), we prepared extracts from 12- to 15-hour-old embryos derived from crosses of *daGAL4* G32 males with *UAS–HA–Sse* I.1;*stg*, gUAS–thr–myc III.!/TM3, *Ser* or *UAS–HA–Sse* I.1;*stg*, *UAS–pim–myc* III.2/*TM3*, *Ser* or *UAS–HA–Sse* I.1;*stg*, *gUAS–thr–myc* III.1, *UAS–pim–myc* III.2/*TM3*, *Ser* or *UAS–HA–Sse* I.1;*stg*, *gUAS–thr–myc* III.1, *UAS–*pim^2*–myc* III.1/*TM3*, *Ser* females. The embryos were treated and extracts were prepared and analyzed as detailed above. To allow an estimation of the amounts of coprecipitated THR–myc and PIM in the experiment shown in Figure 5A, we loaded onto the same gel a dilution series of a mixture of bacterially expressed full-length protein (PIM) and a C-terminal protein fragment (THR), both of which had been used to raise the antibodies (Leismann et al. 2000). The amounts of protein in this mixture was determined by comparison with protein standards in Coomassie-stained gels. After immunoblotting and detection with ECL, signal intensities of the precipitated protein were compared with the dilution series on nonsaturated exposures.

For the analysis of mitotic cells in larval brains, we dissected these organs from early second instar (48–50 h) and third instar wandering stage larvae. The following genotypes were analyzed: *Df(3L)SseA*, and Sse^{13m}, and *Df(3L)SseA*/Sse^{13m}, and *UAS–HA–Sse* I.1/+; *da–GAL4* G32, *Df(3L)SseA*/*Df(3L)SseA*, and *UAS–HA–Sse* I.1/+; *da–GAL4* G32, *Df(3L)SseA*/Sse^{13m}, and *UAS–HA–*Sse^{C497S}/+; *da–GAL4* G32, *Df(3L)SseA*/Sse^{13m}. These larvae were derived from parents carrying *TM3*, *Ser*, *Act5c–GFP*, which allowed for an identification of individuals lacking endogenous Sse^+ gene function as well as Sse^+ siblings by analyzing GFP fluorescence. Brains were fixed and immunostained as described (Gonzalez and Glover 1993). Double labeling of DNA was achieved with Hoechst 33258. For squash preparations to visualize individual chromosomes, brains from second instar larvae of the genotype *Df(3L)SseA*/Sse^{13m}, and *Df(3L)SseA*/*TM3*, *Ser*, *Act5c–GFP*, or Sse^{13m}/*TM3*, *Ser*, *Act5c–GFP* were prepared. The dissection of brains and subsequent treatment with a hypotonic shock were essentially performed according to Pimpinelli et al. (2000). Fixation and squashing of the brains and staining of DNA with Hoechst 33258 was done according to Gonzales and Glover (1993).

Acknowledgments

We thank M. Gatti for providing *l(3)13m-281* and the staff at the Bloomington and Szeged stock centers for various fly stocks. We thank J. Höflich, M. Schleichert, M. Siedler, A. Uhmann, and O. Leismann for help with the construction of various plasmids, transgenic strains, and with the production of antibodies against SSE. We acknowledge the help provided by BDGP. The work was supported by a DFG fellowship for H.J. (Graduiertenkolleg 190) and DFG grants (DFG Le 987/2–1 and DFG Le 987/3–1).

The publication costs of this article were defrayed in part by payment of page charges. This article must therefore be hereby marked "advertisement" in accordance with 18 USC section 1734 solely to indicate this fact.

References

Brand, A.H. and Perrimon, N. 1993. Targeted gene expression as a means of altering cell fates and generating dominant phenotypes. *Development* **118:** 401–415.

Brown, N.H. and Kafatos, F.C. 1988. Functional cDNA libraries from *Drosophila* embryos. *J. Mol. Biol.* **203:** 425–437.

Ciosk, R., Zachariae, W., Michaelis, C., Shevchenko, A., Mann, M., and. Nasmyth, K. 1998. An ESP1/PDS1 complex regulates loss of sister chromatid cohesion at the metaphase to anaphase transition in yeast. *Cell* **93:** 1067–1076.

Cohen-Fix, O. and Koshland, D. 1999. Pds1p of budding yeast has dual roles: Inhibition of anaphase initiation and regulation of mitotic exit. *Genes & Dev.* **13:** 1950–1959.

D'Andrea, R.J., Stratmann, R., Lehner, C.F., John, U.P., and Saint, R. 1993. The *three rows* gene of *Drosophila melanogaster* encodes a novel protein that is required for chromosome disjunction during mitosis. *Mol. Biol. Cell* **4:** 1161–1174.

Dej, K.J. and Orr-Weaver, T.L. 2000. Separation anxiety at the centromere. *Trends Cell. Biol.* **10:** 392–399.

Evan, G.I., Lewis, G.K., Ramsay, G., and Bishop, J.M. 1985. Isolation of monoclonal antibodies specific for human c-myc proto-oncogene product. *Mol. Cell. Biol.* **5:** 3610–3616.

Funabiki, H., Kumada, K., and Yanagida, M. 1996. Fission yeast Cut1 and Cut2 are essential for sister separation, concentrate along the metaphase spindle and form large complexes. *EMBO J.* **15:** 6617–6628.

Gatti, M. and Baker, B.S. 1989. Genes controlling essential cell-cycle functions in *Drosophila melanogaster*. *Genes & Dev.* **3:** 438–453.

Gonzalez, C. and Glover, D.M. 1993. Techniques for studying mitosis in *Drosophila*. In *The cell cycle: A practical approach* (ed. E. Brookes and D. Fantes), pp. 143–175. IRL press, Oxford, UK.

Guacci, V., Koshland, D., and Strunnikov, A. 1997. A direct link between sister chromatid cohesion and chromosome condensation revealed through the analysis of MCD1 in *S. cerevisiae*. *Cell* **91:** 47–57.

Hirano, T. 2000. Chromosome cohesion, condensation, and separation. *Annu. Rev. Biochem.* **69:** 115–144.

Horn, C. and Wimmer, E.A. 2000. A versatile vector set for animal transgenesis. *Dev. Genes Evol.* **210:** 630–637.

Jensen, S., Segal, M., Clarke, D.J., and Reed, S.I. 2001. A novel role of the budding yeast separin Esp1 in anaphase spindle elongation: Evidence that proper spindle association of Esp1 is regulated by Pds1. *J. Cell Biol.* **152:** 27–40.

Knoblich, J.A. and Lehner, C.F. 1993. Synergistic action of *Drosophila* cyclin A and cyclin B during the G2-M transition. *EMBO J.* **12:** 65–74.

Knop, M., Siegers, K., Pereira, G., Zachariae, W., Winsor, B.,

Nasmyth, K., and Schiebel, E. 1999. Epitope tagging of yeast genes using a PCR-based strategy: More tags and improved practical routines. *Yeast* **15:** 963–972.

Koshland, D.E. and Guacci, V. 2000. Sister chromatid cohesion: The beginning of a long and beautiful relationship. *Curr. Opin. Cell Biol.* **12:** 297–301.

Kumada, K., Nakamura, T., Nagao, K., Funabiki, H., Nakagawa, T., and Yanagida, M. 1998. Cut1 is loaded onto the spindle by binding to Cut2 and promotes anaphase spindle movement upon Cut2 proteolysis. *Curr. Biol.* **8:** 633–641.

Leismann, O., Herzig, A., Heidmann, S., and Lehner, C.F. 2000. Degradation of *Drosophila* PIM regulates sister chromatid separation during mitosis. *Genes & Dev.* **14:** 2192–2205.

Losada, A., Hirano, M., and Hirano, T. 1998. Identification of *Xenopus* SMC protein complexes required for sister chromatid cohesion. *Genes & Dev.* **12:** 1986–1997.

Michaelis, C., Ciosk, R., and Nasmyth, K. 1997. Cohesins: Chromosomal proteins that prevent premature separation of sister chromatids. *Cell* **91:** 35–45.

Nasmyth, K., Peters, J.M., and Uhlmann, F. 2000. Splitting the chromosome: Cutting the ties that bind sister chromatids. *Science* **288:** 1379–1385.

Niman, H.L., Houghten, R.A., Walker, L.E., Reisfeld, R.A., Wilson, I.A., Hogle, J.M., and Lerner, R.A. 1983. Generation of protein-reactive antibodies by short peptides is an event of high frequency: Implications for the structural basis of immune recognition. *Proc. Natl. Acad. Sci.* **80:** 4949–4953.

Philp, A.V., Axton, J.M., Saunders, R.D.C., and Glover, D.M. 1993. Mutations in the *Drosophila melanogaster* gene *three rows* permit aspects of mitosis to continue in the absence of chromatid segregation. *J. Cell Sci.* **106:** 87–98.

Pimpinelli, S., Bonaccorsi, S., Fanti, L., and Gatti, M. 2000. Preparation and analysis of *Drosophila* mitotic chromosomes. In Drosophila *protocols*. (eds. W. Sullivan, M. Ashburner, and R.S. Hawley), pp. 3–23. Cold Spring Harbor Laboratory Press, Cold Spring Harbor, New York.

Preston, C.R. and Engels, W.R. 1996. P-element-induced male recombination and gene conversion in *Drosophila*. *Genetics* **144:** 1611–1622.

Preston, C.R., Sved, J.A., and Engels, W.R. 1996. Flanking duplications and deletions associated with P-induced male recombination in *Drosophila*. *Genetics* **144:** 1623–1638.

Rørth, P. 1998. Gal4 in the *Drosophila* female germline. *Mech. Dev.* **78:** 113–118.

Sanson, B., White, P., and Vincent, J.P. 1996. Uncoupling cadherin-based adhesion from wingless signalling in *Drosophila*. *Nature* **383:** 627–630.

Skibbens, R.V., Corson, L.B., Koshland, D., and Hieter, P. 1999. Ctf7p is essential for sister chromatid cohesion and links mitotic chromosome structure to the DNA replication machinery. *Genes & Dev.* **13:** 307–319.

Sone, M., Suzuki, E., Hoshino, M., Hou, D., Kuromi, H., Fukata, M., Kuroda, S., Kaibuchi, K., Nabeshima, Y., and Hama, C. 2000. Synaptic development is controlled in the periactive zones of *Drosophila* synapses. *Development* **127:** 4157–4168.

Stratmann, R. and Lehner, C.F. 1996. Separation of sister chromatids in mitosis requires the *Drosophila* pimples product, a protein degraded after the metaphase anaphase transition. *Cell* **84:** 25–35.

Sumara, I., Vorlaufer, E., Gieffers, C., Peters, B.H., and Peters, J.M 2000. Characterization of vertebrate cohesin complexes and their regulation in prophase. *J. Cell Biol.* **151:** 749–762.

Tang, T.T., Bickel, S.E., Young, L.M., and Orr-Weaver, T.L. 1998. Maintenance of sister-chromatid cohesion at the centromere by the *Drosophila* MEI-S332 protein. *Genes & Dev.* **12:** 3843–3856.

Tinker-Kulberg, R.L. and Morgan, D.O. 1999. Pds1 and Esp1 control both anaphase and mitotic exit in normal cells and after DNA damage. *Genes & Dev.* **13:** 1936–1949.

Tomonaga, T., Nagao, K., Kawasaki, Y., Furuya, K., Murakami, A., Morishita, J., Yuasa, T., Sutani, T., Kearsey, S.E., Uhlmann, F., et al. 2000. Characterization of fission yeast cohesin: Essential anaphase proteolysis of Rad21 phosphorylated in the S phase. *Genes & Dev.* **14:** 2757–2770.

Uhlmann, F. and Nasmyth, K. 1998. Cohesion between sister chromatids must be established during DNA replication. *Curr. Biol.* **8:** 1095–1101.

Uhlmann, F., Wernic, D., Poupart, M.A., Koonin, E.V., and Nasmyth, K. 2000. Cleavage of cohesin by the CD clan protease separin triggers anaphase in yeast. *Cell* **103:** 375–386.

Uzawa, S., Samejima, I., Hirano, T., Tanaka, K., and Yanagida, M. 1990. The fission yeast *cut1+* gene regulates spindle pole body duplication and has homology to the budding yeast *ESP1* gene. *Cell* **62:** 913–925.

Waizenegger, I.C., Hauf, S., Meinke, A., and Peters, J.M. 2000. Two distinct pathways remove mammalian cohesin from chromosome arms in prophase and from centromeres in anaphase. *Cell* **103:** 399–410.

Warren, W.D., Steffensen, S., Lin, E., Coelho, P., Loupart, M., Cobbe, N., Lee, J.Y., McKay, M.J., Orr-Weaver, T., Heck, M.M., et al. 2000. The *Drosophila* RAD21 cohesin persists at the centromere region in mitosis. *Curr. Biol.* **10:** 1463–1466.

Wodarz, A., Hinz, U., Engelbert, M., and Knust, E. 1995. Expression of *crumbs* confers apical character on plasma-membrane domains of ectodermal epithelia of *Drosophila*. *Cell* **82:** 67–76.

Yanagida, M. 2000. Cell cycle mechanisms of sister chromatid separation; roles of Cut1/separin and Cut2/securin. *Genes Cells* **5:** 1–8.

Zachariae, W. and Nasmyth, K. 1999. Whose end is destruction: Cell division and the anaphase-promoting complex. *Genes & Dev.* **13:** 2039–2058.

Zou, H., McGarry, T.J., Bernal, T., and Kirschner, M.W. 1999. Identification of a vertebrate sister-chromatid separation inhibitor involved in transformation and tumorigenesis. *Science* **285:** 418–422..

Teilarbeit C

Proteolytic cleavage of the THR subunit during anaphase limits Drosophila separase function.

Alf Herzig, Christian F. Lehner and Stefan Heidmann

Genes and Development 16, 2443-2454 (2002).

Darstellung des Eigenanteils in Teilarbeit C

Mit Ausnahme des in Fig. 1G dargestellten Experiments, gehen alle Ergebnisse dieser Teilarbeit auf meine Arbeit zurück.

Diese Teilarbeit wurde von allen Autoren verfasst.

Proteolytic cleavage of the THR subunit during anaphase limits *Drosophila* separase function

Alf Herzig, Christian F. Lehner, and Stefan Heidmann[1]

Department of Genetics, University of Bayreuth, 95440 Bayreuth, Germany

Sister-chromatid separation in mitosis requires proteolytic cleavage of a cohesin subunit. Separase, the corresponding protease, is activated at the metaphase-to-anaphase transition. Activation involves proteolysis of an inhibitory subunit, securin, following ubiquitination mediated by the anaphase-promoting complex/cyclosome. In *Drosophila*, the securin PIM associates not only with separase (SSE), but also with an additional protein, THR. Here we show that THR is cleaved after the metaphase-to-anaphase transition. THR cleavage only occurs in functional SSE complexes and in a region that matches the separase cleavage-site consensus. Mutations in this region abolish mitotic THR cleavage. These results indicate that THR is cleaved by SSE. Expression of noncleavable THR variants results in cold-sensitive maternal-effect lethality. This lethality can be suppressed by a reduction of catalytically active SSE levels, indicating that THR cleavage inactivates SSE complexes. THR cleavage is particularly important during the process of cellularization, which follows completion of the last syncytial mitosis of early embryogenesis, suggesting that *Drosophila* separase has other targets in addition to cohesin subunits.

[*Keywords*: Mitosis; sister-chromatid separation; securin; separase; *pimples*; *three rows*]

Received March 11, 2002; revised version accepted July 29, 2002.

Separase is a eukaryotic endopeptidase that resolves the cohesion between sister chromatids by cleaving the Scc1/Mcd1/Rad21 subunit of the cohesin complex (Uhlmann et al. 1999, 2000). Scc1 should be cleaved neither during S phase, when sister-chromatid cohesion needs to be established, nor during G_2 phase and early mitosis, when cohesion is required for the correct bipolar orientation of sister chromatids within the mitotic spindle. However, at the metaphase-to-anaphase transition cohesion must be resolved efficiently and completely to allow faithful segregation of sister chromatids to daughter cells. Separase activity, therefore, is subject to careful regulation. Although separase has been shown to be required for sister-chromatid separation in a wide range of eukaryotes (Funabiki et al. 1996a; Ciosk et al. 1998; Zou et al. 1999; Jäger et al. 2001; Siomos et al. 2001), its regulation is poorly understood and appears to be surprisingly divergent in different organisms.

Regulatory subunits that associate with separase have been identified in diverse species (budding yeast Pds1, fission yeast Cut2, *Drosophila* PIM, vertebrate PTTG; Funabiki et al. 1996a; Ciosk et al. 1998; Zou et al. 1999; Jäger et al. 2001). These securin proteins share almost no sequence similarity and appear to have different additional roles beyond a shared inhibitory function. Separase inhibition by securins is canceled at the metaphase-to-anaphase transition by ubiquitin-dependent degradation (Ciosk et al. 1998). Securin ubiquitination is mediated by the anaphase-promoting complex/cyclosome (APC/C), which, in turn, is regulated by the mitotic spindle checkpoint (for review, see Shah and Cleveland 2000). The mitotic securin degradation, therefore, is only initiated when all chromosomes have reached the correct bipolar orientation within a functional mitotic spindle.

Securins not only function as separase inhibitors, they also act as positive regulators of separase function. Therefore, the securins of fission yeast and *Drosophila* are absolutely required for sister-chromatid separation during mitosis (Funabiki et al. 1996b; Stratmann and Lehner 1996). In contrast, the securins of budding yeast and vertebrates are not essential (Yamamoto et al. 1996; Jallepalli et al. 2001; Mei et al. 2001; Wang et al. 2001). However, the mild consequences of securin gene inactivation in vertebrates might be explained by the presence of redundant securins, as two additional highly similar *PTTG* genes have been identified in the human genome sequence (Chen et al. 2000).

Separase is also regulated by securin-independent mechanisms. A recent study revealed that vertebrate separase activity is inhibited by Cdk1-dependent phosphorylation (Stemmann et al. 2001). In addition, activa-

[1]**Corresponding author.**
E-MAIL stefan.heidmann@uni-bayreuth.de; FAX 49-921-55-2710.
Article and publication are at http://www.genesdev.org/cgi/doi/10.1101/gad.242202.

tion of human but not of yeast separase is accompanied by self-cleavage (Waizenegger et al. 2000; Stemmann et al. 2001). Although self-cleavage clearly does not result in complete inactivation (Stemmann et al. 2001), it is not yet known whether this autoprocessing is causally involved in human separase activation.

The apparent mechanistic diversity of separase regulation in different organisms is paralleled by a lack of primary sequence similarity among not only the securins but also the N-terminal separase domains. These N-terminal regions encompass more than 110 kD in all separases except the *Drosophila* separase homolog SSE. SSE is an exceptionally small separase family member, which consists almost entirely of the conserved cysteine endoprotease domain (Jäger et al. 2001). However, SSE associates not only with the securin Pimples (PIM), but also with the Three rows protein (THR), which does not appear to have orthologs outside *Drosophila* (Jäger et al. 2001). We have speculated, therefore, that *thr* might encode an N-terminal separase domain, which was separated by a gene split from an ancient separase gene during *Drosophila* evolution (Jäger et al. 2001). Consistent with this proposal, PIM binds to THR (Leismann et al. 2000; Jäger et al. 2001), whereas securins bind to the N-terminal domains of separases in yeast (Kumada et al. 1998; Jensen et al. 2001). Like SSE and PIM, THR is also absolutely required for sister-chromatid separation (D'Andrea et al. 1993; Philp et al. 1993).

To clarify SSE regulation, we have analyzed the role of THR in further detail. Interestingly, we find that THR is cleaved after the metaphase-to-anaphase transition, apparently by the associated SSE. Moreover, our analysis of cleavage-resistant mutations suggests that THR cleavage is most important for separase inhibition during early embryogenesis of *Drosophila*.

Results

THR is proteolytically cleaved during mitosis

To analyze the intracellular distribution of THR during the cell cycle, we immunolabeled *Drosophila* embryos with antibodies against THR. In addition, we studied the behavior of a myc-epitope-tagged THR protein expressed from a transgene under control of the *thr* regulatory region. This *gthr–myc* transgene rescues *thr* null mutants completely (Leismann et al. 2000). THR–myc (Fig. 1C,F) as well as THR (data not shown) were found to be cytoplasmic during interphase and distributed throughout the cell during early mitosis. This intracellular distribution is therefore identical to that previously described for the securin PIM, which is known to form a complex with THR and SSE (Stratmann and Lehner 1996; Leismann et al. 2000; Jäger et al. 2001).

Interestingly, THR and THR–myc signals were observed to decline during exit from mitosis. This decline was most clearly detected during mitosis 14 in embryos with only maternal and no zygotic *gthr–myc* expression (Fig. 1A–F). Maternal *thr* transcripts are rapidly degraded during interphase 14 (D'Andrea et al. 1993). As a consequence, maternally derived THR protein can no longer be synthesized after mitosis 14. The disappearance of the maternally derived THR–myc protein during exit from mitosis 14, therefore, is not concealed by THR–myc reaccumulation in embryos that cannot express *gthr–myc* zygotically. Mitosis 14 occurs in a highly reproducible pattern (Foe 1989), which is readily revealed by immunolabeling with antibodies against cyclin B. Anti-cyclin B immunolabeling is absent from cells that have just completed mitosis, but is present in the cytoplasm of cells that have not yet progressed through mitosis (Fig. 1B). Double labeling showed that the distribution of

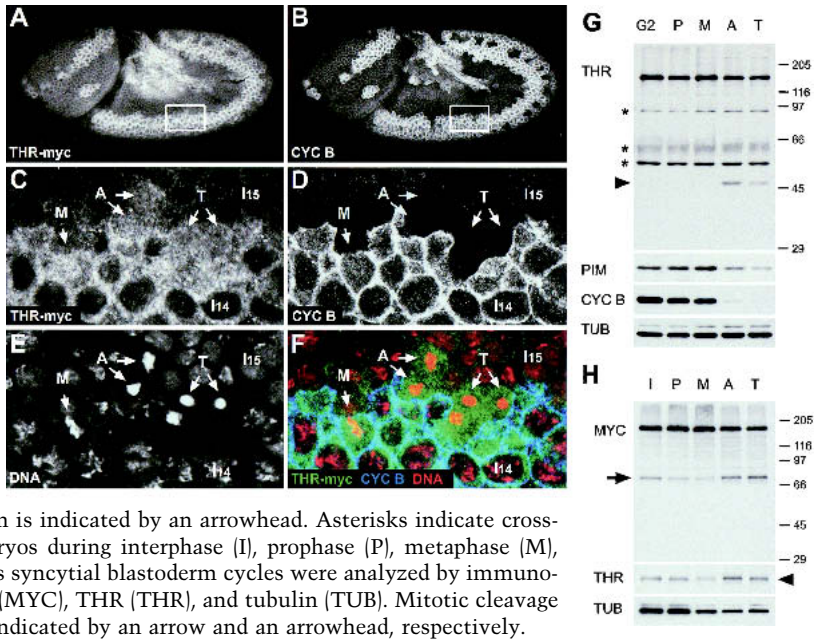

Figure 1. THR is degraded during mitosis. Embryos (*A*,*B*) expressing *gthr–myc* were fixed at the stage of mitosis 14 and labeled with antibodies against the myc epitope (*A*,*C*,*F*), cyclin B (*B*,*D*,*F*), and a DNA stain (*E*,*F*). The boxed area in *A* and *B* is shown in *C–F*. Red, green, and blue in the merged panel *F* represent DNA, anti-myc, and anti-cyclin B labeling, respectively. M, metaphase; A, anaphase; T, telophase; I_{14}, interphase 14; I_{15}, interphase 15. (*G*) Synchronous progression through mitosis 14 was induced, and extracts were prepared from embryos with all cells in G_2 before mitosis 14 (G2), as well as in prophase (P), metaphase (M), anaphase (A), and telophase (T) of mitosis 14. Extracts were analyzed by immunoblotting using antibodies against THR (THR), PIM (PIM), cyclin B (CYC B), and tubulin (TUB). A 47-kD fragment appearing after the metaphase-to-anaphase transition is indicated by an arrowhead. Asterisks indicate cross-reacting bands. (*H*) Extracts from *gthr–myc* embryos during interphase (I), prophase (P), metaphase (M), anaphase (A), and telophase (T) of the synchronous syncytial blastoderm cycles were analyzed by immunoblotting using antibodies against the myc epitope (MYC), THR (THR), and tubulin (TUB). Mitotic cleavage products of THR–myc and endogenous THR are indicated by an arrow and an arrowhead, respectively.

THR–myc was almost indistinguishable from that of cyclin B (Fig. 1, cf. A and B), clearly indicating that the decline of THR–myc is coupled to progression through mitosis. However, careful comparisons indicated that cyclin B is degraded more rapidly and completely than THR–myc (Fig. 1C–F).

To confirm mitotic THR degradation by immunoblotting, we induced a synchronous progression through mitosis 14 (see Materials and Methods). As expected, cyclin B was readily detected up to metaphase and essentially absent in anaphase and telophase (Fig. 1G). PIM degradation was found to be less rapid and complete than cyclin B destruction (Fig. 1G). Immunoblotting with antibodies against THR indicated that the disappearance of full-length THR was also limited (Fig. 1G). However, a distinct 47-kD band was observed exclusively in anaphase and telophase extracts (Fig. 1G, see arrowhead), indicating that a fraction of THR is proteolytically cleaved after the metaphase-to-anaphase transition.

Because our antibodies detected proteins other than THR in the extracts, it was important to confirm that the 47-kD band observed after the metaphase-to-anaphase transition was derived from THR. Therefore, we analyzed *gthr–myc* embryo extracts with antibodies against myc (Fig. 1H). To prepare these extracts, we pooled embryos at distinct stages of the synchronous syncytial mitoses before cellularization. Similarly as in the mitosis 14 extracts (Fig. 1G), a THR fragment that strongly increased in intensity after the metaphase-to-anaphase transition was specifically detected by anti-myc (Fig. 1H, see arrow). Taking the C-terminal myc tags into account, this 70-kD fragment appeared to indicate the same proteolytic event as the 47-kD fragment observed by our antibodies against a C-terminal THR domain (Fig. 1G). Moreover, reprobing the blot of the syncytial *gthr–myc* extracts with these latter antibodies revealed the 47-kD THR fragment with intensities that closely paralleled those of the 70-kD THR–myc fragment (Fig. 1H, see arrowhead).

THR and THR–myc cleavage fragments were also observed in phases other than anaphase and telophase (Fig. 1H), but only during the syncytial cycles. The cleavage products are therefore presumably not completely degraded during the extremely brief syncytial interphases of only a few minutes. The instability of these C-terminal cleavage fragments, however, explains the decline of THR signals during exit from mitosis 14 observed by immunofluorescence, as our antibodies recognize C-terminal epitopes. We have no information concerning the stability and intracellular distribution of the N-terminal THR part, because our antibodies do not recognize the THR N terminus and because N-terminal epitope tags were found to abolish THR function (data not shown).

A separase cleavage consensus motif is required for mitotic THR cleavage

To assess the regulatory significance of THR cleavage, we mapped and mutated the cleavage site. Based on the size of the mitotic THR and THR–myc fragments, the mitotic cleavage was predicted to occur approximately between amino acids 930 and 1030. C-terminal THR fragments starting at different positions within this region were generated by in vitro translation, and their electrophoretic mobility was compared with the mobility of the fragment generated during mitosis in vivo (Fig. 2A). The mitotic in vivo cleavage fragment comigrated with the smallest in vitro fragment starting at position 1032. Interestingly, the region surrounding this position (1031–VEPIRKQ–1037) displays significant similarity to the separase cleavage-site consensus derived from various mitotically and meiotically cleaved cohesin subunits (Fig. 2B; Hauf et al. 2001). Moreover, comparison of THR proteins from *D. melanogaster*, *Drosophila pseudoobscura*, and *Drosophila virilis* revealed that the VEPIRKQ motif is invariant (H. Jäger, C.F. Lehner, and S. Heidmann, unpubl.). We point out that THR is a fast-evolving protein and apart from this potential cleavage region, there is only one other region with more extensive conservation.

To test whether the conserved separase cleavage-site consensus region is, indeed, important for cleavage, we generated mutants (Fig. 2B). In the first mutant, we deleted the separase cleavage-site consensus ($THR^{\Delta VQ}$, deletion of amino acids 1031–VEPIRKQ–1037). In the second mutant, the arginine residue at position 1035 was exchanged for an aspartate (THR^{RD}). The identical mutation in the separase cleavage sites of Scc1 has been shown to abolish cleavage in yeast (Uhlmann et al. 1999), and similar mutations (arginine to alanine) rendered human Scc1 resistant to separase cleavage (Hauf et al. 2001). We established transgenic lines expressing myc-epitope-tagged variants of these two THR mutants and analyzed their cleavage. Both mutant proteins were completely refractory to mitotic cleavage, whereas endogenous THR was still cleaved (Fig. 2C,D). Immunofluorescence analysis during mitosis 14 indicated that the cleavage-resistant mutants $THR^{\Delta VQ}$–myc and THR^{RD}–myc were not degraded during exit from mitosis (Fig. 2E–H; data not shown). We conclude that the separase cleavage-site consensus region in THR is required for mitotic THR cleavage and that this cleavage causes the decline of THR during exit from mitosis.

Mitotic THR cleavage requires functional SSE complexes

If SSE is the protease responsible for THR cleavage, then THR should be stable in cells arrested by the mitotic spindle checkpoint. Immunofluorescence analysis of *gthr–myc* embryos permeabilized and treated with the microtubule inhibitor demecolcine showed that THR–myc is, indeed, stabilized in checkpoint-arrested cells. These cells were identified by double labeling with antibodies against cyclin A (Fig. 3C) and a DNA stain (Fig. 3E). Cyclin A is known to be degraded in arrested cells, which are also characterized by condensed chromosomes (Whitfield et al. 1990). All arrested cells were found to contain high THR–myc levels (Fig. 3A), whereas, as expected, THR–myc levels were very low in cells of mock-

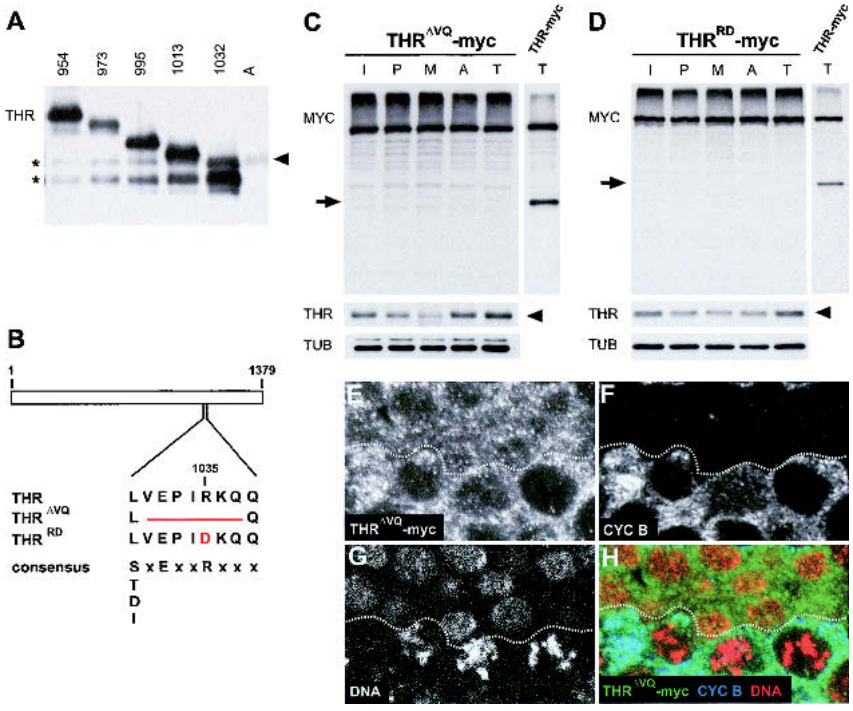

Figure 2. Mapping the mitotic THR cleavage site. (*A*) C-terminal THR fragments were generated in vitro and resolved next to an anaphase embryo extract (lane *A*, same extract as in Fig. 1G, lane A). THR fragments were detected by immunoblotting with anti-THR antibodies. The numbers above the lanes indicate the amino acid position at which the C-terminal THR fragments start. The arrowhead indicates the C-terminal THR fragment generated in vivo after the metaphase-to-anaphase transition. Asterisks indicate partial products of the THR fragments generated in vitro. (*B*) Schematic illustration of the mitotic cleavage region within THR, $THR^{\Delta VQ}$, and THR^{RD}. In addition, the separase cleavage-site consensus sequence (Hauf et al. 2001) is shown below the THR sequences. Cleavage by separase occurs C-terminal from the conserved arginine residue. (*C*,*D*) Extracts from *gthr*$^{\Delta VQ}$*–myc* (*C*) or *gthr*RD*–myc* (*D*) embryos during interphase (I), prophase (P), metaphase (M), anaphase (A), and telophase (T) of the synchronous syncytial blastoderm cycles were analyzed by immunoblotting using antibodies against the myc epitope (MYC), THR (THR), and tubulin (TUB). In addition, a telophase extract from *gthr–myc* embryos was analyzed in parallel (*right* lanes). Mitotic cleavage products of THR–myc and endogenous THR are indicated by arrows and arrowheads, respectively. (*E–H*) Embryos expressing *gthr*$^{\Delta VQ}$*–myc* were fixed at the stage of mitosis 14 and labeled with antibodies against the myc epitope (*E*), cyclin B (*F*), and a DNA stain (*G*). Red, green, and blue in the merged image (*H*) represent labeling of DNA, myc, and cyclin B, respectively. The epidermal region shown corresponds to the boxed region in Figure 1A. Cells below the dotted line are in G_2 before mitosis 14, whereas cells above the dotted line have progressed through mitosis 14 and are mostly in early interphase of cycle 15. Note that $THR^{\Delta VQ}$–myc is still present at high levels in these cells, in contrast to THR–myc (see Fig. 1C–F).

treated embryos that had completed mitosis 14 (Fig. 3B). Furthermore, immunoblot analysis of demecolcine-treated syncytial embryos clearly showed a drastic reduction in the abundance of the THR–myc cleavage product (Fig. 3G).

Phenotypic analyses of various mutants provided additional evidence supporting the suggestion that THR is cleaved by SSE. Cytologically, the mutant phenotypes resulting from the loss of *thr*, *Sse*, or *pim* function have been shown to be identical (D'Andrea et al. 1993; Philp et al. 1993; Stratmann and Lehner 1996; Jäger et al. 2001). Sister-chromatid separation fails in all three mutants. Moreover, we have previously shown that THR, PIM, and SSE form a trimeric complex (Jäger et al. 2001), which appears to be a prerequisite for activation of separase activity at the metaphase-to-anaphase transition. Accordingly, *pim* mutants presumably lack separase activity. Therefore, we analyzed THR–myc stability during exit from mitosis in *pim* mutant embryos. Mitosis 15 is the first division that is affected in *pim* mutant embryos, but the previous mitoses proceed normally because of a maternally provided *pim*$^+$ contribution (Stratmann and Lehner 1996). We observed that THR–myc is no longer degraded during mitosis 15 in *pim* mutant embryos (Fig. 3H), whereas it declined normally in *pim*$^+$ sibling embryos as expected (Fig. 3I).

Additional evidence for the role of SSE in THR cleavage was obtained with transgenes encoding different THR deletion mutants. We have previously shown that a mutant (THR 445–1379–myc) lacking the N-terminal PIM-binding site can still associate with SSE (Jäger et al. 2001). However, this mutant is unable to rescue mutations in the endogenous *thr* gene (data not shown). As this mutant still contains the normal C-terminal region with the cleavage site, we analyzed its cleavage. Analysis in syncytial embryos indicated that THR 445–1379–myc is not cleaved (Fig. 4A). Moreover, THR 445–1379–myc was also not degraded during mitosis 14 (Fig. 4C). We point out that THR 445–1379–myc was expressed in a *thr*$^+$ background in these experiments. Thus, despite the presence of functional and active SSE complexes in this background, THR 445–1379–myc that still binds to SSE was not cleaved during mitosis. A C-terminal deletion mutant (THR 1–1204–myc) is also unable to provide *thr*$^+$ function, even though this mutant can bind to both PIM and SSE to a degree comparable with full-length THR 1–1379–myc (data not shown). The analysis of THR 1–1204–myc, which also still contains the cleavage region, revealed that its cleavage in syncytial embryos is greatly reduced (Fig. 4B) and that the protein is stabilized in mitosis 14 (Fig. 4D).

We conclude that our findings in checkpoint-arrested cells, in *pim* mutants, and with the different *thr* deletion mutants all strongly support the argument that THR

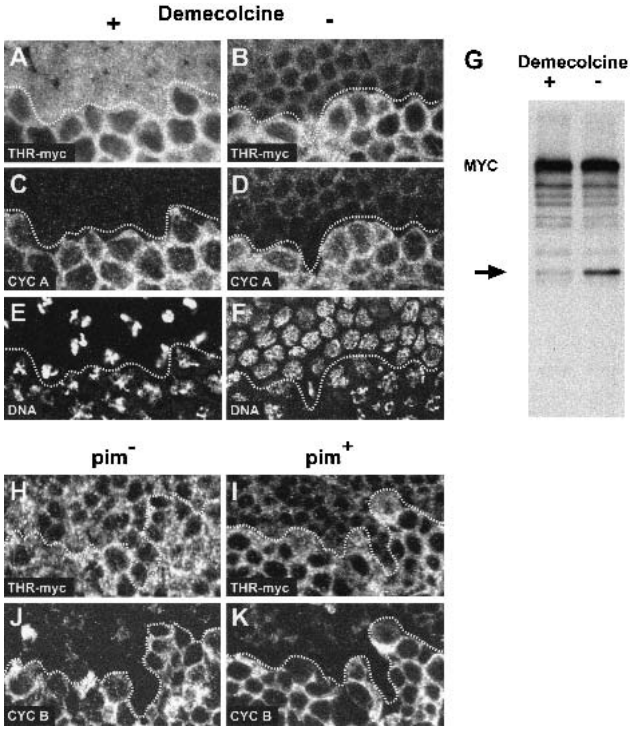

Figure 3. THR cleavage is inhibited in cells arrested by the mitotic spindle checkpoint and in *pim* mutants. (*A–F*) Embryos expressing *gthr–myc* were permeabilized and incubated in the presence (*A*,*C*,*E*) or absence (*B*,*D*,*F*) of the microtubule inhibitor demecolcine while progressing through mitosis 14. After fixation, embryos were labeled with antibodies against the myc epitope (*A*,*B*), cyclin A (*C*,*D*), and a DNA stain (*E*,*F*). Comparable epidermal regions are shown. Cells below the dotted line are in G_2 before mitosis 14, whereas cells above the dotted line have progressed into mitosis 14 and are arrested with condensed chromatin (*E*) or are already in early interphase of cycle 15 (*F*). THR–myc is present at high levels in arrested cells (*A*), and only at low levels in interphase 15 cells (*B*). (*G*) *gthr–myc* embryos during the syncytial blastoderm cycles were permeabilized and incubated in the presence (+) or absence (–) of demecolcine. Embryo extracts were analyzed by immunoblotting with anti-myc. The THR–myc fragment appearing after the metaphase-to-anaphase transition is indicated by an arrow. (*H–K*) *pim*$^-$ embryos (*H*,*J*) and *pim*$^+$ sibling embryos (*I*,*K*) expressing *gthr–myc* were fixed at the stage of mitosis 15 and labeled with antibodies against the myc epitope (*H*,*I*) and cyclin B (*J*,*K*). In the epidermal region shown, cells below the dotted line are in G_2 before mitosis 15, whereas cells above the dotted line have progressed through mitosis 15 and are mostly in early interphase of cycle 16. These latter cells have high levels of THR–myc in *pim*$^-$ embryos (*H*), and only low levels in *pim*$^+$ sibling embryos (*I*).

cleavage can only proceed within complexes that contain active SSE.

Expression of noncleavable THR results in a cellularization defect

To address the physiological significance of mitotic THR cleavage, we characterized the phenotype associated with the mutations abolishing cleavage. The transgenes *gthr*$^{\Delta VQ}$*–myc* and *gthr*RD*–myc* include the wild-type *thr* regulatory region. By crossing these transgenes into a *thr* null mutant background, we analyzed whether the noncleavable THR proteins can functionally replace wild-type THR. The *gthr*$^{\Delta VQ}$*–myc* and *gthr*RD*–myc* transgenes complemented the embryonic lethality associated with null mutations in the endogenous *thr* gene and supported development to the adult stage. The rescued flies hatched with the expected frequency and displayed no apparent morphological defects. Thus, the noncleavable THR variants must be at least partially functional.

However, the *gthr*$^{\Delta VQ}$*–myc* and *gthr*RD*–myc* transgenes resulted in cold-sensitive female sterility. Females with two transgene copies in a wild-type background were almost completely sterile at 18°C, whereas at 25°C they were fertile. Even at 18°C, plenty of eggs were laid. However, very few larvae were observed to hatch from these eggs. This maternal-effect lethality at 18°C was observed with females homozygous for either single *gthr*$^{\Delta VQ}$*–myc* or *gthr*RD*–myc* insertions, and also with females heterozygous for one of six different chromosomes carrying recombined pairs of independent *gthr*$^{\Delta VQ}$*–myc* insertions, ruling out position effects of transgene insertions (Fig. 5A, 6A, below; data not shown). Moreover, the maternal-effect lethality was not observed with females carrying two copies of *gthr–myc* (Fig. 5A), showing that this phenotype does not result from an increased *thr*$^+$ gene dose. However, the dose of *gthr*$^{\Delta VQ}$*–myc* or *gthr*RD*–myc* was found to be critical. Maternal-effect lethality was not observed with females carrying only one transgene copy (Fig. 5A).

The cold-sensitive developmental period of the maternal-effect lethality was defined by temperature-shift experiments. When eggs were collected at 25°C for 1 h and allowed to develop further at 25°C, the larval hatch rate of progeny from females with two *gthr*RD*–myc*, *gthr*$^{\Delta VQ}$*–myc*, or *gthr–myc* transgene copies was indistinguishably high (Fig. 5A, gray bars). However, when the eggs were incubated at 18°C for 4.5 h followed by an up-shift to 25°C for the rest of embryogenesis, we observed a dramatic decrease in the larval hatch rates of progeny from females with either two *gthr*RD*–myc* or *gthr*$^{\Delta VQ}$*–myc* transgenes, whereas the progeny from females with two *gthr–myc* transgenes still hatched with high efficiency (Fig. 5A, black bars). A reciprocal temperature-shift experiment revealed that embryonic lethality of progeny from females with two *gthr*$^{\Delta VQ}$*–myc* transgenes is no longer observed when the whole embryogenesis, except for the first 3.5 h, takes place at 18°C (Fig. 5A, hatched bar). We conclude, therefore, that the cold-sensitive period covers the early stages of *Drosophila* embryogenesis that are characterized by rapid syncytial division cycles followed by cellularization.

To analyze the maternal-effect phenotype caused by noncleavable THR variants on a cellular level, we first examined embryos that had progressed through early development at 18°C, after fixation and DNA labeling (Fig. 5B,C; data not shown). These stainings suggested that progression through the rapid syncytial cycles is affected

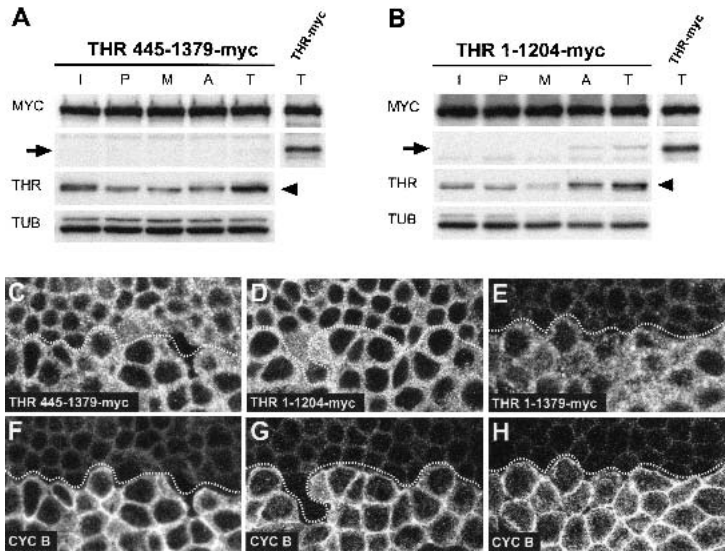

Figure 4. THR cleavage occurs only within functional SSE complexes. (*A*,*B*) Extracts from *gthr 445–1379–myc* (*A*) or *gthr 1–1204–myc* (*B*) embryos during interphase (I), prophase (P), metaphase (M), anaphase (A), and telophase (T) of the synchronous syncytial blastoderm cycles were analyzed by immunoblotting using antibodies against the myc epitope (MYC), THR (THR), and tubulin (TUB). In addition, a telophase extract from *gthr–myc* embryos was analyzed in parallel (*right* lanes). The proteins THR 445–1379–myc, THR 1–1204–myc, and THR–myc all contain the cleavage region and associate with SSE. Mitotic cleavage products of THR–myc and endogenous THR are indicated by arrows and arrowheads, respectively. (*C–H*) Embryos expressing *gthr 445–1379–myc* (*C*,*F*), *gthr 1–1204–myc* (*D*,*G*), or *gthr–myc* (*E*,*H*) were fixed at the stage of mitosis 14 and labeled with antibodies against the myc epitope (*C–E*) and cyclin B (*F–H*). Comparable epidermal regions are shown. Cells below the dotted lines are in G_2 before mitosis 14, whereas cells above the dotted lines have progressed through mitosis 14 and are in early interphase of cycle 15. Note that THR 445–1379–myc (*C*) and THR 1–1204–myc (*D*) are still present at high levels in these cells, in contrast to THR–myc (*E*).

by noncleavable THR, although not severely. In the following, we refer to progeny from females with two $gthr^{RD}$*–myc*, $gthr^{\Delta VQ}$*–myc*, or *gthr–myc* transgene copies as THR^{RD}, $THR^{\Delta VQ}$, and THR embryos, respectively. A fraction of the syncytial THR^{RD} (19%, $n = 317$) and $THR^{\Delta VQ}$ embryos (35%, $n = 269$) displayed various irregularities that were less frequent in THR embryos (12%, $n = 250$). Irregularities included embryonic regions with prominent mitotic asynchrony, abnormal mitotic figures or lower nuclear densities. Moreover, many $THR^{\Delta VQ}$ and THR^{RD} embryos with an apparently regular nuclear distribution were found to have fewer nuclei compared with THR embryos of the same age. All these observations indicate that the noncleavable THR variants cause occasional cell cycle defects during the syncytial cycles with limited penetrance.

A much more severe and highly penetrant phenotype was observed during cellularization. This developmental process follows after the last syncytial division, mitosis 13. During cellularization, the ~6000 nuclei at the syncytial egg periphery are enclosed by cell membranes and thereby transformed into individual cells forming a single layer epithelium (Foe et al. 1993). At this stage, $THR^{\Delta VQ}$ and THR^{RD} embryos were found to lose a large fraction of nuclei from the egg periphery (Fig. 5C,H–J). These nuclei accumulated in the yolk region in the egg interior (Fig. 5C). In contrast, THR embryos had a normal appearance, with the majority of the nuclei at the periphery and only few yolk nuclei in the interior (Fig. 5B). This cellularization defect was displayed by 99% of the $THR^{\Delta VQ}$ embryos ($n = 112$) and 98% of the THR^{RD} embryos ($n = 53$), but none of the THR embryos was affected ($n = 49$). Time-lapse imaging of $THR^{\Delta VQ}$ embryos expressing a histone–GFP fusion (Clarkson and Saint 1999) indicated that this massive loss of nuclei from the egg periphery started well after completion of mitosis 13, concomitant with the early slow phase of cellularization, which is paralleled by nuclear elongation (Foe et al. 1993). The loss of nuclei from the periphery of $THR^{\Delta VQ}$ embryos was found to continue throughout cellularization (data not shown).

Immunolabeling of fixed $THR^{\Delta VQ}$ embryos with an antibody against the *Drosophila* β-catenin homolog Armadillo (ARM), which displays a well-characterized dynamic behavior during cellularization (Hunter and Wieschaus 2000), confirmed that the massive nuclear loss started simultaneously with cellularization (Fig. 5D–J). Moreover, these stainings also indicated that cellularization, as revealed by ARM relocalization, was delayed in $THR^{\Delta VQ}$ embryos compared with nuclear elongation.

Immunolabeling with antibodies against γ-tubulin and α-tubulin indicated that parallel with the onset of cellularization, microtubule organization also became abnormal in $THR^{\Delta VQ}$ embryos. γ-Tubulin labeling in centrosomes was reproducibly weaker and revealed an impaired centrosome separation in $THR^{\Delta VQ}$ embryos (Fig. 5, cf. K and O). Microtubule asters were found to be slightly smaller (Fig. 5, cf. L and P). Centrosomes and associated microtubule asters were observed to stay at the cortex above interiorly displaced nuclei (Fig. 5O–R, arrowheads).

SSE is negatively regulated by mitotic THR cleavage

Mitotic THR cleavage might regulate the activity of the associated SSE. The maternal-effect lethality resulting from noncleavable THR at 18°C therefore might reflect either hyper- or hypoactivation of SSE. To address this issue, we analyzed the effects of a reduced Sse^{+} gene dose on the $gthr^{\Delta VQ}$*–myc* phenotype. A reduction from two to one functional Sse^{+} gene copies was found to result in a strong suppression of the maternal-effect lethality

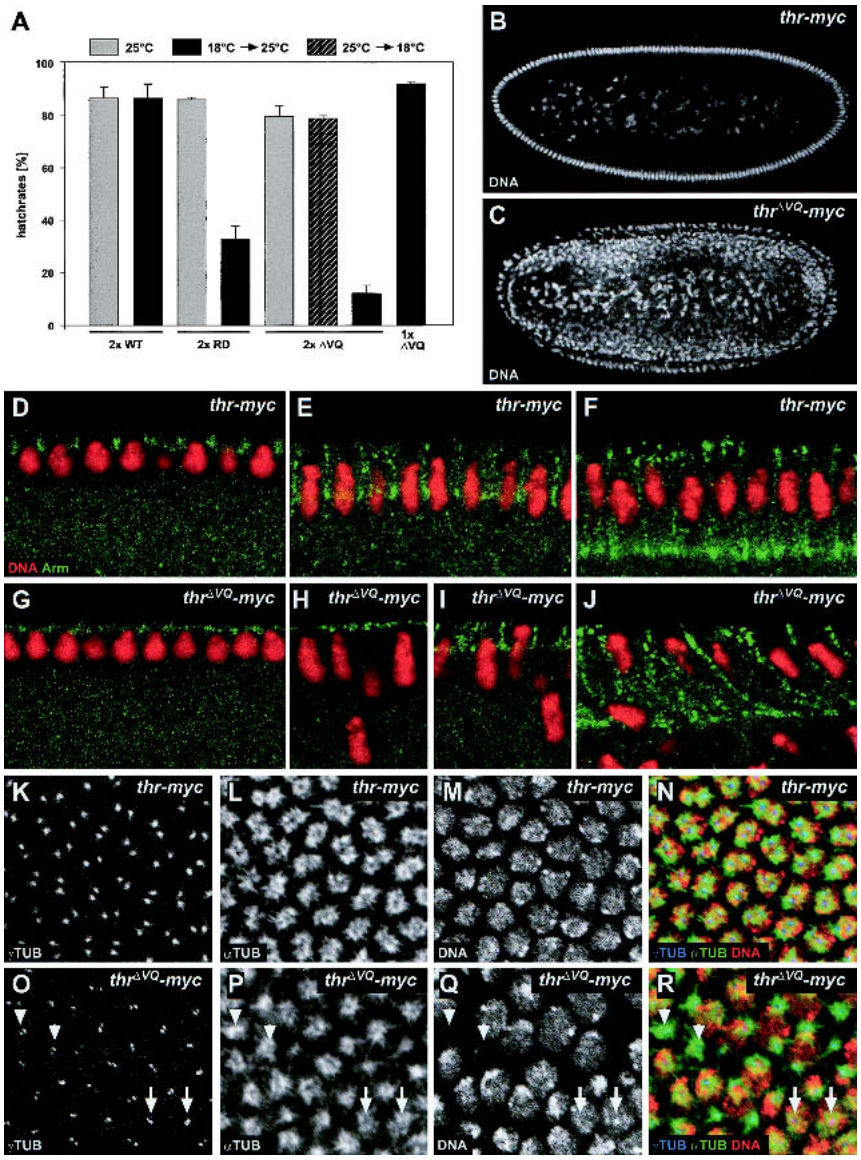

Figure 5. Phenotype associated with expression of noncleavable THR. (*A*) Noncleavable THR present during early embryonic development causes cold-sensitive, maternal-effect lethality. Eggs were collected at 25°C for 1 h from females homozygous for the transgene insertions *gthr–myc* (2× WT), *gthrRD–myc* (2× RD), or *gthr$^{\Delta VQ}$–myc* (2× ΔVQ), or heterozygous for *gthr$^{\Delta VQ}$–myc* (1× ΔVQ). Eggs were incubated at 25°C (gray bars); or shifted to 18°C after 3.5 h (hatched bar); or shifted to 18°C for 4.5 h, followed by a shift back to 25°C (black bars). The larval hatch rates (% of hatched eggs) are given as average values obtained from three independent experiments. (*B,C*) Noncleavable THR causes internalization of nuclei during early embryonic development. Embryos derived from females homozygous for *gthr–myc* (*B*) or *gthr$^{\Delta VQ}$–myc* (*C*) were incubated during their early development at 18°C, fixed, and stained for DNA. (*D–J*) Cellularization is delayed in THR$^{\Delta VQ}$ embryos. Cellularizing THR (*D–F*) and THR$^{\Delta VQ}$ (*G–J*) embryos were fixed and labeled with an antibody against Armadillo (Arm, green) and a DNA stain (DNA, red). (*K–R*) Noncleavable THR affects centrosome separation. THR (*K–N*) or THR$^{\Delta VQ}$ (*O–R*) embryos were fixed during cellularization at 18°C, stained for DNA, and labeled with antibodies against γ-tubulin (γTUB) and α-tubulin (αTUB). Apical confocal sections that contained the γTUB signals were stacked (*K,L,O,P*), and a lower section was taken for DNA (*M,Q*). Arrows indicate unseparated centrosomes. Arrowheads denote positions where nuclei had dropped into the interior of the embryo and had left behind centrosomes and microtubule asters. (*N*) Merge of *K*, *L*, and *M*; (*R*) merge of *O*, *P*, and *Q*. Red, green, and blue in the merged images indicate labeling of DNA, αTUB, and γTUB, respectively.

caused by two *gthr$^{\Delta VQ}$–myc* transgene copies at 18°C (Fig. 6A). This suppression was completely reverted, when one copy of a fully functional genomic *Sse^{+}* transgene was crossed into the females with only one endogenous *Sse^{+}* locus and two *gthr$^{\Delta VQ}$–myc* transgene copies (Fig. 6A), showing that it is in fact the *Sse^{+}* copy number, and not potential second-site mutations, that affects the expression of the *gthr$^{\Delta VQ}$–myc* phenotype.

Not only maternal-effect lethality but also the cellularization defects were affected by the *Sse^{+}* copy number. Massive nuclear loss from the egg periphery at 18°C was observed in 7% of THR$^{\Delta VQ}$ embryos (n = 133), when the mothers had only one *Sse^{+}* copy. In contrast, 95% of THR$^{\Delta VQ}$ embryos derived from sibling females with two *Sse^{+}* copies were affected (n = 119). Quantitative immunoblotting experiments showed that SSE protein levels during early embryogenesis were almost twofold higher in these THR$^{\Delta VQ}$ embryos from mothers with two *Sse^{+}* copies (Fig. 6B, cf. lane labeled Sse^{13m}, 1× and lane labeled Sse^{+}, 0.5×). We conclude, therefore, that the cellularization defects caused by noncleavable THR variants depend on high SSE protein levels.

To assess whether catalytic activity of SSE is required for the cellularization defects caused by noncleavable THR variants, we expressed a transgene (*UAS–HA–Sse^{C497S}*) encoding a catalytically inactive SSE mutant with a serine residue instead of the predicted catalytic cysteine residue (Jäger et al. 2001). Significantly, *UAS–HA–Sse^{C497S}* expression in THR$^{\Delta VQ}$ embryos from mothers with a single endogenous *Sse^{+}* locus did not increase the frequency and severity of cellularization defects. Only 5% of the embryos suffered from massive nuclear loss during cellularization (n = 300). In contrast, an analogous transgene (*UAS–HA–Sse*) allowing expres-

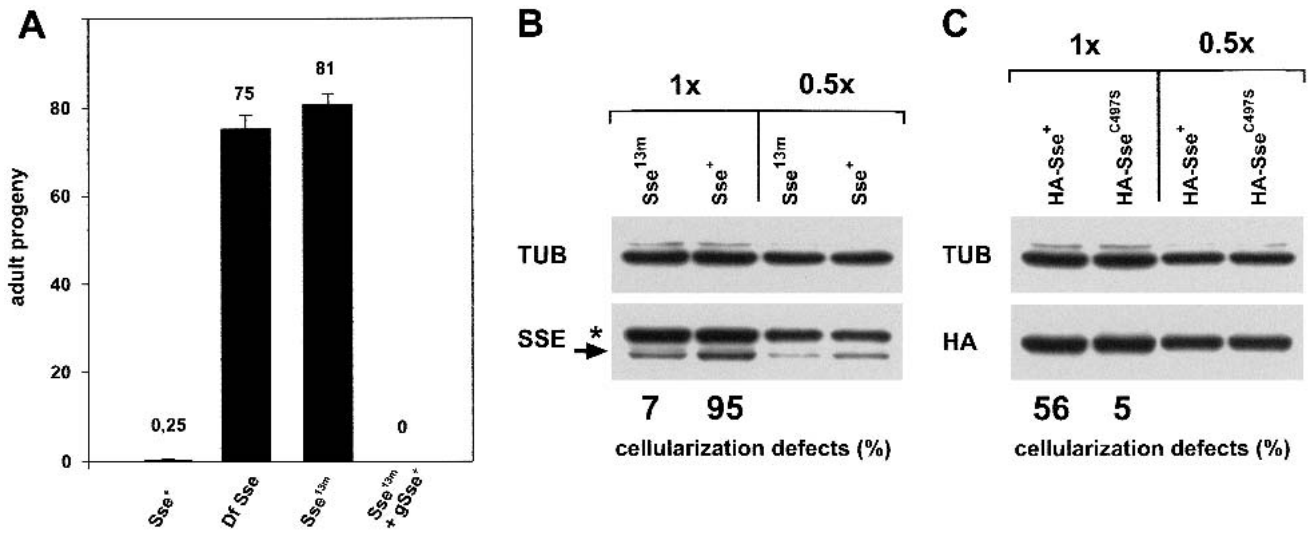

Figure 6. THR cleavage limits SSE activity. (*A*) Females carrying two copies of the $gthr^{\Delta VQ}$–*myc* transgene in a genetic background that was Sse^{+}/Sse^{+} (Sse^{+}), $Df(3L)SseA/Sse^{+}$ (Df Sse), Sse^{13m}/Sse^{+} (Sse^{13m}), or Sse^{13m}, $gSse^{+}/Sse^{+}$ (Sse^{13m} + $gSse^{+}$) were crossed to w^{1} males. *Df(3L)SseA* deletes *Sse*; Sse^{13m} is a null allele and $gSse^{+}$ is a transgene constructed with a genomic fragment providing Sse^{+} function (Jäger et al. 2001). Progeny developing at 18°C were counted. Average values of progeny/day and females obtained from at least four independent experiments are given for each cross. (*B*,*C*) Females carrying two copies of the $gthr^{\Delta VQ}$–*myc* transgene in a genetic background that was either Sse^{+}/Sse^{+} (Sse^{+}) or Sse^{13m}/Sse^{+} (Sse^{13m}) were crossed to w^{1} males (*B*). Females that carried two copies of the $gthr^{\Delta VQ}$–*myc* transgene in an Sse^{13m}/Sse^{+} genetic background and in addition expressed *HA–*Sse^{+} (HA–Sse^{+}) or *HA–*Sse^{C497S} (HA–Sse^{C497S}) were also crossed to w^{1} males (*C*). *HA–*Sse^{C497S} encodes a catalytically inactive SSE mutant. Embryos from these crosses were used to quantitate cellularization defects at 18°C and to prepare protein extracts for immunoblotting. Extracts were loaded either undiluted (1×) or in a 1:2 dilution (0.5×). Blots were probed with antibodies against SSE (SSE; arrow in *B*), the HA epitope (HA; *C*) or tubulin (TUB) as a loading control. The asterisk in *B* indicates a cross-reacting band.

sion of wild-type SSE clearly induced cellularization defects in $THR^{\Delta VQ}$ embryos from mothers with a single endogenous Sse^{+} copy. In this case, 56% of the embryos displayed nuclear loss during cellularization ($n = 317$). Quantitative immunoblotting experiments showed that *HA–*Sse^{C497S} and *HA–Sse* were expressed at the same level (Fig. 6C). We conclude that noncleavable THR variants result in cellularization defects only in combination with catalytically active SSE. The cellularization defects caused by noncleavable THR versions at 18°C in embryos with wild-type SSE levels therefore reflect SSE hyperactivity. Consequently, our findings indicate that THR cleavage contributes to inactivation of SSE.

Discussion

Genetic stability in eukaryotes is critically dependent on the careful regulation of sister-chromatid cohesion. Cohesion between sister chromatids needs to be established during S phase and maintained until the metaphase-to-anaphase transition, when it must be rapidly and completely eliminated. This final elimination of cohesion is known to result from proteolytic cleavage of the Scc1 subunit of the cohesion complex by the endopeptidase separase. Because Scc1 cleavage is irreversible, separase activity has to be tightly regulated. Previous findings have implicated the securins, which bind as inhibitory regulatory subunits to separase in the corresponding control pathway (Funabiki et al. 1996a; Ciosk et al. 1998; Zou et al. 1999). In addition, recent studies have emphasized the regulatory role of phosphorylation of Scc1 and separase (Alexandru et al. 2001; Stemmann et al. 2001). Our studies indicate yet an additional level of control, the proteolytic cleavage of the THR subunit of the *Drosophila* separase complex. Moreover, they emphasize that *Drosophila* separase regulation is not only crucial for controlled cleavage of cohesin subunits, but for that of additional substrates as well.

Immunolabeling revealed that THR is partially degraded after the metaphase-to-anaphase transition, similar to PIM. However, the mitotic degradation of PIM and THR is mechanistically and functionally distinct. Mitotic degradation of PIM is dependent on the presence of a destruction box (D-Box) and on Fizzy-APC/C, which promotes ubiquitination and subsequent degradation by the proteasome (Leismann et al. 2000). This PIM degradation presumably leads to activation of SSE.

In contrast, THR does not seem to contain a functional D-box (data not shown), and mitotic degradation of THR is dependent on SSE. The initial THR cleavage event is followed by degradation of the C-terminal cleavage product. By analogy with the fate of the C-terminal cleavage product of *Saccharomyces cerevisiae* Scc1, we assume that this degradation follows the N-end rule (Rao et al. 2001). Furthermore, rather than activating SSE as in the case of PIM degradation, THR cleavage contributes to inactivation of SSE.

According to this proposal, degradation of PIM should

precede THR cleavage, as these two events would define a window of SSE activity. THR cleavage should not occur too fast after PIM degradation so that SSE can cleave its other targets. THR cleavage therefore might be regulated (for instance, by Scc1 cleavage fragments) or might not lead to SSE inactivation immediately. SSE inactivation might occur only once THR cleavage fragments have been removed. Alternatively, SSE might cleave its substrates with different kinetics. Fast and efficient Scc1 cleavage may be followed by less efficient and slower THR cleavage.

We emphasize that we do not have direct evidence for our proposal from biochemical separase activity assays. The assay developed for human separase in the *Xenopus* extract system (Waizenegger et al. 2000) does not work for *Drosophila* SSE complexes for unknown reasons (A. Herzig, C.F. Lehner, and S. Heidmann, unpubl.). Perhaps activation of *Drosophila* SSE complexes is only possible in a particular cellular context, for instance, on the mitotic spindle or at the kinetochore. Consistent with this proposal, only a fraction of PIM and THR is degraded during mitosis in *Drosophila* embryos, and a slight enrichment of PIM and THR on mitotic spindles, similar to securin and separase in yeast (Ciosk et al. 1998; Kumada et al. 1998; Jensen et al. 2001), can be visualized with appropriate fixation procedures in the syncytial blastoderm (A. Herzig, C.F. Lehner, and S. Heidmann, unpubl.).

Even without biochemical evidence, our data strongly support the notion that THR is cleaved by SSE. Cleavage occurs at a conserved separase-cleavage consensus sequence. Substitution of a single arginine by an aspartate within this region abolishes cleavage, as previously observed for cleavage of yeast and human Scc1 by separase (Uhlmann et al. 1999; Hauf et al. 2001). Furthermore, mitotic THR cleavage requires functional SSE complexes, as THR is neither cleaved in *pim* mutants, nor in SSE complexes containing nonfunctional THR mutants, nor in cells arrested in the mitotic checkpoint, when SSE is inactive.

The idea that THR cleavage and the consequential THR degradation contribute to inactivation of SSE is supported by our genetic analyses. Expression of noncleavable THR variants results in a phenotype that is highly dependent on the level of SSE protein. The phenotype is only observed with wild-type, but not with reduced levels of SSE. Moreover, noncleavable THR generates a phenotype only in combination with functional, but not with catalytically inactive SSE, having a serine instead of the cysteine residue in the catalytic center.

Does THR cleavage represent a general aspect of separase regulation or is it specific for *Drosophila*? THR is not conserved during evolution but might correspond to the nonconserved N-terminal domain found in separases from other eukaryotes. Therefore, mitotic THR cleavage might conceivably correspond to the mitotic separase cleavage, which has been observed in human tissue culture and in vitro (Waizenegger et al. 2000; Stemmann et al. 2001). This separase cleavage also appears to be autocatalytic. The cleavage sites in human separase have not yet been mapped precisely, and the functional consequences of cleavage-site mutations are not yet known (Stemmann et al. 2001). However, extrapolating from the reported size of the human separase cleavage fragments to *Drosophila*, the corresponding processing events should occur within SSE and not within THR, the putative N-terminal separase domain released during evolution. We have not detected SSE processing in *Drosophila*. But the hypothesized evolutionary gene split resulting in the independent Sse^+ and thr^+ genes of *Drosophila* might represent a permanent separation of those separase fragments that are generated by mitotic cleavage in human cells. The theory that mitotic THR cleavage does not correspond to human separase self-cleavage is also supported by the apparently distinct functional consequences of these processing events. Whereas THR cleavage contributes to SSE inactivation, cleaved human separase is clearly active (Stemmann et al. 2001). Mitotic THR cleavage therefore might be an event specific for insects with their characteristic early embryogenesis including syncytial division cycles followed by cellularization. Early embryogenesis is precisely the developmental period that is most dependent on THR cleavage. We do not understand why THR cleavage is essential at 18°C but largely dispensable at 25°C. The reason for this cold-sensitivity is not simply stress per se, because we did not observe sensitivity at elevated temperatures. We note that microtubule-dependent processes tend to be sensitive to cold temperatures (Brinkley and Cartwright 1975; Rieder 1981).

At present, we also do not understand why THR cleavage is particularly crucial for the process of cellularization, whereas it is less important during other developmental stages. As THR cleavage contributes to SSE inactivation, the phenotypes caused by noncleavable THR variants presumably reflect SSE hyperactivation. Persistence of SSE activity into S phase might be expected to interfere with the establishment of sister-chromatid cohesion by premature degradation of the Scc1 cohesin subunit. A rapid SSE inactivation resulting from mitotic THR cleavage, therefore, would be expected to be most important during the extremely rapid syncytial division cycles, during which the alternative pathway of SSE inhibition by resynthesis of the securin PIM during interphase might not be fast enough. In principle, the various irregularities observed during the syncytial cycles in $THR^{\Delta VQ}$ embryos might reflect consequences from premature Scc1 degradation by hyperactive SSE. The limited penetrance and expressivity of these defects during the syncytial cycles, however, makes a detailed characterization difficult.

The highly penetrant phenotype observed during cellularization is very unlikely to result from premature Scc1 degradation. The extensive cellularization defects start well after completion of mitosis 13, which is at most subtly defective in a few nuclei. We therefore assume that hyperactive SSE results in the degradation of an unknown protein that is crucial for cellularization.

Observations in other organisms have also indicated that separase has other targets in addition to cohesin subunits. *Caenorhabditis elegans* separase appears to

have targets whose cleavage is important for osmotic barrier and anterior–posterior axis formation in the fertilized egg (Siomos et al. 2001; Rappleye et al. 2002). Moreover, a bioinformatics survey has revealed 26 potential separase targets in the *S. cerevisiae* proteome (Rao et al. 2001), and the kinetochore-associated protein Slk19 has in fact been confirmed as a separase target. Cleavage of Slk19 has been shown to contribute to anaphase spindle stability (Sullivan et al. 2001). Even though a *Drosophila* ortholog for Slk19 cannot be identified, it is conceivable that spindle-associated proteins are also SSE targets in *Drosophila*. Excess cleavage of microtubule-associated targets important for cytoskeletal organization might thus cause the cellularization defects in $THR^{\Delta VQ}$ embryos, which clearly have an abnormal γ-tubulin distribution during interphase 14. The putative additional SSE targets might be exclusively or particularly important during cellularization. Alternatively, it is not excluded that the alternative pathway of SSE inhibition by PIM resynthesis is particularly inefficient before cellularization, because the decrease of maternal *pim* mRNA levels at this stage might not yet be fully compensated by zygotic *pim* expression.

In conclusion, although mitotic and meiotic cohesin subunits have been shown to be crucial targets of eukaryotic separases, recent results point to additional substrates involved in processes beyond sister-chromatid separation and to novel regulatory mechanisms. Analyses in different organisms, which have revealed surprisingly distinct aspects of separase regulation and function, will perhaps rapidly converge toward a complete picture.

Materials and methods

Fly stocks and crosses

The transgenic lines *gthr–myc* III.1 and *gthr 445–1379–myc* III.1 have been described previously (Leismann et al. 2000; Jäger et al. 2001). *gthr 1–1204–myc* lines were generated analogously. $gthr^{\Delta VQ}$*–myc* and $gthr^{RD}$*–myc* lines were generated with modified *gthr–myc* constructs carrying the desired mutations introduced with the QuikChange Mutagenesis kit (Stratagene). Sse^{13m}, *Df(3L)SseA* (Jäger et al. 2001), pim^{1} (Stratmann and Lehner 1996), and thr^{1B} (Nüsslein-Volhard et al. 1984) have been described previously. An Sse^{13m} chromosome carrying the transgene $gSse^{+}$ III.1 was constructed by meiotic recombination. $gSse^{+}$ III.1, *UAS–HA–Sse* III.1, and *UAS–HA–*Sse^{C497S} III.2 have been described previously (Jäger et al. 2001). The UAS transgenes were expressed using *α4tub–GAL4–VP16* (Micklem et al. 1997). The *T(2;3) TSTL CyO; TM6B, Tb* balancer stock (*TSTL*) was a gift from Konrad Basler (Institute of Molecular Biology, University of Zürich, Zürich, Switzerland).

To investigate the phenotype resulting from two $gthr^{\Delta VQ}$*–myc* transgenes in a thr^{+} background, all six possible pairs of the transgenes $gthr^{\Delta VQ}$*–myc* II.1, $gthr^{\Delta VQ}$*–myc* II.2, $gthr^{\Delta VQ}$*–myc* II.3, and $gthr^{\Delta VQ}$*–myc* II.4 were combined by meiotic recombination. Females with the genotypes $gthr^{\Delta VQ}$*–myc* II.*n*, $gthr^{\Delta VQ}$*–myc* II.*m*/+; *Df(3L)SseA*/+ or $gthr^{\Delta VQ}$*–myc* II.*n*, $gthr^{\Delta VQ}$*–myc* II.*m*/+; Sse^{13m}/+ or $gthr^{\Delta VQ}$*–myc* II.*n*, $gthr^{\Delta VQ}$*–myc* II.*m*/+; Sse^{13m}, $gSse^{+}$ III.1/+ or $gthr^{\Delta VQ}$*–myc* II.*n*, $gthr^{\Delta VQ}$*–myc* II.*m*/+; *TM3, Ser Act5c-GFP*/+ were crossed to w^{1} males at 18°C. The letters *n* and *m* refer to the different transgene insertion numbers. For the experiment shown in Figure 6A, the chromosome $gthr^{\Delta VQ}$*–myc* II.2, $gthr^{\Delta VQ}$*–myc* II.3 was used. At least four vials with six females and eight to ten w^{1} males were set up for each cross; eggs were allowed to be laid for 7 days, and all eclosing progeny were counted. In all cases, the cold-sensitivity caused by the two $gthr^{\Delta VQ}$*–myc* transgene insertions was strongly suppressed (at least 100-fold more progeny when the maternal *Sse* dose was reduced by 50%).

To determine the cold-sensitive period of the maternal-effect lethality resulting from noncleavable *thr* variants, eggs were collected from $gthr^{RD}$*–myc* III.1, or $gthr^{\Delta VQ}$*–myc* II.3, or *gthr–myc* III.1, or $gthr^{\Delta VQ}$*–myc* II.3/+ females at 25°C for 1 h on apple juice agar plates. The agar plates were divided into three sectors. One sector was left at 25°C, one sector was shifted to 18°C after 3.5 h, and a third sector was incubated at 18°C for 4.5 h and then shifted back to 25°C for the rest of embryonic development. Each sector was used for the determination of larval hatch rates.

For the analysis of the phenotype associated with the maternal expression of two $gthr^{\Delta VQ}$*–myc* transgenes in the presence of Gal4-inducible *Sse* transgenes, females with the genotype $gthr^{\Delta VQ}$*–myc* II.3, $gthr^{\Delta VQ}$*–myc* II.4/*α4tub–GAL4–VP16; UAS–HA–Sse* III.1/Sse^{13m}, or $gthr^{\Delta VQ}$*–myc* II.3, $gthr^{\Delta VQ}$*–myc* II.4/*α4tub–GAL4–VP16; UAS–HA–*Sse^{C497S} III.2/Sse^{13m} were generated. Control females had the genotype $gthr^{\Delta VQ}$*–myc* II.3, $gthr^{\Delta VQ}$*–myc* II.4/*TSTL; UAS–HA–*Sse^{C497S} III.2/*TSTL* or $gthr^{\Delta VQ}$*–myc* II.3, $gthr^{\Delta VQ}$*–myc* II.4/*TSTL;* Sse^{13m}/*TSTL*. All females were crossed to w^{1} males. Eggs were collected at 25°C for 1 h and then incubated at 18°C for 4.5 h before fixation and DNA labeling. In addition, eggs were collected at 25°C for 2 h and used to prepare protein extracts for immunoblotting.

Coupled in vitro transcription and translation

To generate THR fragments in vitro, the regions coding for C-terminal domains starting at amino acids 954, 973, 995, 1013, and 1032 were enzymatically amplified and cloned into the vector pCITE2a (Novagen). The forward primers were designed to introduce a start codon immediately upstream of the following *thr* coding regions. The resulting plasmids were used as templates in coupled in vitro transcription and translation reactions using the TNT system (Promega). Next 0.1 μL of each in vitro reaction was run on a SDS-PAGE next to an extract prepared from pooled embryos synchronously progressing through anaphase 14 (see Fig. 1G). The extracts were subsequently analyzed by immunoblotting with an anti-THR antibody.

Antibodies

Antibodies against α-tubulin (mAB DM1A; Neomarkers), γ-tubulin (GTU-88; Sigma), and secondary antibodies (Jackson Immunoresearch) were obtained commercially. The anti-Armadillo antibody (mAb N2 7A1; Peifer et al. 1994) was obtained from the Developmental Studies Hybridoma Bank (University of Iowa). Antibodies against the human c-myc-epitope (mAb 9E10; Evan et al. 1985), the HA-epitope (mAb 12CA5; Niman et al. 1983), cyclin B (Jacobs et al. 1998), cyclin A (Lehner and O'Farrell 1989), PIM and SSE (Jäger et al. 2001), and THR (Leismann et al. 2000) have been described previously.

Immunoblotting and immunolabeling

Extracts from embryos at defined stages of mitosis 14 were obtained as described (Sauer et al. 1995). For the analysis of defined cell cycle stages during the syncytial blastoderm, embryos were

fixed, stained with Hoechst 33258, and stored as described (Edgar et al. 1994). Embryos at the desired cell cycle stage were selected under an inverted fluorescence microscope and subsequently solubilized in SDS-PAGE sample buffer. Hybond-ECL membranes and ECL-detection (Amersham Biosciences) were used for immunoblotting experiments.

For the analysis of THR during mitosis 14 by immunofluorescence, females with the genotype *gthr–myc* III.1/+, or *gthr*$^{\Delta VQ}$*–myc* II.3/+, or *gthr 445–1379–myc* III.1/+, or *gthr 1–1204–myc* III.1/+ were crossed with *w*^{1} males. Embryos were collected from these crosses and fixed at the stage of mitosis 14.

To analyze the stability of THR in spindle checkpoint-arrested cells, we collected eggs from a cross between *w*^{1} males and *gthr–myc* III.1/+ females. Eggs were collected for 30 min and aged at 25°C for 150 min. The subsequent permeabilization and incubation with demecolcine (Sigma) were performed as described (Leismann et al. 2000). Control embryos were treated identically, except that demecolcine was omitted. For the immunoblot analysis shown in Figure 3G, methanol-fixed embryos were stained with Hoechst 33258 and examined microscopically. Only fertilized and morphologically intact embryos were selected for extract preparation.

For the analysis of THR–myc behavior in *pim* mutants, eggs were collected from a cross of *pim*^{1}*/CyO, P[w*$^{+}$*, ftz–lacZ]; gthr–myc* III.1/+ females and *pim*^{1}*/CyO, P[w*$^{+}$*, ftz–lacZ]* males. Eggs were collected for 90 min and aged at 25°C for 270 min, fixed and immunolabeled. *pim* mutant embryos progressing through mitosis 15 were identified by the characteristic *pim* phenotype revealed by the DNA staining (Stratmann and Lehner 1996).

For the analysis of the cellular phenotype caused by the presence of noncleavable THR, eggs were collected from *gthr*$^{\Delta VQ}$*–myc* III.3, or *gthr*RD*–myc* III.1, or *gthr–myc* III.1 females at 25°C for 1 h. The eggs were incubated at 18°C for 3.5 h and then fixed and labeled with a DNA stain.

To quantify defects during syncytial divisions, embryos were counted that had a nuclear density lower than expected for cycle 13 and that displayed abnormalities in their DNA stain (mitotic arrest, asynchronous mitoses, large areas devoid of nuclei, very low density of nuclei on the embryo surface). Percentages were calculated from the total number of embryos that were examined.

To quantify defects during cellularization, all embryos were scored that had completed cellularization (as judged by nuclear morphology). Among these, embryos with >20 nuclei detached from the cortex were classified as having a cellularization defect. Percentages were calculated from the total number of scored cellularized embryos.

Some embryos of the same collections were fixed by heat/methanol treatment and labeled with an antibody against Armadillo and propidium iodide to stain DNA. Some embryos were formaldehyde fixed in the presence of taxol and double-labeled with antibodies against α-tubulin and γ-tubulin to visualize microtubules and centrosomes, respectively. Images were acquired using a Leica TCS-SP inverted confocal laser scanning microscope and the Leica confocal software package. Images were processed using Adobe Photoshop.

Acknowledgments

We are very grateful to Jan-Michael Peters and Irene Waizenegger for generously providing *Xenopus* extract and information. We thank K. Angermann and K. Neugebauer for technical help. We also thank H. Jäger for information concerning the *thr* orthologs from *D. pseudoobscura* and *D. virilis*. The work was supported by DFG grants (LE 987/2-1 and LE 987/3-1).

The publication costs of this article were defrayed in part by payment of page charges. This article must therefore be hereby marked "advertisement" in accordance with 18 USC section 1734 solely to indicate this fact.

References

Alexandru, G., Uhlmann, F., Mechtler, K., Poupart, M.A., and Nasmyth, K. 2001. Phosphorylation of the cohesin subunit Scc1 by Polo/Cdc5 kinase regulates sister chromatid separation in yeast. *Cell* **105:** 459–472.

Brinkley, B.R. and Cartwright, Jr. J., 1975. Cold-labile and cold-stable microtubules in the mitotic spindle of mammalian cells. *Ann. NY Acad. Sci.* **253:** 428–439.

Chen, L., Puri, R., Lefkowitz, E.J., and Kakar, S.S. 2000. Identification of the human pituitary tumor transforming gene (hPTTG) family: Molecular structure, expression, and chromosomal localization. *Gene* **248:** 41–50.

Ciosk, R., Zachariae, W., Michaelis, C., Shevchenko, A., Mann, M., and Nasmyth, K. 1998. An ESP1/PDS1 complex regulates loss of sister chromatid cohesion at the metaphase to anaphase transition in yeast. *Cell* **93:** 1067–1076.

Clarkson, M. and Saint, R. 1999. A His2AvDGFP fusion gene complements a lethal His2AvD mutant allele and provides an in vivo marker for *Drosophila* chromosome behavior. *DNA Cell Biol.* **18:** 457–462.

D'Andrea, R.J., Stratmann, R., Lehner, C.F., John, U.P., and Saint, R. 1993. The *three rows* gene of *Drosophila melanogaster* encodes a novel protein that is required for chromosome disjunction during mitosis. *Mol. Biol. Cell* **4:** 1161–1174.

Edgar, B.A., Sprenger, F., Duronio, R.J., Leopold, P., and O'Farrell, P.H. 1994. Distinct molecular mechanisms regulate cell cycle timing at successive stages of *Drosophila* embryogenesis. *Genes & Dev.* **8:** 440–452.

Evan, G.I., Lewis, G.K., Ramsay, G., and Bishop, J.M. 1985. Isolation of monoclonal antibodies specific for human c-myc proto-oncogene product. *Mol. Cell Biol.* **5:** 3610–3616.

Foe, V.E. 1989. Mitotic domains reveal early commitment of cells in *Drosophila* embryos. *Development* **107:** 1–22.

Foe, V.E., Odell, G.M., and Edgar, B.A. 1993. Mitosis and morphogenesis in the *Drosophila* embryo: point and counterpoint. In *The development of* Drosophila melanogaster (eds. M. Bate and A. Martinez Arias), pp. 149–300. Cold Spring Harbor Laboratory Press, Cold Spring Harbor, NY.

Funabiki, H., Kumada, K., and Yanagida, M. 1996a. Fission yeast Cut1 and Cut2 are essential for sister separation, concentrate along the metaphase spindle and form large complexes. *EMBO J.* **15:** 6617–6628.

Funabiki, H., Yamano, H., Kumada, K., Nagao, K., Hunt, T., and Yanagida, M. 1996b. Cut2 proteolysis required for sister-chromatid separation in fission yeast. *Nature* **381:** 438–441.

Hauf, S., Waizenegger, I.C., and Peters, J.M. 2001. Cohesin cleavage by separase required for anaphase and cytokinesis in human cells. *Science* **293:** 1320–1323.

Hunter, C. and Wieschaus, E. 2000. Regulated expression of *nullo* is required for the formation of distinct apical and basal adherens junctions in the *Drosophila* blastoderm. *J. Cell Biol.* **150:** 391–401.

Jacobs, H.W., Knoblich, J.A., and Lehner, C.F. 1998. *Drosophila* cyclin B3 is required for female fertility and is dispensable for mitosis like cyclin B. *Genes & Dev.* **12:** 3741–3751.

Jäger, H., Herzig, A., Lehner, C.F., and Heidmann, S. 2001. *Drosophila* separase is required for sister chromatid separation and binds to PIM and THR. *Genes & Dev.* **15:** 2572–2584.

Jallepalli, P.V., Waizenegger, I.C., Bunz, F., Langer, S., Speicher, M.R., Peters, J.M., Kinzler, K.W., Vogelstein, B., and Lengauer, C. 2001. Securin is required for chromosomal stability in human cells. *Cell* **105:** 445–457.

Jensen, S., Segal, M., Clarke, D.J., and Reed, S.I. 2001. A novel role of the budding yeast separin Esp1 in anaphase spindle elongation: Evidence that proper spindle association of Esp1 is regulated by Pds1. *J. Cell Biol.* **152:** 27–40.

Kumada, K., Nakamura, T., Nagao, K., Funabiki, H., Nakagawa, T., and Yanagida, M. 1998. Cut1 is loaded onto the spindle by binding to Cut2 and promotes anaphase spindle movement upon Cut2 proteolysis. *Curr. Biol.* **8:** 633–641.

Lehner, C.F. and O'Farrell, P.H. 1989. Expression and function of *Drosophila* cyclin A during embryonic cell cycle progression. *Cell* **56:** 957–968.

Leismann, O., Herzig, A., Heidmann, S., and Lehner, C.F. 2000. Degradation of *Drosophila* PIM regulates sister chromatid separation during mitosis. *Genes & Dev.* **14:** 2192–2205.

Mei, J., Huang, X., and Zhang, P. 2001. Securin is not required for cellular viability, but is required for normal growth of mouse embryonic fibroblasts. *Curr. Biol.* **11:** 1197–1201.

Micklem, D.R., Dasgupta, R., Elliott, H., Gergely, F., Davidson, C., Brand, A., González-Reyes, A., and St. Johnston, D. 1997. The *mago nashi* gene is required for the polarisation of the oocyte and the formation of perpendicular axes in *Drosophila*. *Curr. Biol.* **7:** 468–478.

Niman, H.L., Houghten, R.A., Walker, L.E., Reisfeld, R.A., Wilson, I.A., Hogle, J.M., and Lerner, R.A. 1983. Generation of protein-reactive antibodies by short peptides is an event of high frequency: Implications for the structural basis of immune recognition. *Proc. Natl. Acad. Sci.* **80:** 4949–4953.

Nüsslein-Volhard, C., Wieschaus, E., and Kluding, H. 1984. Mutations affecting the pattern of the larval cuticle in *Drosophila melanogaster*. I. Zygotic loci on the second chromosome. *Roux's Arch. Dev. Biol.* **193:** 267–282.

Peifer, M., Sweeton, D., Casey, M., and Wieschaus, E. 1994. Wingless signal and Zeste-white 3 kinase trigger opposing changes in the intracellular distribution of Armadillo. *Development* **120:** 369–380.

Philp, A.V., Axton, J.M., Saunders, R.D.C., and Glover, D.M. 1993. Mutations in the *Drosophila melanogaster* gene *three rows* permit aspects of mitosis to continue in the absence of chromatid segregation. *J. Cell Sci.* **106:** 87–98.

Rao, H., Uhlmann, F., Nasmyth, K., and Varshavsky, A. 2001. Degradation of a cohesin subunit by the N-end rule pathway is essential for chromosome stability. *Nature* **410:** 955–959.

Rappleye, C.A., Tagawa, A., Lyczak, R., Bowerman, B., and Aroian, R.V. 2002. The anaphase-promoting complex and separin are required for embryonic anterior–posterior axis formation. *Dev. Cell* **2:** 195–206.

Rieder, C.L. 1981. The structure of the cold-stable kinetochore fiber in metaphase PtK1 cells. *Chromosoma* **84:** 145–158.

Sauer, K., Knoblich, J.A., Richardson, H., and Lehner, C.F. 1995. Distinct modes of cyclin E/cdc2c kinase regulation and S phase control in mitotic and endoreduplication cycles of *Drosophila* embryogenesis. *Genes & Dev.* **9:** 1327–1339.

Shah, J.V. and Cleveland, D.W. 2000. Waiting for anaphase: Mad2 and the spindle assembly checkpoint. *Cell* **103:** 997–1000.

Siomos, M.F., Badrinath, A., Pasierbek, P., Livingstone, D., White, J., Glotzer, M., and Nasmyth, K. 2001. Separase is required for chromosome segregation during meiosis I in *Caenorhabditis elegans*. *Curr. Biol.* **11:** 1825–1835.

Stemmann, O., Zou, H., Gerber, S.A., Gygi, S.P., and Kirschner, M.W. 2001. Dual inhibition of sister chromatid separation at metaphase. *Cell* **107:** 715–726.

Stratmann, R. and Lehner, C.F. 1996. Separation of sister chromatids in mitosis requires the *Drosophila pimples* product, a protein degraded after the metaphase anaphase transition. *Cell* **84:** 25–35.

Sullivan, M., Lehane, C., and Uhlmann, F. 2001. Orchestrating anaphase and mitotic exit: Separase cleavage and localization of Slk19. *Nat. Cell Biol.* **3:** 771–777.

Uhlmann, F., Lottspeich, F., and Nasmyth, K. 1999. Sister-chromatid separation at anaphase onset is promoted by cleavage of the cohesin subunit Scc1. *Nature* **400:** 37–42.

Uhlmann, F., Wernic, D., Poupart, M.A., Koonin, E.V., and Nasmyth, K. 2000. Cleavage of cohesin by the CD clan protease separin triggers anaphase in yeast. *Cell* **103:** 375–386.

Waizenegger, I.C., Hauf, S., Meinke, A., and Peters, J.M. 2000. Two distinct pathways remove mammalian cohesin from chromosome arms in prophase and from centromeres in anaphase. *Cell* **103:** 399–410.

Wang, Z., Yu, R., and Melmed, S. 2001. Mice lacking pituitary tumor transforming gene show testicular and splenic hypoplasia, thymic hyperplasia, thrombocytopenia, aberrant cell cycle progression, and premature centromere division. *Mol. Endocrinol.* **15:** 1870–1879.

Whitfield, W.G.F., Gonzalez, C., Maldonado-Codina, G., and Glover, D.M. 1990. The A-type and B-type cyclins of *Drosophila* are accumulated and destroyed in temporally distinct events that define separable phases of the G_2–M transition. *EMBO J.* **9:** 2563–2572.

Yamamoto, A., Guacci, V., and Koshland, D. 1996. Pds1p, an inhibitor of anaphase in budding yeast, plays a critical role in the APC and checkpoint pathway(s). *J. Cell Biol.* **133:** 99–110.

Zou, H., McGarry, T.J., Bernal, T., and Kirschner, M.W. 1999. Identification of a vertebrate sister-chromatid separation inhibitor involved in transformation and tumorigenesis. *Science* **285:** 418–422.

Erklärung:

Hiermit versichere ich, die vorliegende Arbeit selbstständig verfasst und keine anderen als die von mir angegebenen Quellen und Hilfsmittel benutzt zu haben.

Ferner erkläre ich, dass ich weder an der Universität Bayreuth, noch an einer anderen Hochschule versucht habe, eine Dissertation einzureichen, oder mich einer Promotionsprüfung zu unterziehen.

Alf Herzig
Bayreuth,